# Nanoscopic Metal Fluoride Based Novel Solid Catalysts

**DISSERTATION**

zur Erlangung des akademischen Grades

**Doctor rerum naturalium**

(Dr. rer. nat.)

im Fach Chemie

eingereicht an der

Mathematisch-Naturwissenschaftlichen Fakultät I

der Humboldt-Universität zu Berlin

von

Pratap T. Patil, M. Sc.

geboren am 21.07.1978 in Mirkhal, Indien

Präsident der Humboldt-Universität zu Berlin

Prof. Dr. Christoph Markschies

Dekan der Mathematisch-Naturwissenschaftlichen Fakultät I

Prof. Dr. Lutz-Helmut Schön

Gutachter: 1. Prof. Dr. Erhard Kemnitz

2. Prof. Dr. Klaus Rademann

3. PD Dr. Andreas Martin

Tag der mündlichen Prüfung: 19 Dezember 2008

*……Dedicated to my*

*beloved parents….*

***Sou*. Bhartidevi Tukaram Patil & *Shri* Tukaram Devrao Patil**

# Abstract

Because of their high chemical and thermal stabilities, metal fluorides have found to be advantageous over metal oxides in such cases where reactions involving generation of corrosive acids like HCl and HF are concerned. The Sol-gel method is known for the synthesis of materials with considerably different properties to those prepared by classical routes. In this work, sol-gel route has been employed for the synthesis of binary fluorides ($AlF_3$, $MgF_2$, $CaF_2$, $CuF_2$ and $FeF_3$), hydroxyfluorides [$AlF_{3-x}(OH)_x$, $MgF_{2-x}(OH)_x$] complex fluorides ($KMgF_3$, $K_3AlF_6$), metal fluoride supported nanoscopic noble metals (Pd, Pt) and host-guest fluoride systems ($CuF_2/AlF_3$, $FeF_3/AlF_3$).

Besides the successful synthesis of metal fluorides described above, the present thesis deals with investigation of their bulk and surface properties using various analytical and spectroscopic methods (XRD, BET, $NH_3$-TPD FTIR-pyridine adsorption, XPS, microscopic studies) as well as with their catalytic properties for the reactions of academic and industrial interest. Metal fluorides prepared via sol-gel method have shown to possess extraordinary surface properties in terms of surface area, particle size, porosity, Lewis acidity and distortion in their structures as compared to those of classical methods like aqueous synthesis or impregnations. A homogeneous dispersion of Pd nanoparticles supported on high surface area metal fluoride prepared by this method was confirmed by XRD, XPS and TEM imaging.

Catalytic properties of these materials have been investigated for dehydrofluorination of hydrofluorocarbons, isomerization of citronellal, hydrodehalogenation of chlorodifluoromethane, Suzuki cross coupling and oxidative fluorination of benzene.

**Keywords:**

Metal fluorides, Sol-Gel Synthesis, Nanoparticles, Supported Palladium Catalysts, Suzuki Coupling, Hydrodehalogenation, Dehydrohalogenation, Fluorination.

# Zusammenfassung

Metallfluoride sind dank ihrer hohen chemischen und thermischen Stabilität, insbesondere bei Reaktionen unter Beteiligung von hoch korrosiven Gasen (HF, HCl, $Cl_2$, $F_2$) den entsprechenden Oxiden überlegen. Über den Sol-Gel Prozess synthetisierte Produkte weisen oft spezifische, zum Teil sehr unterschiedliche Eigenschaften im Vergleich zu klassisch hergestellten Verbindungen auf. In dieser Arbeit wurde der Sol-Gel Prozess zur Herstellung von binären Fluoriden ($AlF_3$, $MgF_2$, $CaF_2$, $CuF_2$ und $FeF_3$) genutzt und zum Teil weiter entwickelt sowie das Synthesepotential dieser Methode als Zugang für komplexe Fluoride ($KMgF_3$, $K_3AlF_6$), für Metallfluorid-geträgerte „nano Edelmetall-Systeme ($Pd/AlF_3$, $Pt/AlF_3$, $Pd/CaF_2$, $Pd/MgF_2$) und für Gast–Wirt–Metallfluorid-Systeme ($CuF_2/AlF_3$, $FeF_3/AlF_3$) untersucht. Die Eigenschaften der als kompakte Materialien hergestellten Metallfluorid Systeme wurden mit Hilfe spektroskopischer Methoden untersucht und dabei insbesondere deren Oberflächeneigenschaften bestimmt. Die neuen Materialien wurden für die Nutzung akademisch und industriell bedeutsamer Katalysereaktionen evaluiert und mit klassischen Katalysatoren verglichen. Es konnte gezeigt werden, dass der Sol-Gel Prozess für Fluoride zu neuartigen Materialien mit außergewöhnlichen Eigenschaften führt. Insbesondere infolge der Synthese-bedingten Vergrößerung der spezifischen Oberflächen um einen bis zu 20-fachen Faktor im Vergleich zu klassisch hergestellten Fluoriden konnten auch eine Reihe von katalytisch interessanten Metallen (Pd, Pt) in die nanoskopischen Festkörperfluoride eingebracht werden. Die TEM Aufnahmen zeigen, dass z. B. 2-5 nm große Palladiumpartikel sehr homogen in ca. 80 nm große $CaF_2$- bzw. 20 nm große $AlF_3$-Matrices in nur einem einzigen Reaktionsschritt eingeführt werden können. Die neuen Materialien wurden in verschiedenen katalytischen Reaktionen getestet und zeigten sich in mehreren Fällen den „Standard Katalysatoren“ überlegen.

**Stichworte:**

Metallfluoride, Sol-Gel Synthese, Palladium Nanopartikel, Suzuki Kopplung, Hydrodehalogenierung, Dehydrohalogenierung, Fluorierung.

# Table of Contents

# 1 INTRODUCTION

## 1.1 Heterogeneous Catalysis

Technology based on the utilization of catalytic processes plays a key role in the economic development and growth of the chemical industry. A major emerging and challenging area of heterogeneous catalysis is that of environmental pollution control, having serious implications with the steady tightening by the legislation on release of waste and toxic emissions. Even though, heterogeneously catalyzed processes are widely used in different areas (e.g. petrochemical industry), many manufacturers of fine and specialty chemicals still depend on homogeneously catalyzed liquid phase reactions. Most of them involve the use of stoichiometric amounts of catalysts, e.g., Friedel Craft acylation using anhydrous $AlCl_3$. Additionally, such processes often suffer from low selectivity leading to impure products and tedious work-up procedures involving the generation of waste with disposal costs often outweighing the costs of the target products. All these facts are continuously driving the industry towards the implementation of innovative "clean technology", including the use of alternative heterogeneously catalyzed processes. There are several intrinsic advantages of the heterogeneous catalysts, e.g. simple product separation with catalyst reuse, easy reactant activation and spillover between supports and active phases, reactor operations in continuous flow mode etc. However, to maintain economic viability, a suitable heterogeneous catalyst system must not only minimize the production of waste, but also exhibit activities and selectivities comparable or superior to the existing homogeneous ones. The developments of "green" and "sustainable" technologies have the focus mainly on the following:

Achieving high activity and selectivity. The challenging target is to achieve almost 100 % yield without any side product formation;

The challenge to develop technology with integrated environmental protection leading to the consequent use of solid Brønsted and Lewis acids as catalysts in order to avoid

the problems caused by homogeneously operating processes, e.g. salt formation, corrosion etc.;

Use of cheaper renewable feed stocks;

Utilization of unavoidable side products, heat of reaction etc. The main goal is the complete usage of feed stock and energy;

Developing multifunctional catalysts, which can perform simultaneously several individual reaction steps. The challenging target is to carry out selectively multi step synthesis as "one-pot reaction";

In addition to the general problems mentioned above, there are still pressing needs for better catalyst systems.[1] At this juncture, there is a real need for developing new class of materials with improved properties. Solid metal fluorides are good examples for such solids, which are indeed special class of materials and possess unique properties and hence can be used as novel materials for the development of new catalysts, especially for their application under highly corrosive halogen containing atmosphere.

## 1.2 Metal Fluorides

Metal fluorides[2-15] are emerging as new hi-tech materials in catalysis,[2-9] ceramics,[11-12] thin optical films,[11, 13-15] anti-reflective coatings,[11] hosts for laser devices[11] and energy storage devices.[11, 16] They are obtained either synthetically or from naturally occurring minerals and ores. As required, they are used in different forms such as simple binary, oxy / hydroxyl, complex or doped fluorides, etc.[5] By using or combining different metal cations in the fluoride matrices, it is possible to prepare materials with a wide range of desired properties. Metal fluorides possess the strongest electronegative element, which generates a higher Lewis acidity on the metal center compared to their corresponding oxides. The most important application of metal fluorides is their use as standard catalysts for the synthesis of fluorocarbons, e.g. the conversion of ozone-depleting chlorofluorocarbons (CFCs) into more environmentally friendly hydrochlorofluorocarbons (HCFCs) and/or hydrofluorocarbons (HFCs),[8] the synthesis of different monomers for fluoropolymers,[17] etc. In such reactions, metal oxides require activation by fluorocarbons to reach maximum activity due to the formation of fluoride-based species on the surface, which also indicates the importance of fluorides on the activation of metal oxides.

Statistical data obtained from the chemical abstract service (SciFinder) shows that research on metal fluorides increased tremendously from 1950 onwards (Fig 1.1) after the

application of metal fluorides as fluorination catalysts in the synthesis of fluorocarbons from chlorinated hydrocarbons.

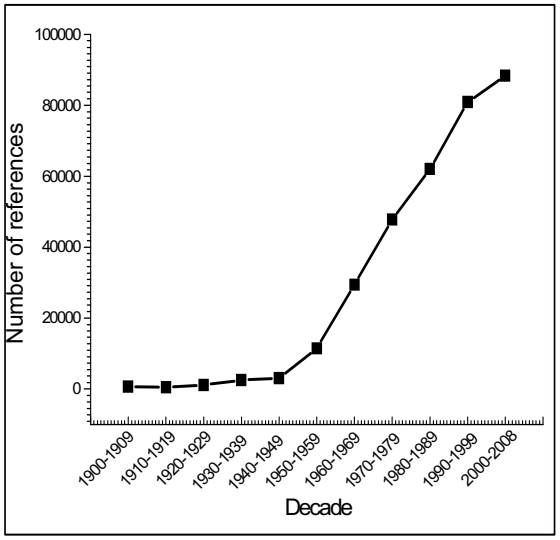


**Fig. 1.1** References found in literature with term "fluoride" per decade since 1900.

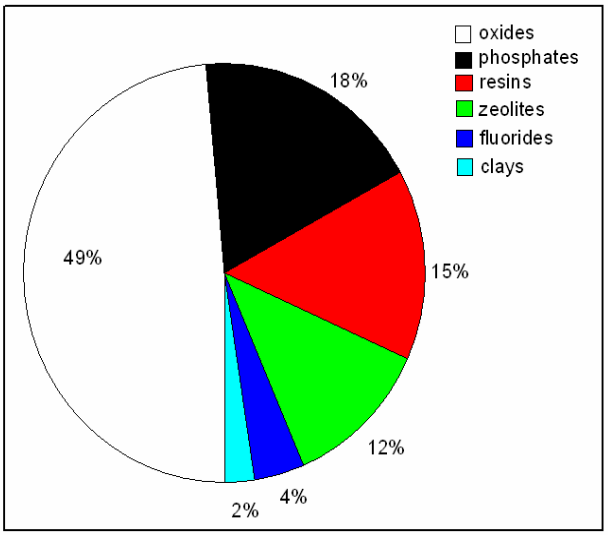


**Fig. 1.2** References found in lit era ture with term "material" (ox ide, fluoride etc) and "catalyst" since 1980.

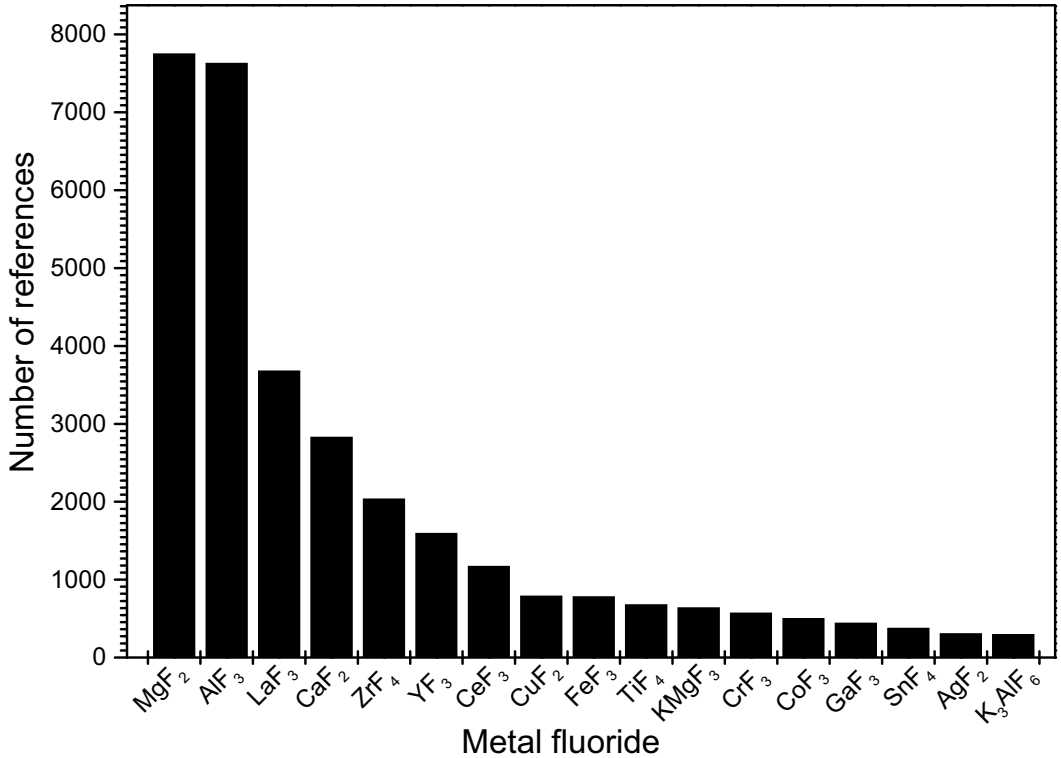


**Fig. 1.3** References found in literature with particular " MFx" since 1950.

Already 4 % of articles in literature collected since 1980 dealt with metal fluoride based materials as catalysts (Fig 1.2). $AlF_3$ and $MgF_2$ are by far the most investigated metal fluorides as shown in Figure 1.3.

## 1.3 Nano-Metal Fluorides via the Sol-Gel Method

Performing chemical reactions under "sol-gel conditions" [18] is a powerful method for the synthesis of high surface area nanoscopic materials. It has several advantages over other synthetic techniques for the preparation of nanoparticles.[19] Because of the very high lattice energies metal fluorides usually undergo crystallization and as a consequence thereof, their surface areas are rather low. For example $AlF_3$ prepared by conventional methods has BET surface areas of about 20 $m^2/g$.[2] Kemnitz and coworkers[20] recently developed a non-aqueous sol-gel method for the synthesis of metal fluorides. $AlF_3$ prepared by this new sol-gel method is an X-ray amorphous nanoscopic solid with very distinct surface and catalytic properties compared to the crystalline phases.[20-21]

The primary goal of this thesis is to generalize the applicability of such new synthesis method of metal fluorides with nanoscopic dimensions and to study their catalytic potential. Besides the investigation of the previously established sol-gel method for simple metal fluorides, the main focus of this work is to develop a potential route for the synthesis of nano-metal fluorides supported Pd nanoparticles.

To achieve above mentioned objectives, various nano-metal fluorides exhibiting varying Lewis acidic properties ranging from very strong acids to completely neutral compounds have been investigated in the present study. The list of metal fluorides investigated is given below.

- Binary fluorides: $AlF_3$, $MgF_2$, $CaF_2$
- Hydroxy fluorides: $AlF_{3-x}(OH)_x$, $MgF_{2-x}(OH)_x$
- Complex fluorides: $KMgF_3$, $K_3AlF_3$
- Metal fluorides as novel supports for palladium: $Pd^0/AlF_3$, $Pd^0/MgF_2$, $Pd^0/CaF_2$ etc.
- Binary fluorides with redox properties: $CuF_2$, $FeF_3$
- Host-guest fluorides: $CuF_2/AlF_3$ and $FeF_3/AlF_3$

The properties of interest concerning the characterizations of the novel materials were:

- Phase purity and crystallinity
- Textural properties such as surface area pore size distribution
- Surface morphology and porosity
- Acid-base characteristics

- Synergetic effects due to interactions between Pd and $MF_x$ –support

The catalyzed reactions chosen for testing the efficiencies of the novel materials were:

- Dehydrofluorination of hydrofluorocarbons
- Isomerization of citronellal
- Suzuki carbon-carbon coupling reactions
- Hydrodehalogenation of $CHClF_2$
- Oxidative fluorination of benzene

# 2 LITERATURE

In this chapter, structural properties, synthesis methods and catalytic applications of metal fluorides based system under investigation are described in detail.

## 2.1 Structure and Properties of Metal Fluorides

*$AlF_3$*

$AlF_3$ exists in five crystallographic phases, such as α, β, η, θ, and κ-$AlF_3$. Among these β and κ are found to be catalytically more active due to their open network structure. While, α-$AlF_3$ is catalytically inactive.[3] The arrangement of [$AlF_6$] octahedrons differs in α-$AlF_3$ and β-$AlF_3$ (Fig 2.1). In rhombohedral α-$AlF_3$, [$AlF_6$] octahedra are corner sharing connected adopting a distorted $ReO_3$ structure. In contrast, β-$AlF_3$ adopts the hexagonal tungsten bronze (HTB) structure, in which six [$AlF_6$] octahedra form hexagonal channels running along the C-axis. Harrison et. al. [22, 23] have explained the high reactivity of β-$AlF_3$[22] in comparison to α-$AlF_3$[23] based on the results obtained from modeling of surface morphologies. According to these calculations, the difference in reactivity arises from substantial difference in accessibility of the reactive, co-ordinatively unsaturated sites of the respective surfaces. In the structure of α-$AlF_3$, Al atoms are effectively covered by fluorine atoms leading to a surface without any acidity. However, in β-$AlF_3$ five fold co-ordination of the surface Al-sites is the reason for its strong Lewis acidity and high catalytic activity. The quantitative Lewis acid strength calculated based on molecular parameters in gas phase given by Christe et. al.[24] is in the order $SbF_5$> $AlF_3$~ $AlFCl_2$~ $AlF_2Cl$~ $AlCl_3$. $AlF_3$ is believed to have equal Lewis acidic character as that of $AlCl_3$ some time ago. However, very recently, Kemnitz and co-workers proved experimentally the superior Lewis acidic properties of high surface area aluminium fluoride (*HS*-$AlF_3$) in comparison to $AlCl_3$.[25]

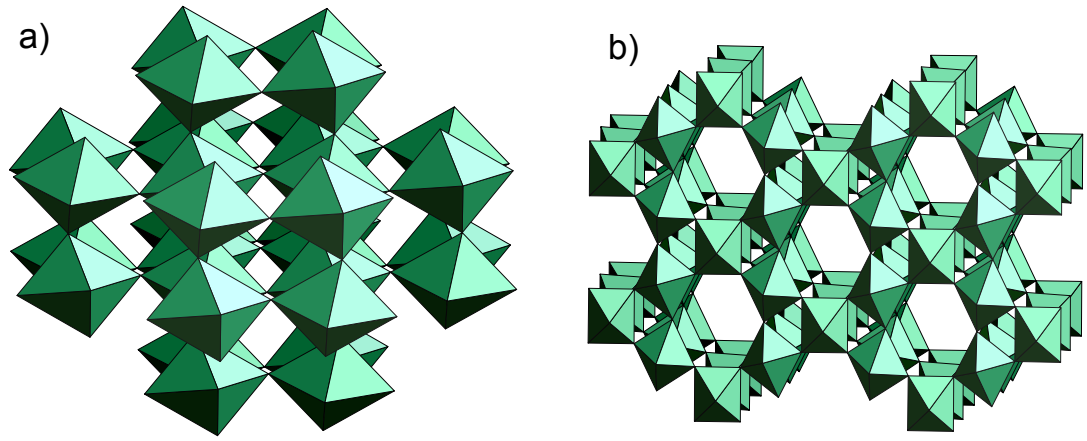


**Fig. 2.1** Linkage of $AlF_6$ octahedra a) in structure of α-$AlF_3$, b) in the HTB structure of β-$AlF_3$.

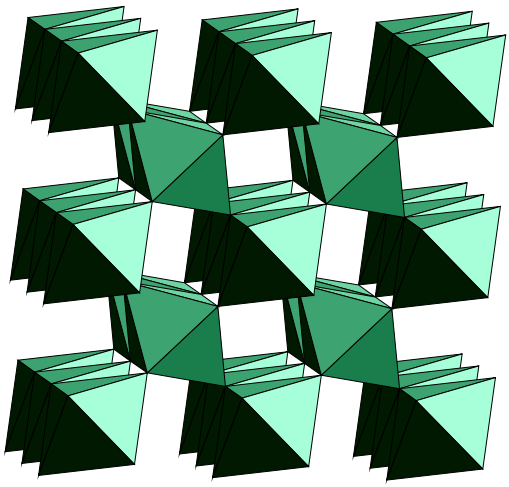

**Fig. 2.2** Crystal structure of $MgF_2$

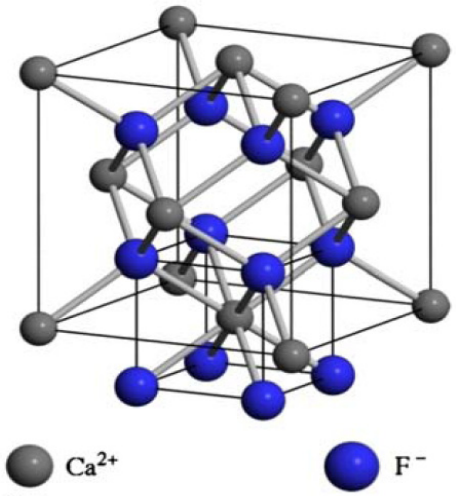


**Fig. 2.3** Crystal structure of $CaF_2$

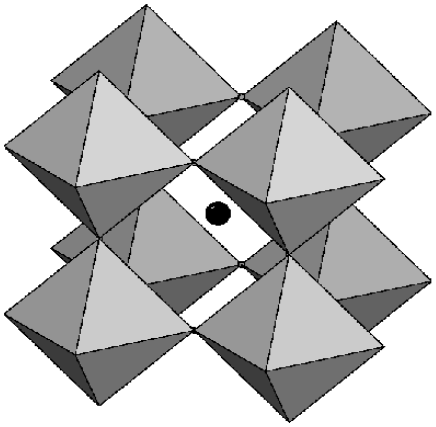

**Fig. 2.4** Crystal structure of $KMgF_3$

*$MgF_2$*

Magnesium difluoride ($MgF_2$) crystallizes in the rutile structure type, in which $Mg^{2+}$ ions are surrounded by six $F^-$ ion and each $F^-$ ion by three $Mg^{2+}$ ions (Fig 2.2).[7] $MgF_2$ possesses a good thermal stability and mechanical strength. It is an insulator with a broad band gap. The first work on magnesium fluoride relevant from heterogeneous catalysis point of view was reported by Wojciechowska el. al. in 1975.[26] The same group has further explored its application as support for different oxides[27-30] and metals[31-32] for several reactions like hydrodechlorination, hydrodesulfurization and reduction of $NO_x$.[26-33] $MgF_2$ is represented to play an important role as support for oxides ($V_2O_5$, $MoO_3$, $WO_3$, CuO, and $Cr_2O_3$),[26-35] fluorides ($FeF_3$, $CrF_3$ etc)[36, 37] and metals (Pd, Pt and Ru).[31-33, 38, 39] $MgF_2$ was considered to be a nearly inert solid fluoride without measurable Lewis acidity,[40] however recently Krishna Murthy et. al.[41] have shown that $MgF_2$ prepared by sol-gel method possesses moderate Lewis acidity.

*$CaF_2$*

Calcium fluoride, $CaF_2$, belongs to the well known fluoride compounds possessing a high symmetric cubic structure (Fig 2.3). The unit cell consists of a face centered cube of $Ca^{2+}$, the $F^-$ ions are centered in the octants of this cube in which each $Ca^{2+}$ ion is surrounded by 8 $F^-$ ions and each $F^-$ by 4 $Ca^{2+}$ ions (Fig 2.3).[42] $CaF_2$ is a chemically inert material. It is used as a window material for both infrared and ultraviolet wavelengths, since it is transparent in these regions (about 0.15 μm to 9 μm) and exhibits extremely weak birefringence. So far $CaF_2$ has been very less investigated for catalytic application. In this thesis, we have shown that $CaF_2$ is neutral material of catalytic interest.[43,44]

*$KMgF_3$*

$KMgF_3$ adopts the perovskite structure in which $Mg^{2+}$ is octahedrally coordinated by $F^-$ anions. $K^+$ appears in the center of the cube formed by eight [$MgF_6$] octahedra (Fig 2.4). Such type of complex fluorides are being used as neutral supports in catalysis.[8]

*Host-guest fluorides*

A model to predict whether Lewis or Brønsted acidity can be generated in a host lattice of oxide by introducing an additional guest metal has been developed by Tanabe.[45] This model is well adapted by metal fluorides.[46] According to this model by doping a divalent host ($MF_2$) with a trivalent guest fluoride ($MF_3$), Lewis acidity is generated because of developed excess positive charge. On the other hand, by doping a trivalent host fluoride ($MF_3$) with a divalent guest fluoride (($MF_2$), Brønsted acidity is generated because of de-

veloped excess negative charge, which becomes compensated by a proton from moisture thus forming e.g. - OH groups.

# 2.2 Synthesis of Metal Fluorides

## 2.2.1 Classical methods

*Crystallization / precipitation from aqueous solutions*

The most widely used method for the synthesis of metal fluorides with the reaction of a metal precursors with 40 %aqueous HF. Metal nitrates, carbonates,[27] chlorides,[47] metal alkyls[48] were used as precursors and the resulting precipitate/ crystalline material was dried at relatively higher temperature. By this method, metal fluoride hydrates are often formed with low surface areas. Similarly, Kleist et. al.[49] have recently used a simple method for the synthesis of $AlF_3$ by fluorination of $Al_2O_3$ in aqueous system.

*Gaseous fluorination of metal oxides (solid-gas reaction)*

Synthesis of metal fluorides by gas phase fluorination of oxides is also another commonly practiced method. It is generally carried out by passing vapors of fluorine containing organic compounds (e.g. $CF_4$, $CHF_3$, $CH_2F_2$, $CF_3COOH$, $CF_3SO_3H$, $CF_3OCF_3$, $CF_3CH_2OH$ etc), fluorosulfur compounds (e.g. $SF_6$, $SO_2F_2$ and $SOF_2$) or inorganic compounds (e.g. HF, $BF_3$, $NH_4F$) on the metal oxides at temperatures between 100-500 °C.[3, 50, 51] The content of fluorine introduced into the fluorinated material however depends on various factors such as fluorination time, temperature and nature of fluorinating agent. There are several reports for the synthesis of fluorinated alumina ($F\text{-}Al_2O_3$)[52-57] and chromia ($F\text{-}Cr_2O_3$)[58-60] based fluorination catalysts using this method. Along with the formation of pure fluorides, complex phases of hydroxy fluorides [$M(OH)_xF_y$; x & y = 1, 2, 3..] and/or oxyfluorides [$MO_xF_y$; x & y = 1, 2 ,3..] has also been reported. The fluorination mechanism depends strongly on the fluorinating agent employed.[57] Acidic protons on fluorinating agent, and the mode of oxygen removal either as $H_2O$ or as CO, for example, may alter the surface structure and the acidic properties of the intermediates that are formed. Changing fluorinating agents may also affect the surface sites that are attacked first during the initial fluorination reaction.

*Special methods for metal fluorides syntheses*

A special method for the preparation of highly dispersed aluminium fluoride was described starting from alumino-silicates, zeolites, which were subjected to a plasma fluorination to remove silicon as gaseous $SiF_4$ and leaving behind this way a highly distorted

$AlF_3$ framework.[51, 62] Besides, physical methods such as CVD and PVD, mechanical milling, laser dispersion or molecular-beam epitaxy have been used for commercially available metal fluorides for their conversion from crystalline into amorphous state.[10] Pyrolysis of fluorine containing compounds,[63] the hydrothermal synthesis[64] as well as microwave-assisted methods have also been reported as a special method for the preparation of nanoscopic aluminium hydroxyfluorides[64] and spherical monodispersed $MgF_2$.[66] In early years, fluorine promoted materials were prepared by impregnation methods in which oxides were saturated with an aqueous solution containing an appropriate amount of a compound such as HF, $BF_3$, $HBF_4$, $NH_4F$, $NH_4BF_4$ or $NH_4SiF_6$ which were reacted at higher temperature.[50-51]

## 2.2.2 Sol-gel method

In addition to the above, there are two more indirect methods are known for sol-gel synthesis of metal fluorides such as

i) Post-fluorination of a metal oxide prepared via a sol-gel route[67-70]
ii) Sol-gel formation of metal trifluoroacetates and their thermal decomposition[71]

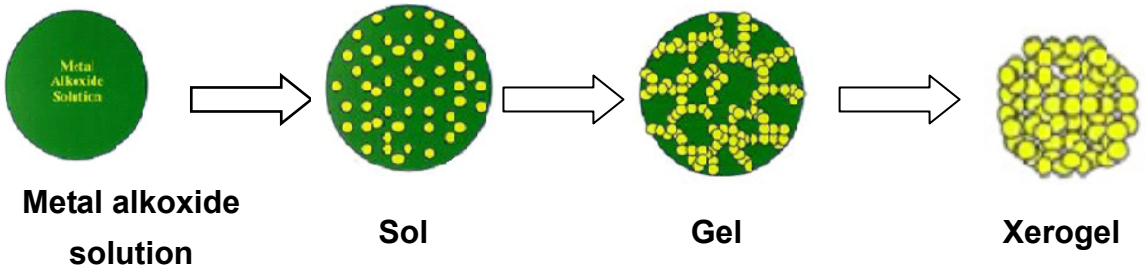


**Scheme 2.1**

Sol-gel method (Scheme 2.1) has shown a wide range of applications in coating, ceramic and glass industries[18]. It is very well investigated for the synthesis of metal oxides based catalytic materials.[71-76] The sol-gel technique as a method for the synthesis of catalytic-nanoscopic materials offers several advantages:

- it is simpler and cheaper than others,
- it offers easy control on porosity and microstructural properties,
- it is a low temperature process,
- a large surface area can be obtained,
- it can be easily modified with uniformly dispersed dopants/modifiers to enhance thermal stability and the catalytic activity,
- the process is potentially easy to scale up,

- and the technology is also well suited for the production of thin-films, coatings and ceramic materials.

Despite the low reproducibility of results and use of relatively expensive alkoxides, the sol-gel process has been proven to be a highly applicable and industrially viable process for synthesizing nanocrystalline materials in general metal fluorides in particular.

*New sol-gel method for the synthesis of nano-metal fluorides*

In contrast to metal oxides, very few efforts have been made to synthesize metal fluoride based materials by sol-gel method by Kemnitz and co-workers.[20] The method developed by Kemnitz et. al. used a non-aqueous soft chemical method for the synthesis of high surface area (*HS*) metal fluorides with extraordinary surface and catalytic properties.[20] $AlF_3$ prepared this way has not only a very large surface area (up to 450 $m^2/g$) but also possess a nanoscopic, mesoporous and highly distorted structure.[20-21] Its Lewis acidity is as high as that of $SbF_5$ and aluminium chlorofluoride (ACF), thus *high surface* $AlF_3$ is obviously - beside ACF[77] - the strongest solid Lewis acid known and can also be used as suitable acidic catalyst or catalyst support.[24] The basics and fields of applications of this new sol-gel synthesis route were reviewed by Rüdiger et. al. recently summarizing the results within this method for preparing nano-structured metal fluorides.[4-5] A very important feature of this method is that it also offers the possibility of incorporating one or more additional co-components of interest into the *HS* metal fluorides, enabling high dispersion of "dopant" at nanoscopic scale. By implementing sol-gel, it becomes possible to produce metal fluoride ceramics transparent in the visible range by cold pressing.[12] This new method is further explored in this thesis for the synthesis of wide range fluorides with different functionalities (Chapter 3).

## 2.3 Metal Fluorides in Catalysis

Metal fluorides in catalysis are of great interest and have been assumed to be of great relevance as an economic alternative to many metal oxide catalyzed, industrially important reactions.[2-9] In particular, the scenario of halogen exchange reactions, a versatile tool for converting the environmentally harmful halogenated compounds into environmentally friendly and useful compounds, have been widely investigated.[2-3] Several studies have demonstrated that the oxide based catalysts need to be activated in a fluorocarbons or HF stream in order to reach maximum catalytic activity in halogen exchange reactions.[2, 73-74] This suggests that surface fluorinated species are active phases for the remarkable catalytic activity. After these early investigations, metal fluorides have taken a considerable boost as catalysts not only in organofluorine chemistry[2-9, 17, 20-21, 25, 36-41, 43, 46, 52,

but also for the synthesis of fine chemicals,[7, 26-32, 34-37, 44, 50-51, 53-54] where for the later type of reactions metal oxides or zeolites were the most widely used materials.

### 2.3.1 Applications in organofluorine chemistry

In organofluorine chemistry, metal fluorides have been extensively used for the conversion of ozone depleting CFCs firstly to HCFCs, later into HFCs. Manzer and Rao have reviewed the important role of metal fluorides for the transformation of CFCs in to CFC alternatives by several catalytic reactions such as Cl/F exchange, dismutation, isomerization, hydrodehalogenation and dehydrohalogenation (Table 2.1).[80]

**Table. 2.1** Applications of metal fluorides in organofluorine chemistry.

| Type of reaction | Example | |
|---|---|---|
| 1) Dismutation | $5\ CHClF_2$ | $3\ CHF_3 + CHCl_2F + CHCl_3$ |
| | $5\ CCl_2F_2$ | $3\ CClF_3 + CCl_3F + CCl_4$ |
| 2) Isomerization | $CF_3\text{-}CH_2F$ | $CHF_2\text{-}CHF_2$ |
| | $CClF_2\text{-}CFCl_2$ | $CF_3\text{-}CCl_3$ |
| | $CF_2Br\text{-}CFBr\text{-}CF_3$ | $CF_3\text{-}CBr_2\text{-}CF_3$ |
| 3) Hydrodehalogenation | $CCl_2F_2 + 2\ H_2$ | $CH_2F_2 + 2\ HCl$ |
| | $CHClF_2 + H_2$ | $CH_2F_2 + HCl$ |
| | $CF_3\text{-}CCl_2F + H_2$ | $CF_3\text{-}CH_2F + 2HCl$ |
| 4) Dehydrohalogenation | $CH_3\text{-}CCl_3$ | $CH_2{=}CCl_2 + HCl$ |
| | $CF_3\text{-}CH_2F$ | $CF_2{=}CHF + HF$ |
| 5) Cl/F-exchange or Fluorination | $CH_2Cl_2 + 2\ HF$ | $CH_2F_2 + 2\ HCl$ |
| | $CF_3\text{-}CH_2Cl + HF$ | $CF_3\text{-}CH_2F + HCl$ |
| | $Ar\text{-}Cl + HF$ | $Ar\text{-}F + HCl$ |
| 6) Hydrofluorination | $CCl_2{=}CCl_2 + HF$ | $CF_3\text{-}CHCl_{2-x}F_x$ ( x= 1,2) + x HCl |

Cl/F exchange is restricted to few compounds, however hydrodehalogenation has been more widely explored for last 25 years for selective conversion of CFCs and HCFCs to HCFCs and HFCs respectively.[33, 38, 39, 43, 47, 81-93] Most prominently, metal based catalysts supported on different carriers are extensively studied. For this purposes, metals like Pd,[8, 33, 38, 39, 43, 47, 56, 81-93] Pt,[8, 38, 39] Ni,[89, 94] Ru,[33] supported on activated carbon,[84] metal oxides[85, 93] and metal fluorides[8, 33, 38, 39, 47, 81-83, 86-92] were used. Among these catalysts, palladium as metals and metal fluorides as supports were promising in terms of activity, selec-

tivity and stability against HCl and/or HF released during the reaction.[8] Similarly, metal fluorides have also been used for dismutation,[2, 20, 21, 36, 37, 43, 57, 79, 95-104] isomerization, [20, 21, 25, 36, 97-101, 105-107] dehydrohalogenation,[101, 108, 109] fluorination[3, 101, 110, 111] and hydrofluorination.[36, 46, 97, 112] As dismutation and isomerization reactions take place exclusively on Lewis acidic centers therefore nowadays these reactions are being used as test reactions for probing Lewis acidity. [20, 21, 36, 37, 97-103]

## 2.3.2 Applications in fine chemical synthesis

**Table. 2.2** Applications of metal fluorides in fine chemical synthesis.

| Type of reaction | Example |
|---|---|
| 1) Friedel-Crafts reaction (Acylation and alkylation) | 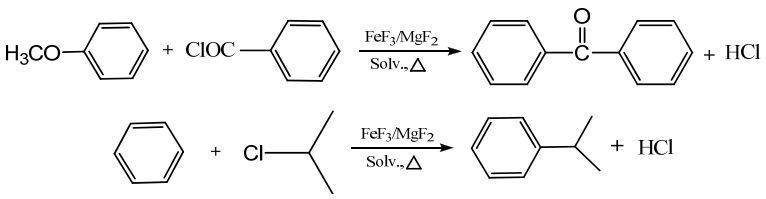 |
| 2) Ethylbenzene oxidation | 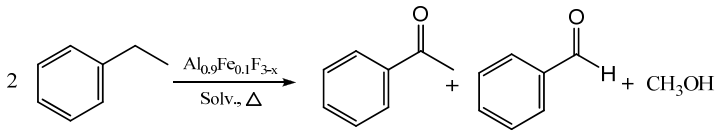 |
| 3) Oxidative dehydrogenation (ODH) | 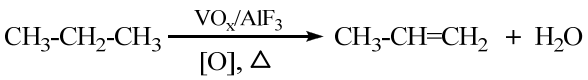 |
| 4) Ammoxidation | 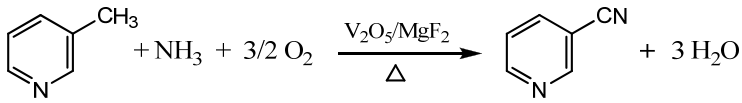 |
| 5) Michael addition | 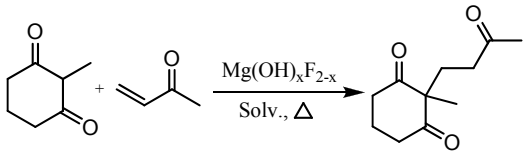 |
| 6) *o*-xylene isomerization | 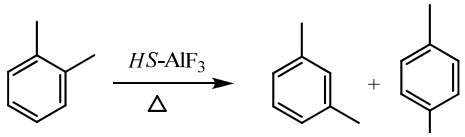 |
| 7) Citronellal isomerization | 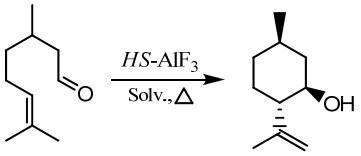 |
| 8) Suzuki coupling | 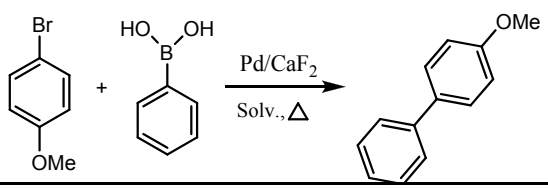 |

The application of metal fluorides as catalysts is not only limited to organofluorine chemistry but there are also promising activities for the fine chemicals synthesis (Table 2.2). In recent years, metal fluorides have been successfully employed for several reactions of academic and industrial interests such as Friedel-Crafts alkylation and acylation,[36, 97] oxidation of ethyl benzene,[113] oxidative dehydrogenation (ODH) of propane,[114, 115] ammoxidation of picoline,[34, 35] *o*-xylene isomerization,[5] Michael additions,[116] Heck and Suzuki cross coupling[44, 117] and synthesis of vitamin E.[118, 119] F-$Al_2O_3$ was the one, which was used for gas phase alkylation's of aromatics.[53, 120-122] Krishnamurthy et. al have showed that $MgF_2$ doped $FeF_3$ and $CrF_3$ can be used for Friedel-Crafts reaction.[36, 97] Iron doped-[113] and Vanadium doped-[114-115] aluminium fluoride has shown remarkable activities for ethylbenzene oxidation and propane ODH, respectively. Similarly, $V_2O_5/MgF_2$ prepared by impregnation method has given high yield for nicotinonitrile during the ammoxidation of 3-picoline.[34, 35] $MgF_{3-x}(OH)_x$ based hydroxyfluorides are found efficient for the Michael addition of 2-methyl cyclohexane-1,3-dione to methyl vinyl ketone.[116] *High surface* $AlF_3$ was an excellent catalyst for gas phase isomerization of o-xylene[5] and liquid phase isomerization of citronellal to isopulegol[123] Nanoscopic $CaF_2$ supported Pd nanoparticles were excellent catalysts for Suzuki coupling as discussed in this thesis (Chapter 5) [44].

## 2.4 Supported Pd Catalysts/Nanoparticles

After the discovery of Palladium in 1803 by W. H. Wollaston, it has become useful for several catalytic applications. It possesses the unique property of absorbing a large amount of hydrogen gas (up to 900 times of its own volume) at room temperature, which leads to one of its main chemical uses, as a hydrogenation catalyst. There are large numbers of reactions, which are catalyzed by supported palladium catalysts, and their importance has surpassed the interest in the fundamental chemistry. The extensive use of the palladium as catalysts is due to its high activity, high selectivity and high durability. Additionally, it also has several advantages such as

- use of minimum amount of catalysts,
- the reactions take place under mild reaction conditions, so it requires minimum equipments and cost utilities,
- excellent selectivity leads to high product yield because of minimum side reactions,
- they can be used regardless of either acid or base solvent,
- easy handling and preservation over a long period of time is possible because they are stable in air,
- no pretreatment is required except some special type of catalysts,

- the recovery and reuse of catalysts is possible in most of the reactions.

Secondly, supported palladium catalysts have several advantages over unsupported materials. Supports can be used to improve the mechanical strength, thermal stability and lifetime of the catalyst. They can also provide the means for increasing the surface area of the active species. In addition, experimental data revealed that supported metal based catalysts frequently have structural features and chemical compositions different from those on the surface of the bulk. This difference arises primarily from the interaction of the metal with the support and the size and shape of the catalytic species. In the last few decades palladium containing homogeneous and heterogeneous catalysts have been used for many organic transformations, particularly in the hydrogenolysis of organohalides[124, 125] and C-C coupling reactions.[126,127] Apart from conventionally used oxides as support, metal fluorides have also been used as non-conventional support for Pd in catalysis.[8, 33, 38, 39, 43, 56, 81-83, 91, 92] The structural and catalytic properties such as particle size, metal dispersion activity, selectivity and stability of Pd catalysts significantly depend on the method of synthesis, Pd precursor and type of support used.[128] Furthermore the nanoparticles of Pd have shown totally different properties than their microscopic counterparts.[129,130]

# 2.5 Reactions Studied in This Thesis

*Dehydrofluorination of hydrofluorocarbons* (Scheme 2.2) is useful reaction for the synthesis of fluoroolefins, which are used as monomer for the synthesis of fluoropolymers. Dehydrofluorination, which involves the activation of stable C-F bond, is a high energy demanding reaction and often carried out catalytically (or non-catalytically) at very high temperatures.

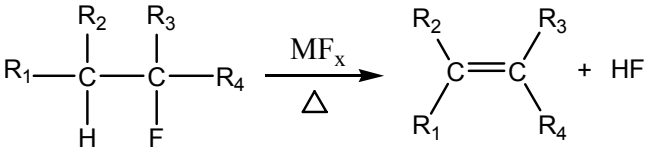


$R_1$, $R_2$, $R_3$, $R_4$ = -H or -F or -$CF_3$

**Scheme 2.2**

The catalysts known for dehydrofluorination have shown low activities and also deactivated after certain period of time.[131] This promoted us to investigate our new sol-gel derived metal fluorides with different functionalities for dehydrofluorination. In this study, initially binary fluorides, host-guest fluorides and metal fluorides supported Pd catalysts are tested for the dehydrofluorination of $CF_3$-$CH_2F$ (HFC-134a). The most active catalyst (HS-$AlF_3$) is further used successfully for the dehydrofluorination of $CF_3$-CHF-$CHF_2$ (HFC-236ea) and $CF_3$-$CH_2$-$CF_3$ (HFC-236fa).

*Citronellal isomerization* (Scheme 2.3) is a crucial step in the industrial production of (-)-menthol by Takasago process[132] involving the use of $ZnBr_2$ as Lewis acid catalyst. It forms four diastereomeric pulegols, among those (-)-isopulegol is important because this only gets transformed into useful (-)-menthol isomer having a specific peppermint odor

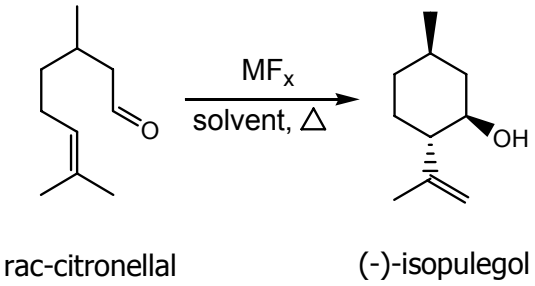


rac-citronellal (-)-isopulegol

**Scheme 2.3**

and cooling sensation on human bodies. Therefore diastereoselective synthesis of (-)-isopulegol from citronellal with the use of heterogeneous catalysts is of immense interest. For this purpose, metal fluoride based materials are investigated for this reaction.

*Suzuki carbon-carbon coupling* (Scheme 2.4) is a Pd - catalyzed cross coupling of aryl halides (or triflates) with organoborone reagents.[133] It is most widely used for the synthesis of biphenyls which are used as intermediates in organic synthesis. It is a structure sensitive reaction and the activity is strongly governed by the Pd particle size as well as its dispersion. Pd nanoparticles supported on different metal fluorides are tested for this reaction and compared with benchmark Pd/C-catalyst.

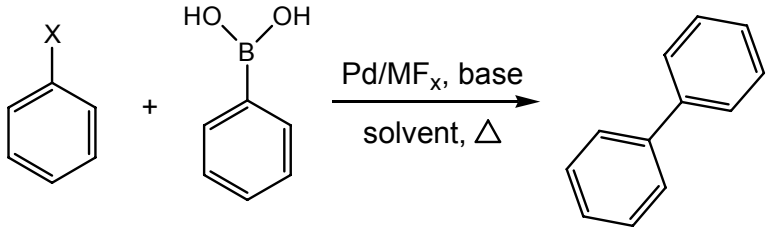


**Scheme 2.4**

*Hydrodehalogenation of chlorodifluoromethane* is an important reaction for the synthesis of CH2F2 (Scheme 2.5), which is being used as low boiling refrigerant in recent years by replacing earlier environmentally harmful CFCs and HCFCs.

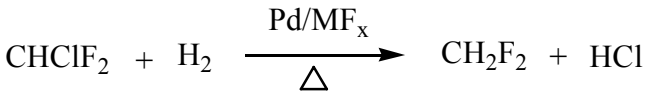


**Scheme 2.5**

Because of their chemical and thermal stabilities in corrosive atmosphere (generation of HCl and/ HF), metal fluorides supported palladium catalyst are most widely used for hydrodehalogenation.[8] For this purpose, $Pd/MF_x$-catalysts prepared by new sol-gel method are investigated. The consecutive as well as competitive reactions are also investigated for achieving high yield for $CH_2F_2$.

*Oxidative fluorination of benzene* selectively to fluorobenzene is recently reported by Subramanian and Manzer by using metal fluorides with specific redox potential ($1 > E^0 > 0$).[134] $CuF_2$ is known for this reaction, however in the present study $FeF_3$ was investigated because of its cheapness and easy regenerability. The reactions are initially carried out in batches and finally efforts are made to carry out selective benzene fluorination in continuous process by *in-situ* oxidizing the used low valent fluoride in presence of HF/oxidant flow.

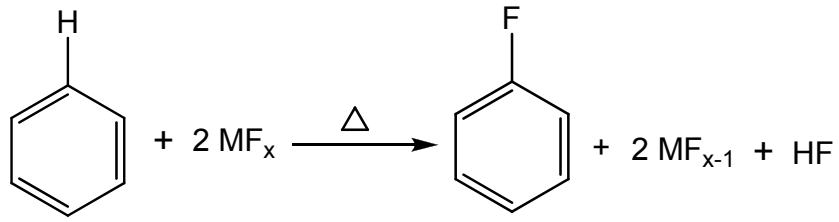


$MF_x = CuF_2$ or $FeF_3$

**Scheme 2.6**

# 2.6 Objectives of This Study

The main goal of this thesis was to explore the newly established non-aqueous sol-gel synthesis of *HS*-$AlF_3$ for other different types of fluorides such as simple binary fluorides ($MgF_2$, $CaF_2$, $FeF_3$, $CuF_2$) complex fluorides ($KMgF_3$, $K_3AlF_6$), hydroxy fluorides [$Al(OH)_xF_{3-x}$, $Mg(OH)_xF_{2-x}$], metal fluorides supported Pd nanoparticles & doped fluorides ($CuF_2/AlF_3$, $FeF_3/AlF_3$). The main intension is to study the effect of synthesis method on intrinsic and morphological properties of product materials. It is anticipated that intimate interactions between Pd and $MF_x$ ($AlF_3$) would depend on the method of preparation. This speculation prompted us to investigate the influence of different supports and different methods of synthesis on properties of support materials (crystallinity, acidity and surface area), metal particle size and dispersion on catalytic activity and selectivity.

Based on this early work, the main objectives at the start of this thesis were

- to explore new sol-gel method for the synthesis of other binary fluorides, hydroxyfluorides & complex fluorides of catalytic interest (support and/catalyst),

- to synthesize Pd nanoparticles supported on high surface area metal fluorides by introducing Pd precursor during the sol-gel synthesis,
- to compare the sol-gel method with traditional methods (aqueous & impregnation),
- to characterize the sol-gel derived materials for understanding bulk and surface properties,
- to study catalytic applications in organofluorine chemistry and in fine chemical synthesis.

# 3 SOL-GEL SYNTHESIS

## 3.1 Introduction

Metal fluorides are usually obtainable as highly ordered polycrystalline solids in accordance to their high lattice energies.[2] However, the recently developed non-aqueous sol-gel method delivers highly disordered aluminum fluoride with large surface areas.[20] Amorphous $AlF_3$ obtained by this way possessed nanoscopic, mesoporous morphologies and showed promising activities in different catalytic reactions.[20, 21]

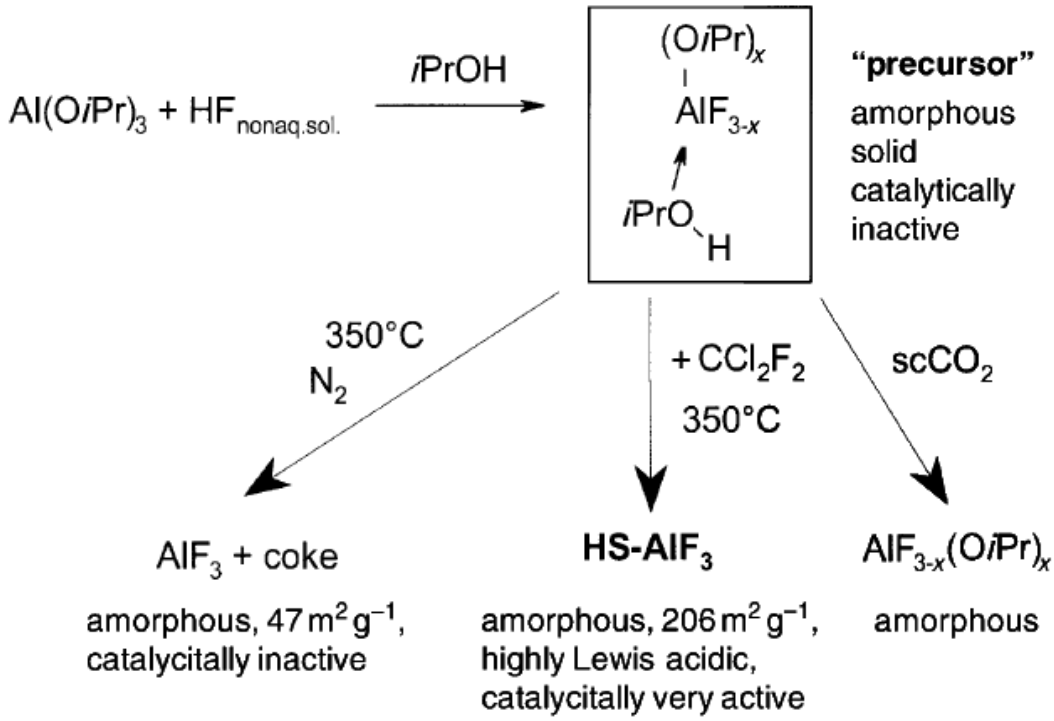


**Scheme 3.1** Route used for the synthesis of *high surface* $AlF_3$ by Kemnitz et. al.[20]

Based on this early work, the main focus was to explore this new method described for $AlF_3$ for other fluorides having different functionalities such as strongly acidic, moderately acidic, neutral, bi-acidic (Lewis and Brønsted), basic, bi-functional and redox properties. In this scenario, several materials were prepared but only some selected systems are described in this thesis. The syntheses, structural and catalytic properties of newly prepared fluorides were compared to *high surface* $AlF_3$.

# 3.2 Synthesis of Binary Fluorides ($MF_x$)

A typical sol-gel method used for the synthesis of nano-metal fluorides is briefly described below: A non-aqueous solution or suspension of a metal alkoxide was reacted with a stoichiometric amount of hydrofluoric acid dissolved in a dry solvent, which was added drop wise in the ice cold alkoxide solution. Depending upon the involved metal, alkoxide group and used solvent, a sol was immediately formed which was transformed in a gel after certain period of stirring followed by overnight ageing (~ 16h). It results into a complex development of a polymer-like network of gel structures. The gelation process strongly depends on several factors such as strength of H-bonding formed, van der Waals interaction forces, partial charge of the metal and properties of the solvent used. The gel stability is again very sensitive to different solvent properties like dielectric constant, ability to hydrogen bonding, polarity and geometric size of the molecule.

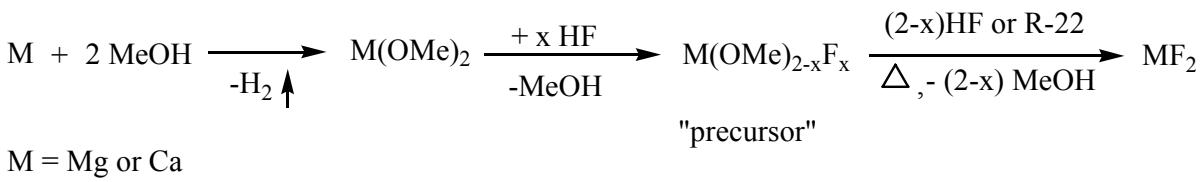


**Scheme 3.2**

The method used for the synthesis of nano-$MgF_2$ and nano-$CaF_2$ is shown in Scheme 3.2. The aged wet gel was dried under vacuum at elevated temperature, 40-70°C, depending on the solvent used, which resulted in a dry gel or a xerogel, which is ascribed as "precursor" (scheme 3.2). The precursor is a highly but not completely fluorinated material which was further post-fluorinated by gaseous HF or $CHClF_2$ (R-22) to obtain a fully fluorinated material by removing the physically and chemically bounded solvent molecule as well as non-fluorinated alkoxide groups which was evidenced by reduction of carbon content (Table 3.1). The gelation process as well as the carbon content in the final material significantly depends on the cations involved in the sol-gel process. $Al(OiPr)_3$ and $Mg(OMe)_2$ undergo a faster gelation resulting in a immediate thick gel, whereas a gel-like precipitate was formed in case of $Ca(OMe)_2$ fluorination. This leads to a different amount of carbon content in the final material. The high amount of carbon present in

$AlF_3$ precursor indicates an incomplete fluorination as well as association of solvent molecule in the polymeric network.

**Table. 3.1** Elemental analysis, BET surface area and textural properties of bulk and palladium supported metal fluorides.

| Catalyst | Elemental analysis (%)[a] | | | | $V_{BJH-d}$[b] ($cm^3/g$) | $d_{avg}$[c] ( Å ) | $S_{BET}$[d] ($m^2/g$) |
|---|---|---|---|---|---|---|---|
| | Pre. | | Post-fluor. | | | | |
| | C | H | C | H | | | |
| $AlF_3$ | 23.9 | 5.9 | 0.8 | 0.2 | 0.47 | 84 | 225 |
| $MgF_2$ | 2.3 | 1.6 | <d.l.[e] | 0.1 | 0.18 | 34 | 218 |
| $CaF_2$ | 1.8 | 0.4 | <d.l. | 0.1 | 0.39 | 132 | 118 |
| $KMgF_3$ | 2.1 | 1.1 | <d.l. | 0.0 | 0.52 | 139 | 148 |
| $Al(OH)_{1.5}F_{1.5}$ | 28.4 | 6.2 | 0.7 | 0.2 | 0.36 | 80 | 178 |
| $Mg(OH)_{0.4}F_{1.6}$ | 4.8 | 1.2 | <d.l. | 0.1 | 0.43 | 68 | 248 |

[a] -Pre.= precursors, Post-fluor.= post-fluorinated samples, [b-] BJH desorption cumulative pore volume of pores between 17 -3000 Å diameters, [c-]average pore diameter by BET, [d-] specific surface area by BET. [e] - below detection limit.

The proposed mechanism for the sol-gel synthesis of metal fluorides resembles the sol-gel synthesis of metal oxides. Principally, the sol-gel method for the synthesis of metal oxides from metal alkoxides involves acid catalyzed hydrolysis and condensation steps (Eq. 3.1). The hydroxyl groups formed after the necleophilic substitution undergo condensation reaction with -OR in a second step forming a -M-O-M- metal oxide network (Eq. 3.1).

$$\text{- M(OR)} \xrightarrow[\text{-ROH}]{H_2O} \text{- M(OH)} \xrightarrow[\text{-ROH}]{M(OR)} \text{- M-O-M-} \qquad (3.1)$$

However, in case of sol-gel synthesis of metal fluorides, hydrolysis is replaced by "fluorolysis" step. The M-F bonds formed in the first step do not undergo a three dimensional network formation because the donating solvent molecules prevent an establishment of regular $MF_6$-octahedra. That means instead of forming well crystallized metal fluorides, highly distorted nano-sized metal fluoride particles become stabilized (Eq. 3.2).

$$x\left[\text{ M(OR)}\right] \xrightarrow[\text{- x ROH}]{\text{x HF}} x\left[\text{ M-F}\right] \longrightarrow \frac{x}{2}\left[\text{—M—F—M—F—}\right] \qquad (3.2)$$

The structural and catalytic properties of the final metal fluorides are strongly determined by the synthesis method as well as the post-fluorination conditions.[2] By using $CHClF_2$ as a post-fluorinating agent one can generate moderately acidic centers even on $MgF_2$ surface,[41] a fluoride which had been prepared only as a neutral material up to now.[46] On going from precursors to catalysts, we always observe significant losses in the BET surface areas. Nevertheless, the post-treated materials (Table 3.1) possess high surface areas which are up to ten times larger than reported from other preparations for $AlF_3$,[2,49, 136] $MgF_2$,[46] and $CaF_2$.[17] The characterization results (chapter 4) have shown that the sol-gel prepared $AlF_3$ possesses extremely strong Lewis acidity, $MgF_2$ possesses moderate Lewis acidity and $CaF_2$ is neutral. The type of reagent used for post-fluorination has shown an influence on the surface area and Lewis acidity of the final material. A high surface area was obtained when HF was used and a strong Lewis acidity was generated by using $CHClF_2$ for post-fluorination.

# 3.3 Synthesis of Hydroxy- and Complex Fluorides

The properties of the above mentioned binary fluorides can be further modified by introducing -OH groups into its structure (hydroxyfluorides) or making complexes with alkali metals like Na or K (complex fluorides). By introducing -OH groups a Brønsted acidity can be generated, neutral materials like $KMgF_3$ and $K_3AlF_6$ can be obtained. The complex fluorides are formed because the cations are perfectly shielded in their structures.[137, 138] For these purposes hydroxy- and complex fluorides of aluminium and magnesium were prepared and investigated in catalysis.

In order to obtain the hydroxyfluorides, two different strategies have been used. In the first step, the fluorination of the metal alkoxide was carried out using a stoichiometric amount of HF as per the amount of -OH groups required in the final compound. The obtained precursor with a certain number of -(OR) groups was either calcined in air at higher temperature (~ 350 °C) according to Eq. 3.3a or hydrolysed using the necessary amount of $H_2O$ according to Eq. 3.3b to generate -(OH) groups in it's structure.[116, 139] However to avoid water in the system, which may decrease surface area of the final material the thermolysis approach was used for the synthesis of aluminium and magnesium hydroxyfluorides with nominal concentrations $Al(OH)_{1.5}F_{1.5}$ and $Mg(OH)_{0.4}F_{1.6}$.

$$M(OR)_x + y\ HF \longrightarrow M(OR)_{x-y}F_y \xrightarrow[\Delta]{\text{air (x-y } H_2O)} M(OH)_{x-y}F_y + x\text{-}y\ ROH \qquad (3.3a)$$

$$M(OR)_{x-y}F_y \xrightarrow{x\text{-}y\ H_2O} M(OH)_{x-y}F_y + x\text{-}y\ ROH \qquad (3.3b)$$

It was expected that $Al(OH)_{1.5}F_{1.5}$ should posses both Lewis and Brønsted acid sites, and $Mg(OH)_{0.4}F_{1.6}$ is acted as a base catalysts for Michael addition.[116] BET surface areas of $Al(OH)_{1.5}F_{1.5}$ and $Mg(OH)_{0.4}F_{1.6}$ was found to be 178 and 248 $m^2/g$ respectively (Table 3.1). Since these materials did not show any promising activities for the reaction under investigation, e.g. citronellal isomerization (see chapter 5), therefore it was not investigated in detail.

Complex fluorides, $KMgF_3$ and $K_3AlF_6$ were prepared according to Eq. 3.4 and 3.5, respectively. Even after the first fluorination step, the carbon content was very low (Table 3.1) and XRD showed formation of pure phases, nevertheless the samples were post-fluorinated with R-22 for comparison purpose.

$$KO^tBu + Mg(OMe)_2 + 3\,HF \xrightarrow{MeOH} KMgF_3 + {}^tBuOH + 2\,MeOH \qquad (3.4)$$

$$3\,KO^tBu + Al(O^iPr)_3 + 6\,HF \xrightarrow{{}^iPrOH} K_3AlF_6 + 3\,{}^tBuOH + 3\,{}^iPrOH \qquad (3.5)$$

$KMgF_3$ was found to be a neutral and a stable material used as bulk or as support for Pd and investigated in detail for its structural (Chapter 4) and catalytic properties (Chapter 5) together with the binary fluorides.

## 3.4 Synthesis of Metal Fluorides Supported Palladium Nanoparticles ($Pd^0/MF_x$)

Dissolving palladium acetylacetonate in the $MF_x$-sols leads to $Pd^{2+}$ containing $MF_x$-gels which can be converted after successive fluorination and reduction steps into $Pd^0/MF_x$-"nanocomposites". The Pd phase is scaled down to nanoparticles of about 2-5 nm, which are finely dispersed on the support-phases (10-50 nm $MF_x$-particles). For this purpose, the well established sol-gel method for preparation of *high surface* $AlF_3$[20] has been modified in such a way, that the introduction of additional components like Pd into the colloidal system during the synthesis does not significantly influence the bulk and surface properties of the resulting gel: it is comparable to a gel from pure metal fluorides but it contains already the palladium precursor in a highly dispersed state. It is of eminent importance to control the colloidal properties of the system (sol and gel formation, coagulation, peptisation etc.) by optimizing the reaction conditions (temp, stirring rate, type and amount of solvents) during the first fluorination step. At this stage, the -OR against -F exchange results in the formation of a viscous sol, which coagulates on further stirring to a three dimensional network of a polymeric semi-solid gel, the so called "wet gel". After ageing and vacuum drying a solid dry gel, so called "precursor", was obtained. The post fluori-

nation of the dry gel is necessary to exchange remaining -OR groups by -F in order to get a fully fluorinated, Lewis acidic catalyst.[4, 5] The final $H_2$-treatment aimed the reduction of $Pd^{II}$ and – as has been proven by XRD (Chapter 4, Fig. 4.8) but especially by TEM measurements (Chapter 4, Fig. 4.16) resulted in the formation of the Pd-metal (no further indication for any $PdF_2$ or $PdCl_2$).

**Table. 3.2** Elemental analysis, BET surface area and textural properties of bulk and palladium supported metal fluorides.

| Catalyst | Elemental analysis (%)[a] | | | | | | $V_{BJH\text{-}d}$[b] ($cm^3/g$) | $d_{avg}$[c] ( Å ) | $S_{BET}$[d] ($m^2/g$) |
|---|---|---|---|---|---|---|---|---|---|
| | Pre. | | Post-fluor. | | AR | | | | |
| | C | H | C | H | C | H | | | |
| $Pd^0/AlF_3$-R22 | 25. | 5.5 | 1.8 | 0.3 | 1.6 | 0.4 | 0.33 | 125 | 106 |
| $Pd^0/MgF_2$-R22 | 3.7 | 1.9 | 1.4 | 0.1 | 1.4 | 0.4 | 0.16 | 83 | 78 |
| $Pd^0/CaF_2$-R22 | 4.9 | 1.5 | 1.3 | 0.2 | 1.2 | 0.2 | 0.27 | 185 | 59 |
| $Pd^0/KMgF_3$-R22 | 6.1 | 1.5 | <d.l. | 0.2 | <d.l. | 0.2 | 0.52 | 205 | 100 |
| $Pd^0/AlF_3$-HF | 21 | 5.0 | 2.4 | 1.7 | 1.6 | 1.4 | 0.29 | 97 | 115 |
| $Pd^0/MgF_2$-HF | 3.8 | 1.9 | 2.3 | 1.4 | 1.2 | 0.6 | 0.85 | 46 | 225 |
| $Pd^0/CaF_2$-HF | 7.2 | 1.4 | 1.5 | 1.0 | 1.3 | 0.5 | 0.22 | 307 | 118 |
| $Pd^0/CaF_2$-aq | 4.1 | 1.6 | <d.l. | 0.4 | <d.l. | 0.2. | 0.29 | 319 | 37 |
| $Pd^0/CaF_2$-imp | 4.8 | 1.0 | - | - | <d.l. | 0.2 | 0.55 | 358 | 62 |
| $Pd^0/Ca(OH)_{0.5}F_{1.5}$ | 8.4 | 1.7 | - | - | 1.5 | 0.8 | 0.45 | 200 | 90 |

[a] -Pre.= precursors, Post-fluor.= post-fluorinated samples, AR= after reduction. [b-] BJH desorption cumulative pore volume of pores between 17 - 3000 Å diameters, [c-]average pore diameter by BET, [d-] specific surface area by BET. [e] - below detection limit.

The elemental analysis of these precursors revealed significant amounts of carbon (17.7-27.3 %) and hydrogen (4.8-6.1%) with varying values within the different metal fluoride supports (Table 3.2). The carbon content is mainly due to strongly adsorbed alcohol (solvent) as well as remaining unconverted alkoxide groups at the metal as has been already shown.[20] The surface areas and the Lewis acidic properties of the final catalysts depend on the synthesis parameters, like type of alkoxides and solvents, molar ratios, time of ageing and post fluorination conditions.[98, 140] For the synthesis of $Pd^0/KMgF_3$, toluene was used as solvent instead of $CHCl_3$ for dissolution of $Pd(acac)_2$ because in the presence of $CHCl_3$, $KO^tBu_4$ reacted vigorously with formation of KCl, which was confirmed by XRD (not shown). The BET surface area, pore volume, pore diameter and elemental analysis data of the metal fluoride supported palladium catalysts together with the data of the corresponding "sol-gel"-derived bulk metal fluorides are summarized in Table 3.2.

The carbon and hydrogen contents of the precursors are quite high, indicating the presence of organics (adsorbed ROH and $RO^-$). Thus after the gas phase post-fluorination by $CHClF_2$, the organic is completely removed as evidenced by elemental analysis (Table 3.2). The pore diameters are between 83 and 205 Å typical for mesoporous materials. In case of supported Pd catalysts, the pore volumes are 28-56% smaller as those of the bulk metal fluoride materials. This decrease in pore volumes might be taken as a hint for the incorporation of Pd nanoparticles inside the pores of the metal fluoride matrices. This is in line with the observed decrease in surface areas on going from $MF_x$ to $Pd^0/MF_x$ (Table 3.1 and Table 3.2) as well as the homogeneous distribution of Pd on the support as evidenced by TEM images. BET surface area of these $Pd^0/AlF_3$ and $Pd^0/MgF_2$ is very high compared to those by earlier methods.[38]

The samples prepared by the sol-gel method followed by post-fluorination with $CHClF_2$ and HF are indicated as $Pd^0/MF_x$-R22 and $Pd^0/MF_x$-HF, respectively (Table 3.2). $Pd^0/CaF_2$-aq was prepared by using 40 % aqueous HF for the first step of fluorination instead of anhydrous HF dissolved in organic solvents followed by usual post-fluorination with HF and reduction. $Pd^0/CaF_2$-imp was prepared by impregnation of $CaF_2$; the procedure involved preparation of *high surface area* $CaF_2$ by our sol-gel method (post-fluorinated samples with BET of 99 $m^2/g$), followed by impregnation with $Pd(acac)_2$ dissolved in $CHCl_3$ and additionally $H_2$ reduction of the vacuum dried samples. $Pd^0/Ca(OH)_{0.5}F_{1.5}$ was prepared by fluorination of a methanolic solution of $Ca(OCH_3)_2$ and $Pd(acac)_2$ with 1.5 equivalents of HF, thus leading to a nominal composition $[Pd^0/CaF_{1.5}(OH)_{0.5}]$. After removal of the solvent, the sample was calcined at 350 °C in air atmosphere and additionally reduced at 200 °C by hydrogen.

The Pd content was adjusted in all catalysts to 5 wt%. All samples were fully characterized by various analytical techniques. Post-fluorination with gaseous HF occurs at low temperature (100-120 °C) and the samples obtained possess very high surface areas. On the other hand, strong acidic centers were generated after the post-fluorination at 250-300°C with fluorocarbons such as $CHClF_2$ (R-22).[100] Although XPS and thermal analysis have shown that the alcoholic residues - bound physically and/or chemically - are acting as reducing agents during the post-fluorination step, to ensure the complete reduction, the samples have to be reduced by $H_2$ at 200 °C. This low reduction temperature prevents Pd-sintering, preserving the former homogeneous distribution of "$Pd^{x+}$" also after its conversion into $Pd^0$, thus, leading to highly dispersed nanoparticles on the support.[135]

# 3.5 Synthesis of Iron and Copper based Binary and Host-Guest Fluorides

Fluorides of iron and copper are of interests because of their redox potential, suitable for selective fluorination of benzene.[134] The sol-gel method was further employed for the synthesis of $FeF_3$ and $CuF_2$ based binary as well as host-guest type redox fluorides. So far there is no report for the synthesis of $FeF_3$ and $CuF_2$ via sol-gel method. Krishnamurthy et. al. have prepared $FeF_3/MgF_2$, however apparently no real evidence for the formation of $FeF_3$ was given.[36] The sol-gel method used for these materials is similar to that of binary fluorides. Since alkoxides of copper are not commercially available and iron alkoxides are very expensive therefore corresponding acetylacetonates e.g., $Fe(acac)_3$ and $Cu(acac)_2$, were used as precursors for the synthesis of $FeF_3$ and $CuF_2$ respectively. The fist step fluorination resulted in a precursor (Eq. 3.6) which was post-fluorinated under different environments in subsequent step.

$$Fe(acac)_3 + 3\,HF \xrightarrow{CH_3OH} \underset{\text{"precursor"}}{FeF_{3-x}(acac)_x} + 3\text{-}x\ Hacac \qquad (3.6)$$

The HF post-fluorination at elevated temperature, at 400°C, led to the formation of $FeF_2$ instead of the desired $FeF_3$, therefore fluorination was carried out using different oxidizing environments such as $O_2$/HF, $Cl_2$/HF, $F_2$ to avoid the reduction of $Fe^{3+}$ to $Fe^{2+}$. The samples are denoted in accordance to the fluorinating reagent used (Scheme 3.4).

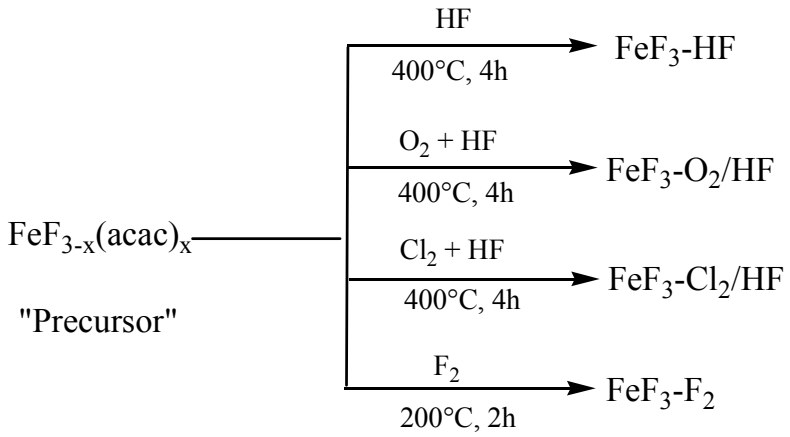


**Scheme 3.4** Post-fluorination of $FeF_{3-x}(acac)_x$ with various fluorinating agents.

Copper fluorides and host-guest fluorides ($FeF_3/AlF_3$ and $CuF_2/AlF_3$) were prepared similarly. The post-fluorination was successful with HF for copper samples. The higher

carbon content even after the high temperature post-fluorination clearly indicates that the -acac ligends are difficult to remove completely from the "precursor" even with the strong fluorinating agent $F_2$. XRD results (Fig. 4.10) showed the formation of $FeF_2$ in $FeF_3$-HF sample and weak reflections corresponding to $FeF_3$ were found in $FeF_3$-HF/$O_2$ and $FeF_3$-HF/$Cl_2$. The formation of $FeF_3$ was clearly observed in $FeF_3$-$F_2$ sample.

**Table. 3.3** Elemental analysis, BET surface area and textural properties of iron and copper based redox fluorides.

| Catalyst | Elemental analysis (%) | | $V_{BJH}$[a] | $d_{avg}$[b] | $S_{BET}$[c] |
|---|---|---|---|---|---|
| | C | H | ($cm^3/g$) | (Å) | $m^2/g$ |
| $FeF_3$-HF | 1.8 | 0.8 | 0.33 | 118 | 113 |
| $FeF_3$-HF/$O_2$ | <d.l.[d] | 0.4 | 0.27 | 362 | 31.1 |
| $FeF_3$-$Cl_2$/HF | 3.5 | 1.4 | 0.02 | 77.1 | 12.2 |
| $FeF_3$-$F_2$ | 2.6 | 0.6 | 0.24 | 91.4 | 97.6 |
| $FeF_3$/$AlF_3$-$F_2$ | 2.2 | 0.4 | 0.31 | 197 | 62.9 |
| $CuF_2$-HF | 1.6 | 0.4 | 0.06 | 161 | 15.6 |
| $CuF_2$/$AlF_3$-HF | 1.8 | 0.3 | 0.52 | 323 | 93.2 |

[a]-BJH desorption cumulative pore volume of pores between 17 - 3000 Å diameters, [b]-average pore diameter by BET, [c]- specific surface area by BET. [d] - below detection limit.

The test reactions showed that $FeF_3$-$F_2$ and $CuF_2$-HF have the potential for oxidative fluorination of benzene, further the activity was increases in host-guest fluorides (Chapter 5, section 5.5).

# 3.6 Summary

In summary, the new sol-gel method was successfully implemented for a wide variety of materials such as binary fluorides ($MgF_2$, $CaF_2$), hydroxy fluorides [$AlF_{3-x}(OH)_x$, $MgF_{2-x}(OH)_x$], complex fluorides ($KMgF_3$ and $K_3AlF_6$), metal fluorides supported Pd nanoparticles (Pd/$AlF_3$, Pd/$CaF_2$ etc) and $FeF_3$ and $CuF_2$ based binary and host-guest ($FeF_3$/$AlF_3$ and $CuF_2$/$AlF_3$) fluorides. The sol-gel derived fluorides have shown very high surface areas, nanoscopic distinctly different structural and catalytic properties compared to the materials prepared by conventional aqueous fluorination and impregnation methods. More details about the structural characterization and the catalytic properties of the materials described here are given in chapter 4 and chapter 5, respectively.

# 4 CHARACTERIZATION

The metal fluorides based samples prepared by using new sol-gel method (chapter 3) were characterized by different methods to understand their bulk and surface properties. Among the samples prepared and investigated for catalytic properties (Chapter 5), few of them which have shown better catalytic potential were chosen for characterization. In this chapter, characterization of binary fluorides (including $KMgF_3$ complex fluoride) (Section 4.1), metal fluorides supported Pd nanoparticles (Section 4.2), and iron and copper based fluorides (Section 4.3) is described.

## 4.1 Characterization of Binary Fluorides

In this section, characterization of sol-gel prepared $AlF_3$, $MgF_2$ and $CaF_2$ based binary fluorides is discussed. Additionally, the ternary $KMgF_3$ based complex fluoride which was used as neutral support for Pd has also included for comparison purpose.

### 4.1.1 X-ray diffraction

X-ray diffraction was carried out to study phase purity and crystallinity. XRD of precursors as well as post-fluorinated samples obtained via sol-gel synthesis (chapter 3) is shown in Fig 4.1. The precursor and post-fluorinated $AlF_3$ samples are amorphous in nature whereas reflections corresponding to microcrystalline $MgF_2$, $CaF_2$ and $KMgF_3$ are found in respective precursors and post-fluorinated samples. The broad reflections of the precursors are transformed into more crystalline after post-fluorination, which can be very clearly seen in case of $MgF_2$. Since the carbon content in $CaF_2$ (1.8 %) and $KMgF_3$ (2.1 %) precursors was low this effect was not observed in these samples.

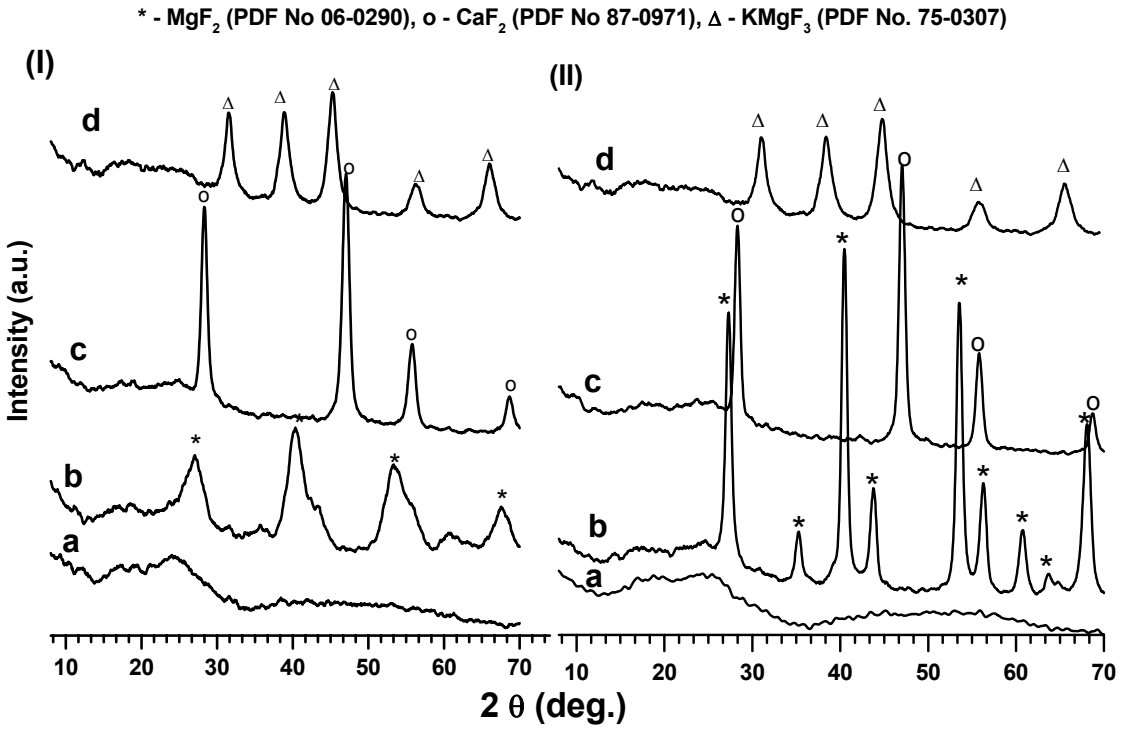


**Fig. 4.1** XRD patterns of $AlF_3$ (a), $MgF_2$ (b), $CaF_2$ (c) and $KMgF_3$ (d) based precursors (I) and post-fluorinated samples (II).

The amorphous nature of $AlF_3$ and the broad XRD-reflection in other samples show high degree of distortion in their structures which was further supported by solid state MAS-NMR measurements (Section 4.1.2).

## 4.1.2 Solid state MAS NMR spectroscopy

The local environment of fluorine and aluminium species in binary fluorides has been investigated by MAS NMR spectroscopy. $^{19}F$ and $^{27}Al$ MAS NMR spectra of an $AlF_3$ precursor and a post fluorinated sample recorded with spinning speed of 25 kHz is given in Fig 4.2. Chupas et. al[141] and König et. al.[142] developed a partial chemical shift scales for $^{19}F$ depending on its environment (fluorine and oxygen). The analysis of the fluorine signal of the precursor compound is given by König et. al.[142] The position of the signal a mixed fluorine/oxygen coordination of aluminium. The chemical shift of highly ordered crystalline α-$AlF_3$ is known to occur at $\delta_F$ = -172 ppm and $\delta_{Al}$ = -16 ppm in $^{19}F$ and $^{27}Al$ MAS NMR spectroscopy respectively.[141] However in the present case the post-fluorinated $AlF_3$ shows for $^{19}F$ a chemical shift value which is slightly high field ($\delta_F$ = -168.3 ppm), which corresponds to a mean $AlF_5O$ coordination in the sample. This change in the chemical shift is clearly due to the presence of high distortion in $AlF_3$ structure. $AlF_{3-x}(O^iPr)_3$ has shown a chemical shift at lower field ($\delta_F$ = -161.1 ppm) in compari-

son to post-fluorinated sample which is due to the presence of -(OiPr) groups coordinated to Al.

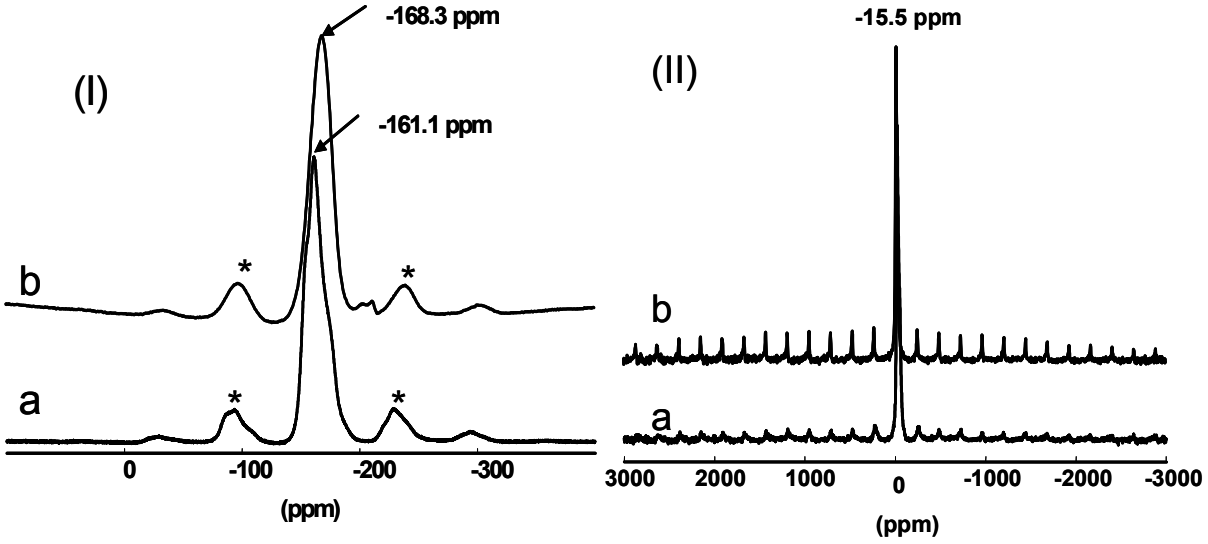


**Fig. 4.2** $^{19}F$ (I) and $^{27}Al$ (II) MAS NMR spectra of precursors (a) and post fluorinated (b) $AlF_3$ samples at a spinning frequency of 25 kHz.

The -(OiPr) groups were completely removed after post-fluorination leading to a completely fluorinated and highly distorted $AlF_3$. The chemical shift of $\delta_{Al}$ = -15.5 ppm observed in $^{27}Al$ MAS NMR spectra of precursor as well as post-fluorinated sample is typical for octahedrally coordinated aluminium $(AlF,O)_6$ octahedra with high F content (Fig 4.2, II).[143]

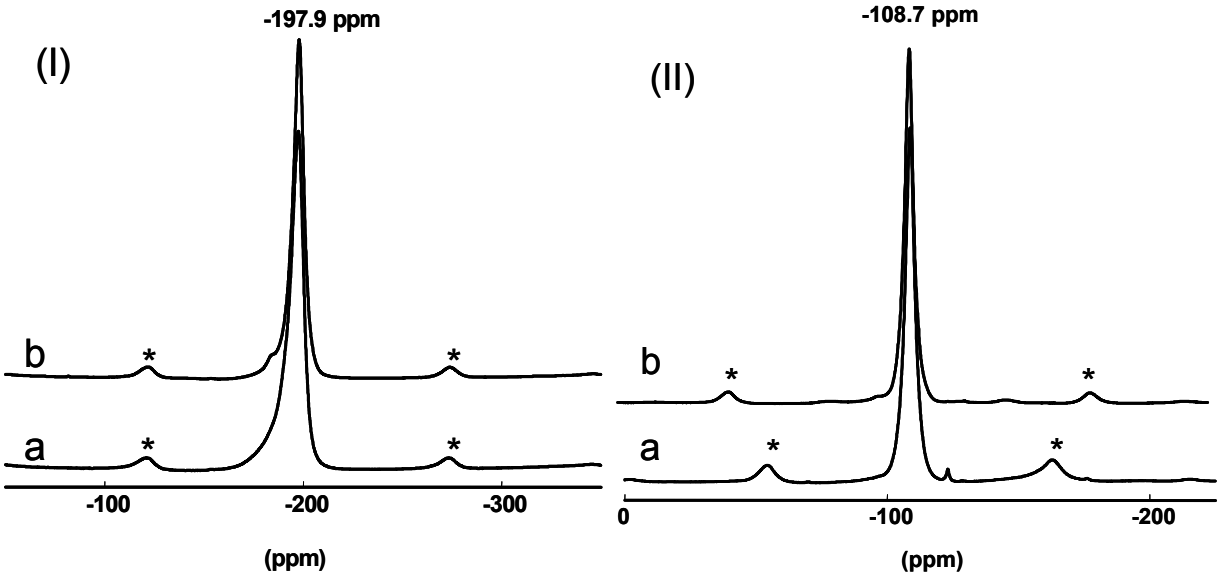


**Fig. 4.3** $^{19}F$ MAS NMR spectra of precursors (a) and post fluorinated (b) of $MgF_2$ (I) and $CaF_2$ (II) samples at a spinning frequency of 25 kHz.

The large number of side bands arises, even at spinning speed of 25 kHz from the $^{27}Al$ satellite transition and indicates large quadrupole coupling constants (QCC) and a highly distorted aluminium environment[144] Neither tetrahedral ($\delta_{Al}$ = - 50-80 ppm) nor fivefold coordinated ($\delta_{Al}$ = - 25-35 ppm) aluminium species were detected by NMR spectroscopy. Similarly, $^{19}F$ MAS NMR spectra of $MgF_2$[145, 140] and $CaF_2$[145, 42] both of precursor and post-fluorinated sample have shown a signal with chemical shift values at -197.9 ppm and -108.7 ppm characteristic of respective fluorides (Fig 4.3). The precursor as well as the post-fluorinated material has shown the same value indicating a high degree of fluorination of $MgF_2$ and $CaF_2$ taking place already at precursor stage.

### 4.1.3 FTIR photoacoustic spectroscopy with pyridine adsorption

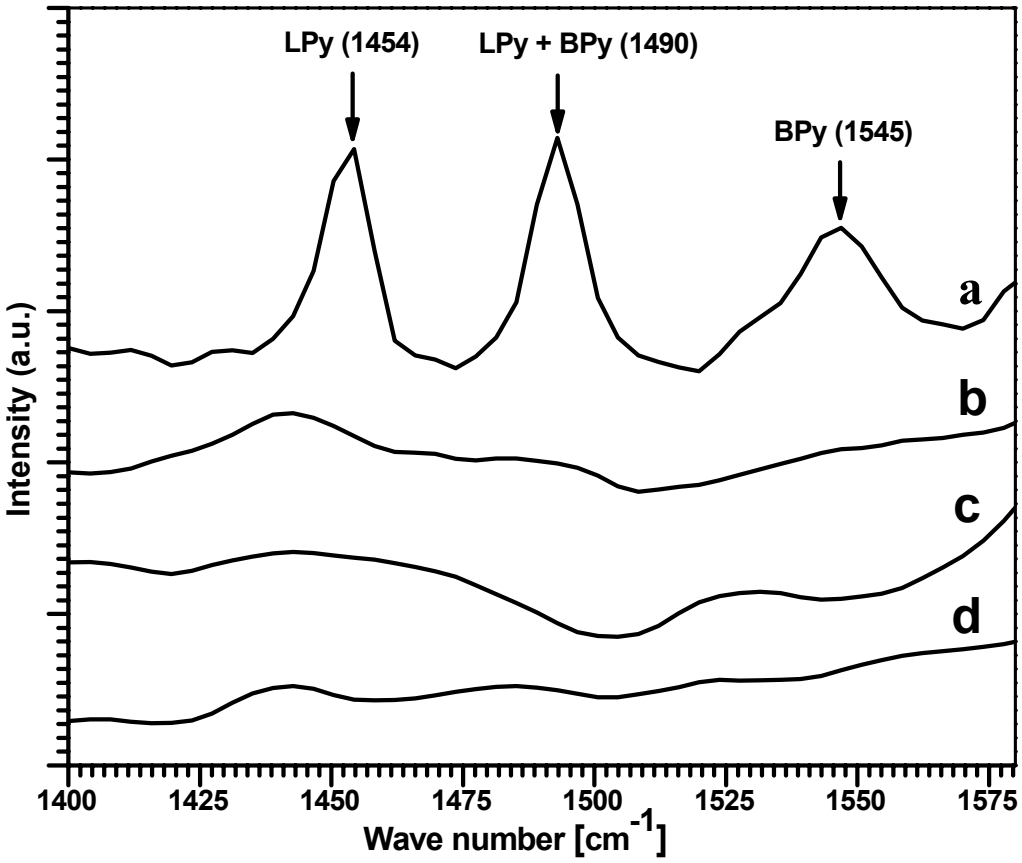


**Fig. 4.4** FTIR photoacoustic spectra of pyridine chemisorption of binary- and complex fluorides (a = AlF3, b = MgF2, c = CaF2 and d = KMgF3).

FTIR photoacoustic spectroscopy (FTIR-PAS) was employed for characterizing the acid sites of binary fluorides by using pyridine (pKa = 5.25) as a basic probe molecule. Figure 4.4 shows FTIR-PAS spectra of $MF_x$-samples. The vibration bands at 1451 ($\upsilon_{19b}$), 1490 ($\upsilon_{19a}$) and 1610 $cm^{-1}$ ($\upsilon_{8a}$) are characteristic for pyridine coordinated on Lewis acid sites (Lpy) and at 1490 ($\upsilon_{19b}$), 1540 ($\upsilon_{19a}$) and 1640 ($\upsilon_{8a}$) on Brønsted acid centers (BPy).[146]

$AlF_3$ has shown the presence of both Lewis and Brønsted acid sites. There was no pyridine adsorption observed on $MgF_2$, $CaF_2$ and $KMgF_3$ samples. However further investigations on acidity by $NH_3$-TPD (discussed below) and dismutation reactions (Section 5.4) have shown that $MgF_2$ posses moderate acid centers.

### 4.1.4 Temperature programmed desorption of ammonia ($NH_3$-TPD)

To study strength of acid sites and their distribution $NH_3$-TPD was carried out. A typical $NH_3$-TPD profile of binary fluorides is shown in Fig 4.5.

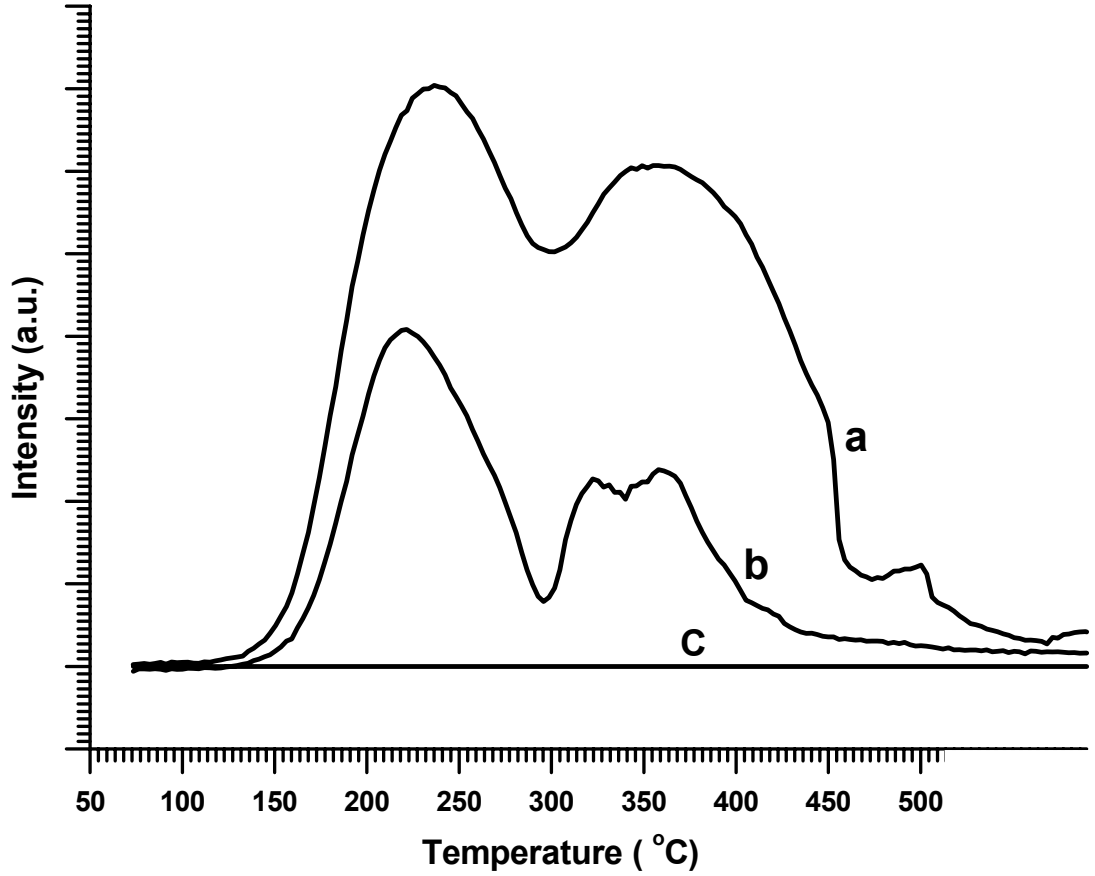


**Fig. 4.5** $NH_3$-TPD of binary fluorides (a = $AlF_3$, b = $MgF_2$ and c = $CaF_2$).

The peak maxima at low temperatures (100-300 ºC) correspond to weak acidic sites; the higher the desorption temperature is the stronger the sites are (300-425 ºC -strong acid sites). The $NH_3$-desorption on $AlF_3$ and $MgF_2$ systems occurred upto 475 and 400 ºC, indicating the presence of strong and moderate acidic sites, respectively. Pure $CaF_2$ did not show adsorption of $NH_3$. The acid strength determined from the amount of $NH_3$ desorbed was 0.899 mmol/g for $AlF_3$, 0.275 mmol/g for $MgF_2$ and 0.0 mmol/g for $CaF_2$. This clearly indicates the presence of strong acidic centers in $AlF_3$ prepared by new sol-gel method

### 4.1.5 Scanning electron microscopy (SEM)

Surface morphology of the binary fluorides and complex fluorides was investigated by SEM (Fig. 4.6).

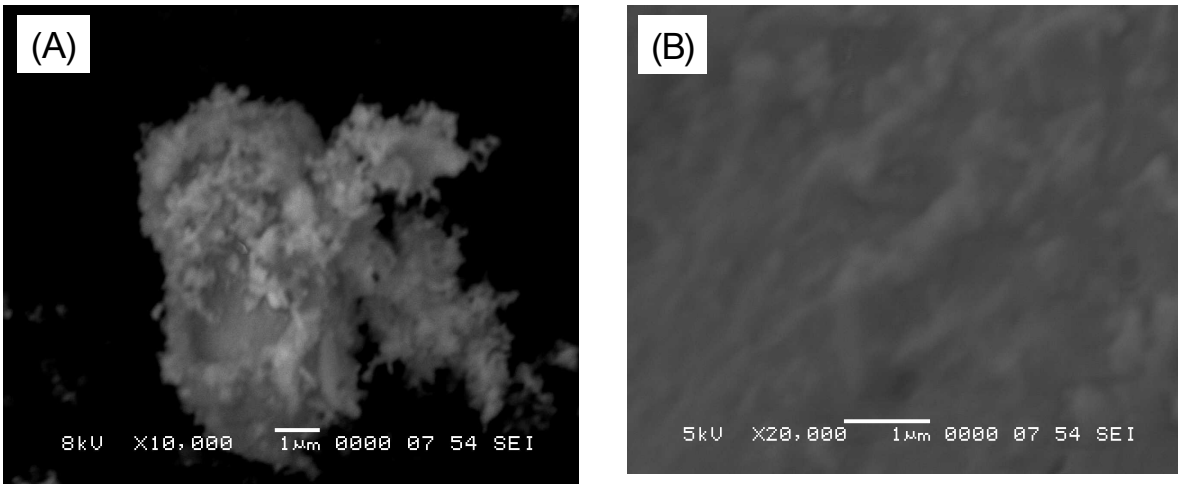


**Fig. 4.6** SEM Image of $CaF_2$ (A) and $KMgF_3$ (B) samples

Typical SEM image of $CaF_2$ (Fig. 4.6A) shows an agglomerated structure of highly porous nature. The SEM image of $KMgF_3$ (Fig. 4.6B) shows a flat and smooth surface even at higher resolution (1µm).

## 4.2 Characterization of Metal Fluorides Supported Pd Nanoparticles

### 4.2.1 X-ray diffraction

In Figure 4.7 the X-ray diffraction patterns of the products in course of the synthesis of metal fluorides supported Pd catalysts are shown. Additionally, the XRD of pure $MF_X$ are included for comparisons. The characteristic diffractograms clearly depict the changes occurring on Pd during the steps of the catalyst preparation. Although the diffractograms of the precursor before and after gas phase fluorination have many features in common, there are some minor differences which need to be discussed. It is obvious that for some samples reflections at low 2 theta-values ($2\theta$ = 11.5, 12.3°) are present which disappear after gas phase fluorination and hydrogen treatment. These can clearly be ascribed to palladium acetylacetonate [PDF No. 55-1251] which was used as $Pd^{II}$ precursor. It is obvious that they disappeared as a result of hydrogen treatment. Moreover, the weak reflection at $2\theta$ = 46.6° in case of the $Pd^0/MgF_2$ and at $2\theta$ = 40.1° in case of $Pd^0/MgF_2$ sample

is indicative for the presence of $Pd^0$ [PDF No. 46-1043], however, obviously with a lower dispersion than in the other samples.

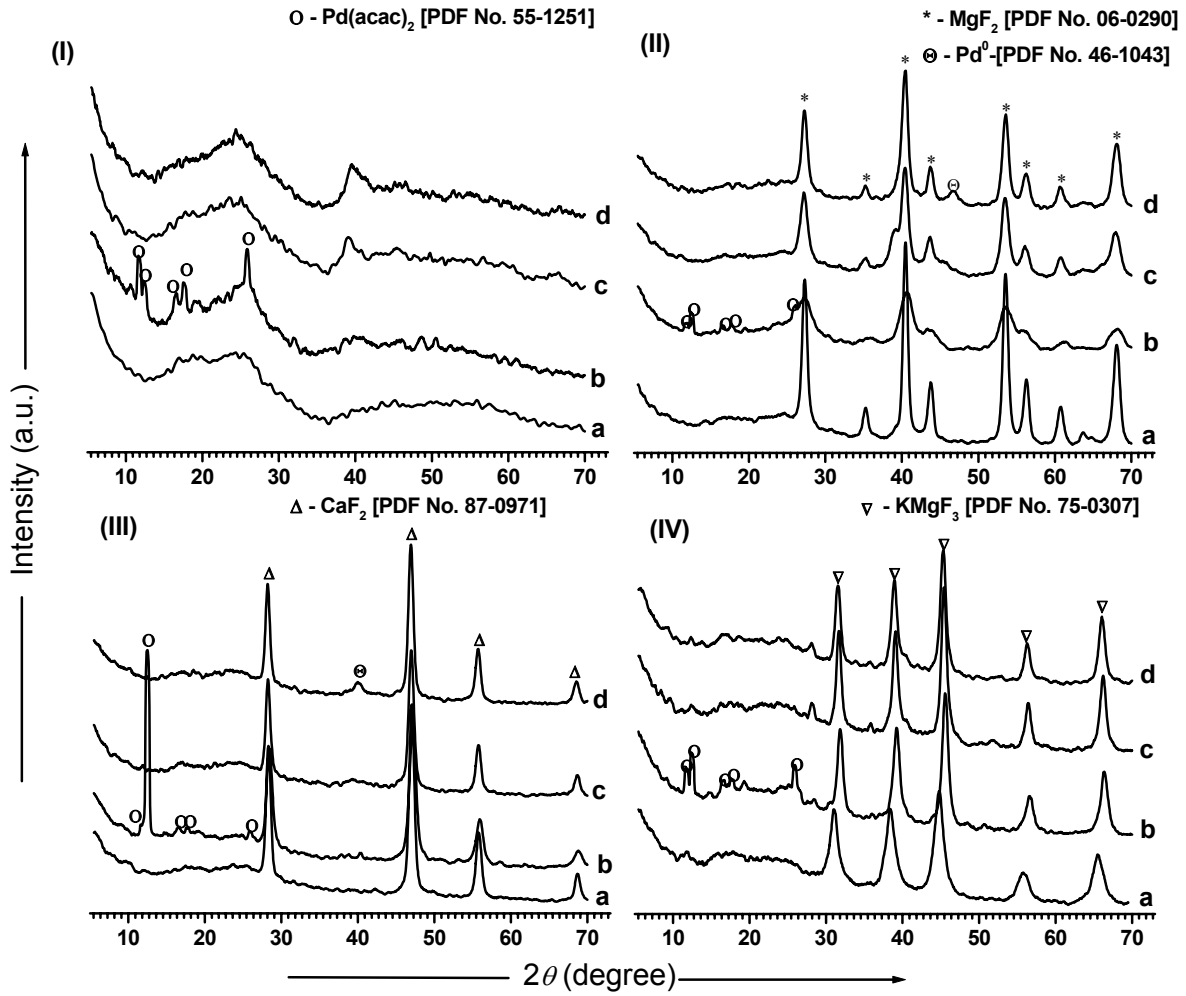


**Fig. 4.7** XRD patterns of $AlF_3$ (I), $MgF_2$ (II), $CaF_2$ (III) and $KMgF_3$ (IV) based catalysts. (a) - pure $MF_x$-supports, (b) - $Pd^{II}/MF_{x-y}(OR)_y$-precursors, (c) - $Pd^{II}/MF_x$-post-fluorinated with $CHClF_2$ and (d) - $Pd^0/MF_x$-reduced samples.

An effect of different supports as well as different preparation methods on Pd dispersion and catalytic activity in Suzuki coupling (Section 5.3) was studied. Reflections of various intensities, corresponding to $Pd^0$ were observed in the XRD pattern of $Pd^0/CaF_2$ samples prepared by different methods (Fig. 4.8, curves d-f). Interestingly enough, by comparing the intensities and widths of Pd (111) reflections at $2\theta = 40.1°$ one can clearly recognize the better dispersion of Pd-nanoparticles in case of using non-aqueous HF in the sol-gel synthesis ($Pd^0/CaF_2$-HF and $Pd^0/CaF_2$-R-22) compared to the samples prepared by aqueous HF ($Pd^0/CaF_2$-aq) fluorination and impregnation ($Pd^0/CaF_2$-imp).

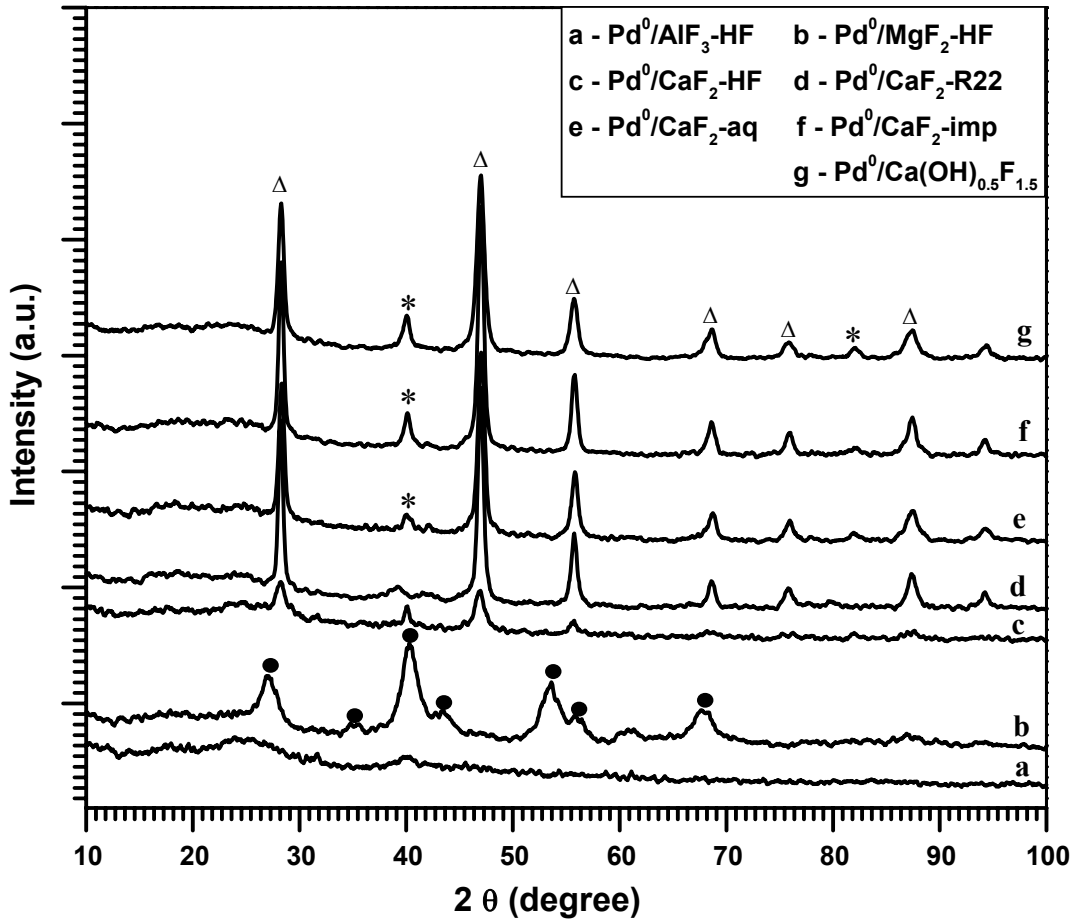


**Fig. 4.8** XRD patterns of metal fluorides supported palladium nanoparticles prepared using different synthesis conditions. ∗ - Pd (PDF No. 46-1043), □ - $CaF_2$ (PDF No. 87-0971), • - $MgF_2$ (PDF No. 06-0290).

## 4.2.2 Thermal analysis coupled with mass spectrometry (TA-MS)

In order to get more insight into the reaction path during the Pd incorporation and understand the thermal behavior of the system, thermal analysis (TA) coupled with mass spectrometry (MS) investigations have been performed. Fig 4.9 presents the TA-MS curves of a $Pd^{II}/AlF_{3-x}(OiPr)_x$ catalyst precursor (25.6 % C and 5.5 % H) which shows the main processes during the catalyst formation. The TG curve exhibits a single step gradual weight loss of 23.7 % up to 520 °C due to the loss of water and physically and chemically bonded organic moieties as confirmed by MS. The DTA curve shows exothermic peaks at 83, 134 and 545 °C which are caused by the reduction of $Pd^{II}$ to $Pd^0$ by $H_2$, decomposition of -(OiPr) group and crystallization of aluminum fluoride, respectively. The decomposition of the remaining alkoxide at 134 °C is evidenced by the mass number 43 ($C_3H_7$) (Fig. 4.9) but the fact that it occurs exothermic is somehow unexpected. Probably the

exothermic effect is due to $H_2$ gas used here which may result in the parallel formation of $H_2O$.

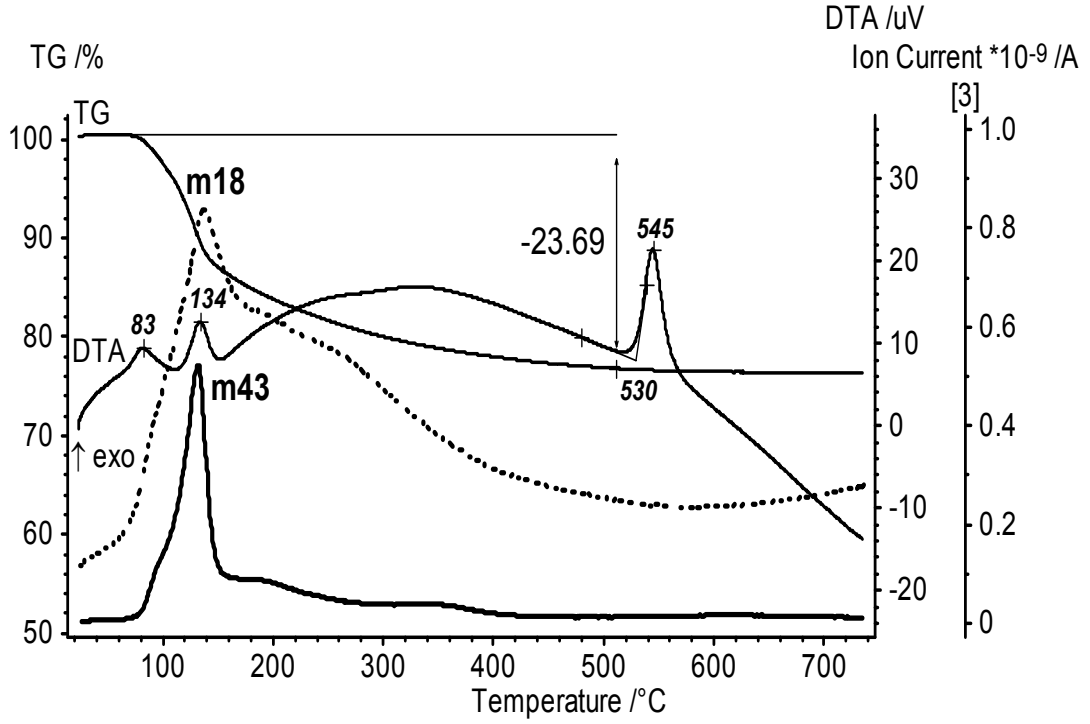


**Fig. 4.9** TA-MS analysis of $Pd^{II}/AlF_{3-x}(OiPr)_x$ catalyst precursor with IC curves for *m/z* 18 for ($H_2O^+$) and *m/z* 43 ($CH_3CO^+$).

The thermal behavior of the $Pd(II)/AlF_{3-x}(OiPr)_x$ system is very similar to that of $AlF_{3-x}(OiPr)_x$ except the observed lowering of crystallization temperature of *HS*-$AlF_3$ (546 against 563)[21] and the occurrence of acetyl ($CH_3CO^+$) fragment stemming from $Pd(acac)_2$ in the precursor matrix indicating the incorporation of acetylacetonate into the gel.

## 4.2.3 $N_2$ adsorption-desorption and BJH pore size distribution

$N_2$ adsorption-desorption profiles of $Pd^0/MF_x$-HF catalyst have been shown in Fig. 4.10. $Pd/AlF_3$ shows type IV nitrogen adsorption isotherm with the characteristic H1 hysteresis at around 0.6-09. The hysteresis loop formed is due to the capillary condensatation within mesopores and is indicative of well ordered uniform shape and size of mesopores. The sharp adsorption increase at higher pressure and the one step capillary condensation indicate the presence of large and uniform mesopores, respectively.[147] $Pd^0/MF_x$-catalysts further differ in their structural morphologies and textural properties as can be seen from BJH pore size distribution (Fig. 4.11). $Pd^0/AlF_3$-HF and $Pd^0/MgF_2$-HF samples possess narrow and unimodal pore size distributions with an average pore diameter of 98 and 40

Å, respectively. On the other hand, broad and bimodal distribution of pores with diameters between 300 and 400 Å was observed in $Pd^0/CaF_2$-HF, indicating the presence of meso- as well as macropores.

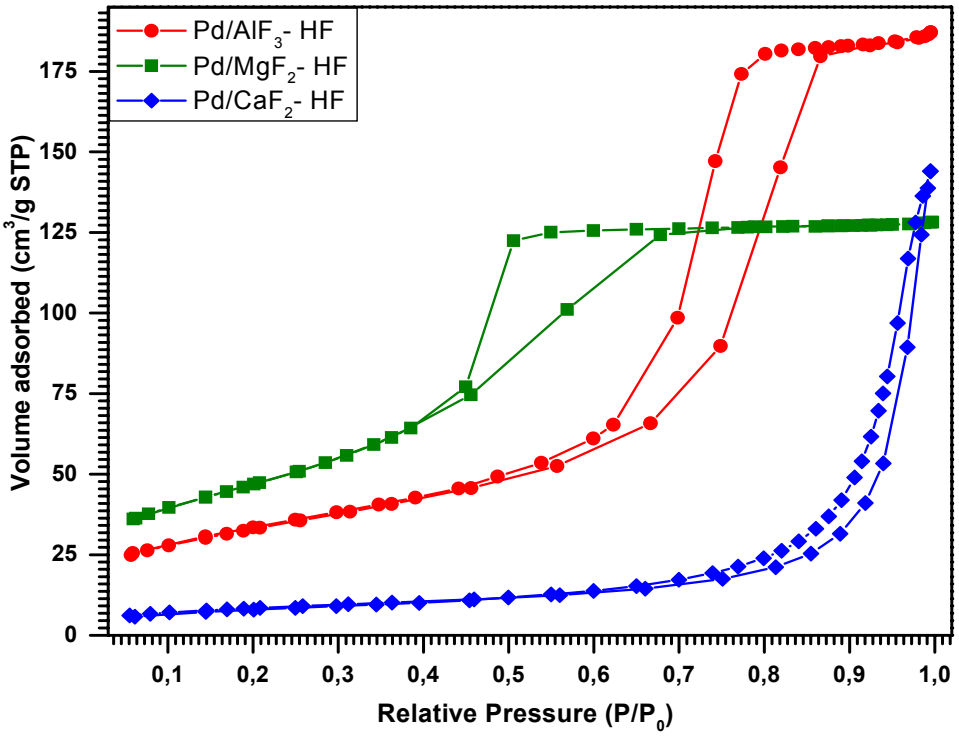


**Fig. 4.10** $N_2$ adsorption-desorption profile of $Pd^0/MF_x$ catalysts

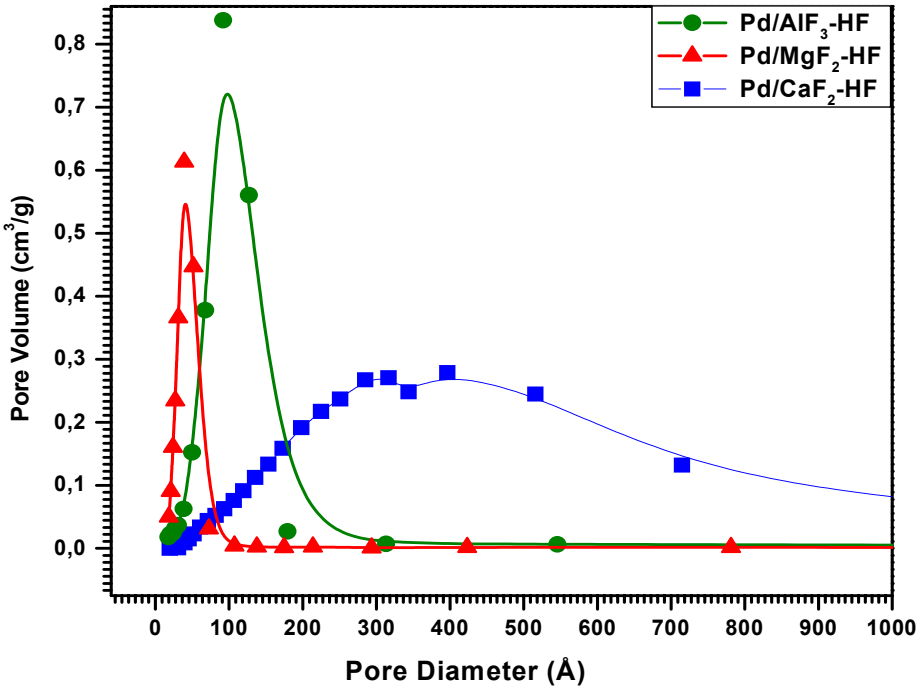


**Fig. 4.11** BJH pore size distributions of $Pd^0/MF_x$ Catalysts.

### 4.2.4 FTIR photoaucoustic spectroscopy with pyridine adsorption (FTIR-PAS).

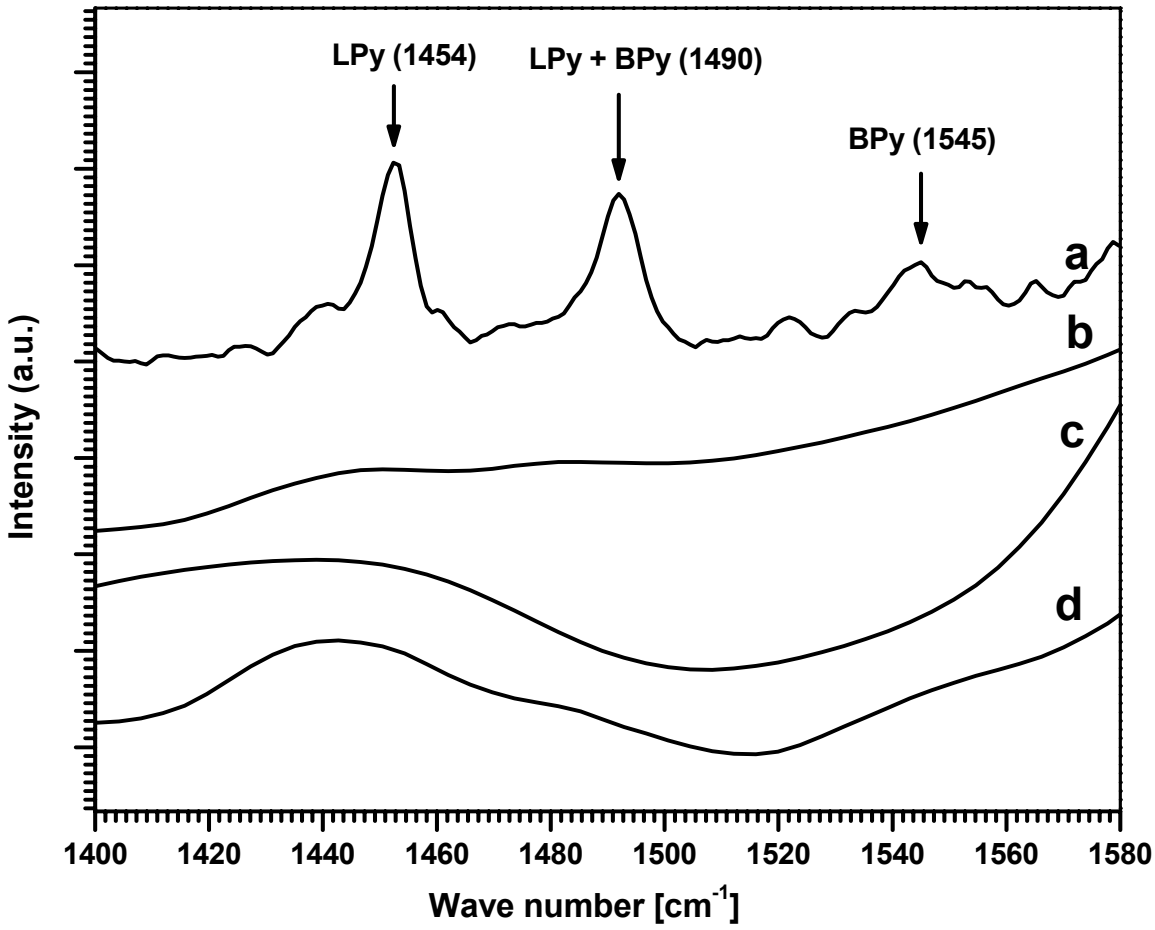


**Fig. 4.12** FTIR photoacoustic spectra of pyridine chemisorption of $Pd^0MF_x$ (a = $Pd^0/AlF_3$, b = $Pd^0/MgF_2$, c = $Pd^0/CaF_2$ and d = $Pd^0/KMgF_3$) samples.

FTIR spectra confirm that the incorporation of Pd does not influence significantly the acidic properties of $MF_x$ supports (Fig. 4.12). Especially in case of the $AlF_3$-system, both pure $AlF_3$ and $Pd^0/AlF_3$-samples contain Lewis acid sites. The peak around 1490 $cm^{-1}$ is representative for Brønsted-sites only if it exceeds the intensity of the peak around 1450, but this is not the case here. No adsorption of pyridine was observed over $MgF_2$, $CaF_2$ and $KMgF_3$ supported Pd samples, revealing the absence of acidic centers. However, both $NH_3$-TPD and catalytic dismutation indicated the presence of moderate acidic centers in $MgF_2$ and $Pd^0/MgF_2$ samples which obviously are too weak to be detected via pyridine FTIR. Moreover, it was shown that $MgF_2$ prepared via sol-gel synthesis clearly exhibits weak Lewis acid sites.[41]

### 4.2.5 Temperature programmed desorption of ammonia ($NH_3$-TPD)

In figure 4.13, $NH_3$-TPD profiles of $Pd^0/MF_x$ samples (a-c) are shown. Since the former FTIR-PAS results indicated exclusively Lewis sites and no Brønsted acid sites at all at the surface of the catalysts, these $NH_3$-TPD profiles give a clear picture of the strength distribution of these Lewis sites.

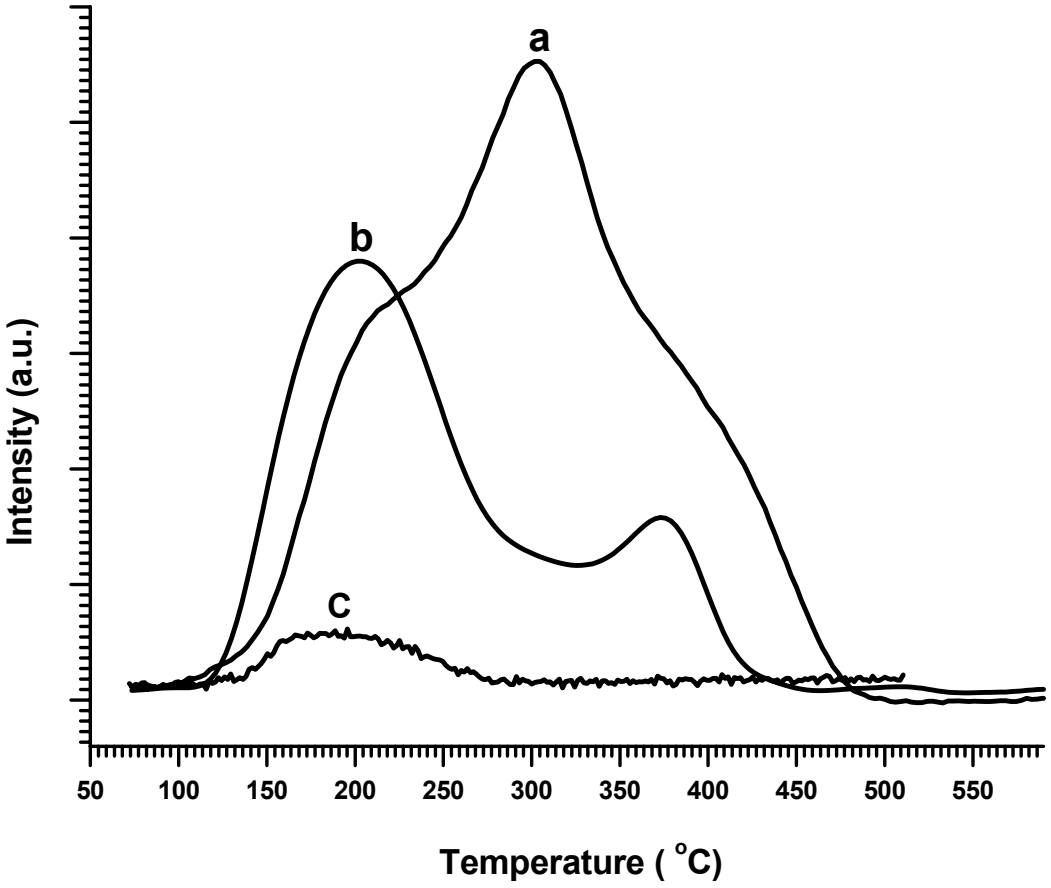


**Fig. 4.13** $NH_3$-TPD profiles of $Pd^0/MF_x$ (a = $Pd^0/AlF_3$, b = $Pd^0/MgF_2$ and c = $Pd^0/CaF_2$) samples.

The order of acidity in $Pd^0/MF_x$ is same as in case of bulk $MF_x$, $Pd^0/AlF_3$ > $Pd^0/MgF_2$ > $Pd^0/CaF_2$. The differences between $MF_x$ and $Pd^0/MF_x$ profiles are significant only in case of $AlF_3$. As a result of Pd loading, an additional acid site (intermediate strength) has obviously been formed. Since the FTIR-PAS does not give any hint to the formation of Brønsted sites, this is obviously a new medium strong Lewis site which could be generated on account of the strong sites in pure $AlF_3$ because the intensity of the deconvoluted peak (not shown) in the region 400 to 450 °C decreased as the intermediate strong site around 300 °C has increased. Obviously, incorporation of Pd into the sol-framework has altered the surface morphology on account of the strongest Lewis acid sites. This has further influence on acidic strength. The amount of $NH_3$ desorbed was comparatively

lower in $Pd^0$/MFx than in $MF_x$ (0.336 mmol/g for $Pd^0/AlF_3$ and 0.121 mmol/g for $Pd^0/MgF_2$). This clearly indicates the incorporation Pd in $MF_x$-structure is blocking the acidic centers of the support materials.

### 4.2.6 X-ray photoelectron spectroscopy

Distinct changes in XPS binding energies (BE) have been observed in $Pd/CaF_2$ catalyst samples not only at the various stages of their synthesis but also depending on the different synthesis routes as well (Fig 4.14).

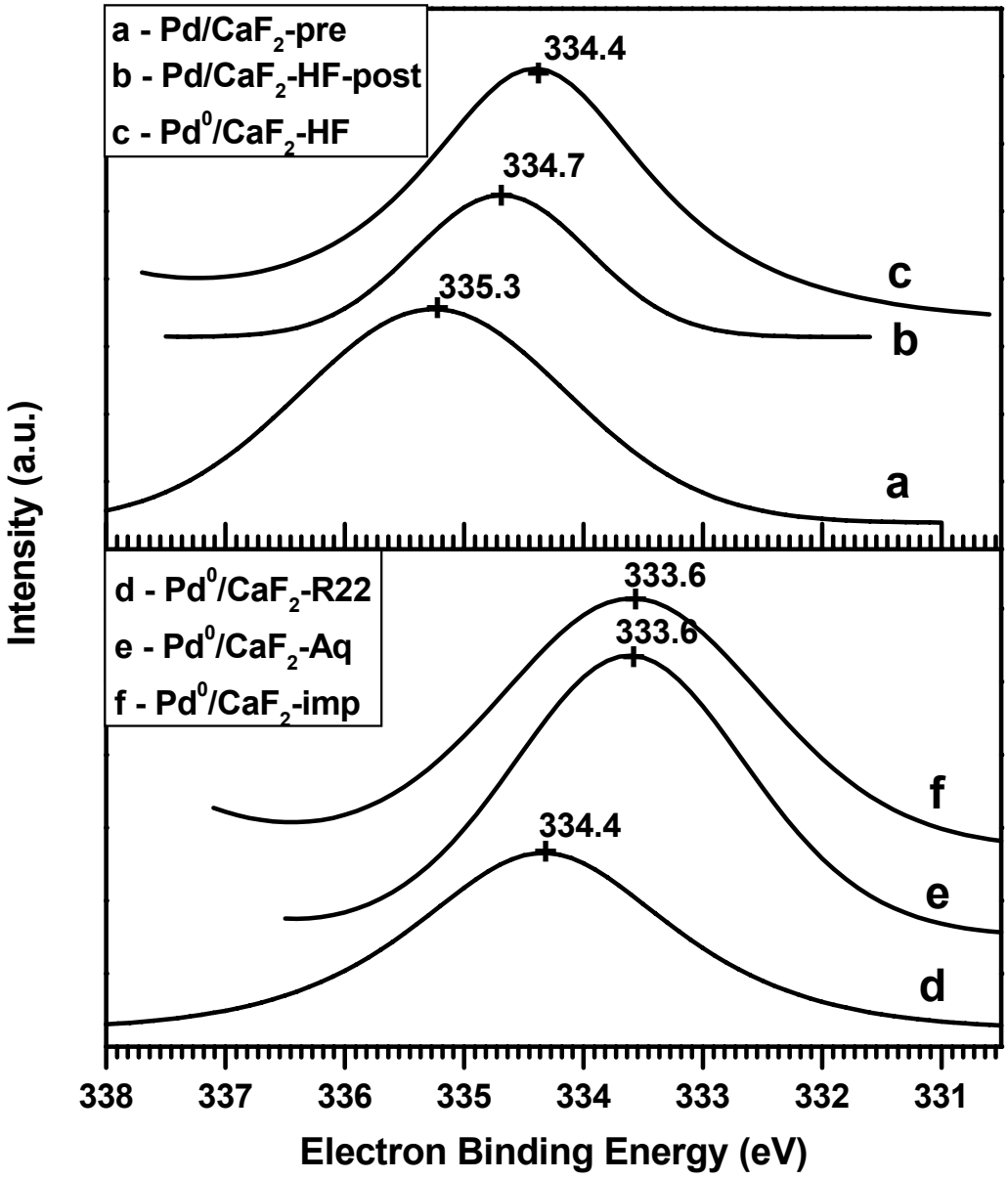


**Fig. 4.14** Pd ($3d_{5/2}$)-Binding Energy observed in $Pd^0/CaF_2$ during various stages of synthesis (a-c) and prepared by different synthesis routes (d-f).

The BE -value of 335.3 eV found for Pd($3d_{5/2}$) in Pd/$CaF_{2-x}(OCH_3)_x$ precursor indicates the presence of $Pd^{II}$ species, whereas the measured BE value of 334.7 eV for the post fluorinated Pd/$CaF_2$ samples is near to the BE of 334.4 eV observed for the final Pd/$CaF_2$-HF and Pd/$CaF_2$-R22 catalysts (Fig. 4.14) and reported for supported $Pd^0$.[17] Thus, the XPS data summarized in figure 4.14 reveal that a partial reduction of Pd species by organic residues takes place along with the post-fluorination treatment during the second step of synthesis. Pd/$CaF_2$-aq and $Pd^0$/$CaF_2$-imp both have 0.8 eV lower BE values observed for Pd ($3d_{5/2}$). However, these samples showed low activity for Suzuki coupling (Table 5.3, Fig 5.6). This can be explained by a different particle-support interaction depending on the preparation and / or by a final state effect due to a different relaxation of the ionized Pd, e.g. particle size effects. [148]

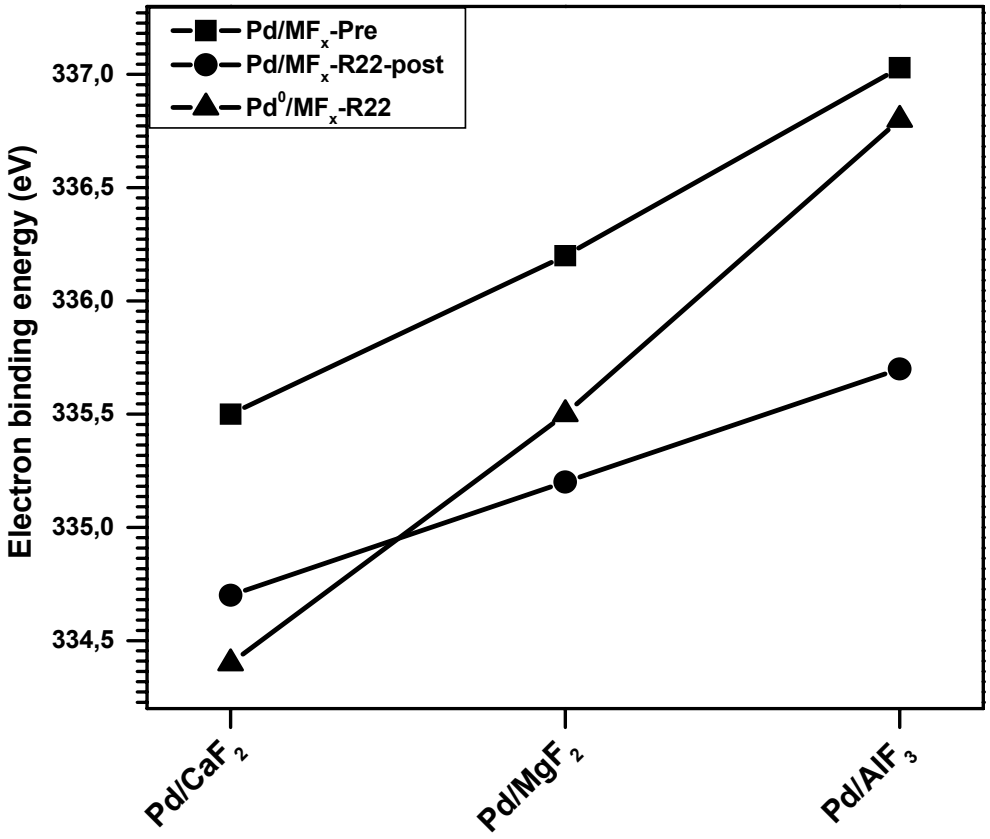


**Fig. 4.15** Changes in Pd ($3d_{5/2}$) Binding Energies observed because of different acidities in Pd/MFx catalysts in precursor (■) and after post-fluorination (•)

Significant changes in BE of Pd($3d_{5/2}$) were observed when metal fluorides of different acidities were used at each step of precursor, post-fluorination as well as reduction. BE of $Pd^0$/$AlF_3$ (337.0 eV) is 1.5 eV higher than $Pd^0$/$CaF_2$ (335.5 eV). This difference is attributed to strong acidity of $AlF_3$, which is pulling electrons of Pd thereby making Pd more electron deficient e.g., electronic effect.

### 4.2.7 Microscopic study

The surface morphology, homogeneity and particle size was characterized by means of transmission electron microscopy (TEM), atomic force microscopy (AFM), and scanning electron microscopy (SEM). TEM images of the $Pd^0/CaF_2$ system show exemplarily the dimension and distribution of the Pd-particles in the fluoride system (Fig. 4.16).

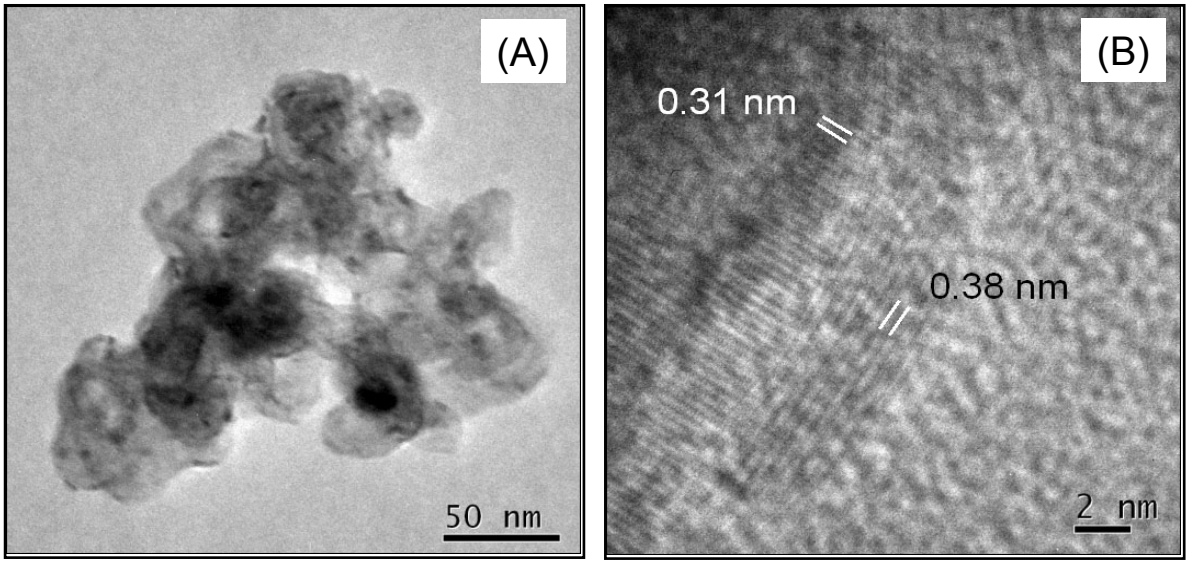


**Fig. 4.16** TEM images of $Pd^0/CaF_2$-HF nanoparticles.

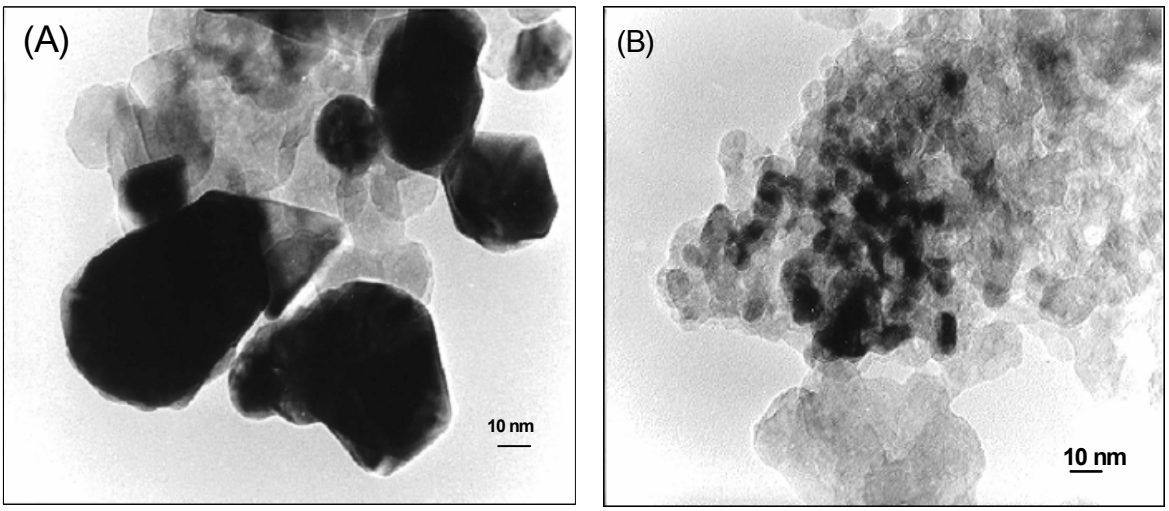


**Fig. 4.17** TEM images of $Pd^0/CaF_2$-aq (A) and $Pd^0/CaF_2$-imp (B) catalysts.

Fig. 1.16a displays a characteristic bright-field image of a freshly prepared $Pd^0/CaF_2$ catalyst. The $CaF_2$ particles exhibit an irregular shape with diameters of about 40 to 50 nm whereas the Pd-particles can be recognized as darker spots with a diameter d ranging between 3 to 8 nm. Only a few bigger Pd-agglomerates (d ~ 15nm) can be seen. Fig. 4.16b

displays the border region of $Pd^0/CaF_2$ in high-resolution TEM mode. Basing on the distance of the marked lattice planes, two different phases can be distinguished. Within $CaF_2$ the distance of the {111} lattice planes of $d_{111}$ = 0.31(4) nm was determined and for metallic Pd the distance of the {100} lattice planes ($d_{100}$ = 0.38(2) nm). For all measured samples just these two phases were identified by TEM, meaning neither $PdF_2$ nor $PdCl_2$ is present. This clearly shows that $Pd^{2+}$ has been quantitatively transformed into the metal stage as already predicted from XRD. SEM investigations indicated for all the samples a homogeneous porous morphology, AFM images indicated a homogeneous dispersion of Pd nanoparticles (both not shown here) thus confirming the TEM results. Bigger particles of size 60-100 nm were observed in catalyst prepared by aqueous fluorination ($Pd^0/CaF_2$-aq) and polydispersed Pd nanoparticles of 10-30 nm were clearly seen in catalyst prepared by impregnation method ($Pd^0/CaF_2$-imp).

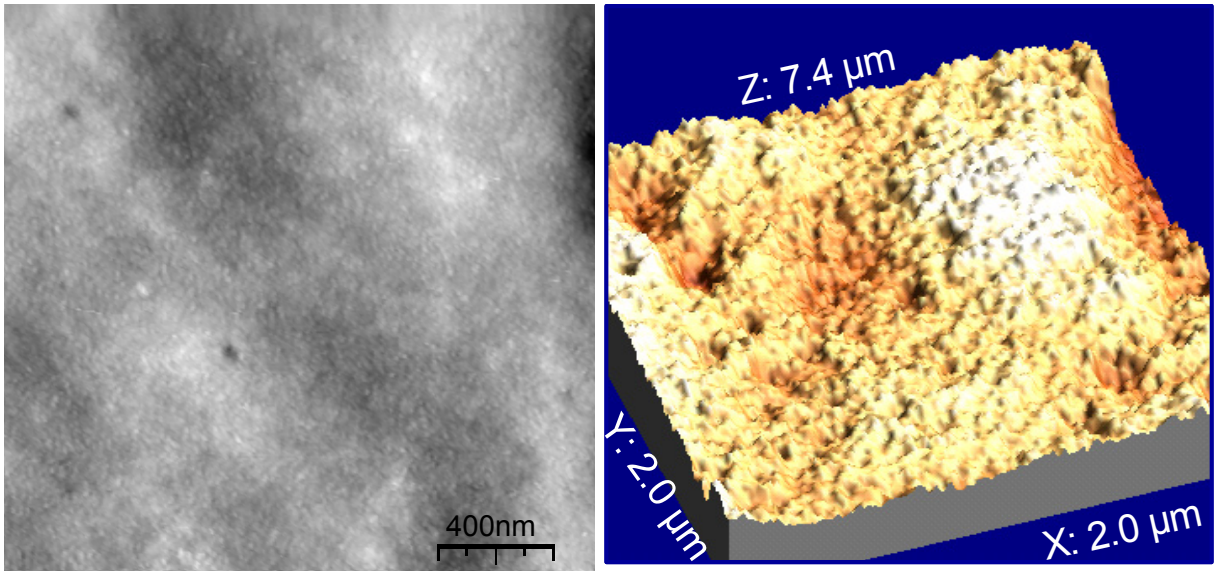


**Fig. 4.18** 2D (left) and 3D (right) AFM images of $Pd^0/MgF_2$.

The surface morphology of $Pd^0/MF_x$ was further studied using atomic (scanning) force microscopy (AFM/SFM). Fig 4.18 presents the typical contact mode for two dimensional and three dimensional AFM images of $Pd/MgF_2$ prepared by dip coating technique. Nanoparticles of average size 20 nm are visible in AFM; however Pd and $MgF_2$ particles can not be differentiated by this method. 3D image of $Pd/MgF_2$ has shown the formation of smooth surface.

## 4.3 Characterization of Iron and Copper based Fluorides

Iron and copper fluorides with redox properties were characterized by XRD, $N_2$-adsorption desorption isotherms together with BJH pore size distribution and scanning electron microscopy.

### 4.3.1 X-ray diffraction

XRD patterns of $FeF_{3-x}(acaca)_x$ precursors and post-fluorinated with different reagents are shown in Fig. 4.19. The precursor obtained after the sol-gel fluorination was amorphous in nature. HF post fluorinated sample ($FeF_3$-HF) has shown major reflections at 2θ = 26.8, 33.1, 38.4 and 51.5° corresponding to $FeF_2$ indicating reduction of formed $FeF_3$ in alcohol atmosphere. $FeF_3$-HF/$O_2$ and $FeF_3$-HF/$Cl_2$ have shown a single reflection for $FeF_3$ at 2θ = 26.8° along with some reflection for $FeF_2$. The reflection corresponding to only $FeF_3$, 2θ = 24.2, 33.8, 40.5, 49.1, 54,6 were found in $FeF_3$-$F_2$. The synthesis of pure $FeF_3$ phase was successful only by the post fluorination of $FeF_{3-x}(acaca)_x$ precursors by $F_2$ as strong fluorinating and oxidizing agent.

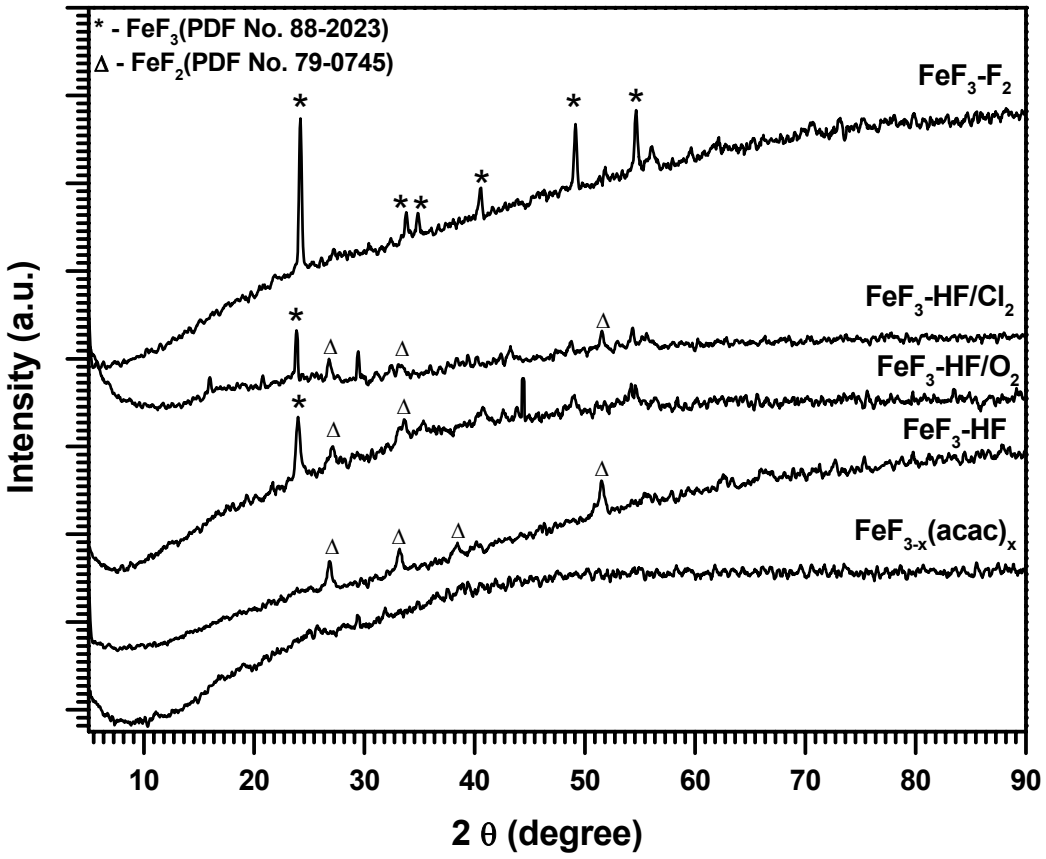


**Fig. 4.19** XRD of precursor and post-fluorinated of $FeF_3$ samples.

In case of copper samples (Fig. 4.20), post fluorination of $CuF_{2-x}(acac)_2$ precursor was successful with gaseous HF. Weak reflections corresponding to $CuF_2$ at 2 θ = 27.7, 31.5, 33.5, 37.3, 50.0, 51.5, 54.1, 55.7° were observed even at precursor stage. After the post-fluorination, more reflections of crystalline $CuF_2$ along with a little CuO reflections at 2θ = 36.4, 42.3, 61.4 were seen (Fig. 4.20, A). CuO formation attributes to the occurrence of hydropyrolysis ($CuF_2 + H_2O \rightarrow CuO + HF$) because of the moisture adsorbed on the sur-

face when the precursor was handled in open atmosphere. In case of $FeF_3/AlF_3$-$F_2$ (Fig. 4.20, B) and $CuF_2/AlF_3$ (Fig. 4.20, C) only $AlF_3$ reflection at $2\theta$ = 25.2, 51.8, 58.1° can be seen without any $FeF_3$ and $CuF_2$, respectively. It clearly indicates that high surface $AlF_3$ is offering a fine dispersion for $FeF_3$ and $CuF_2$.

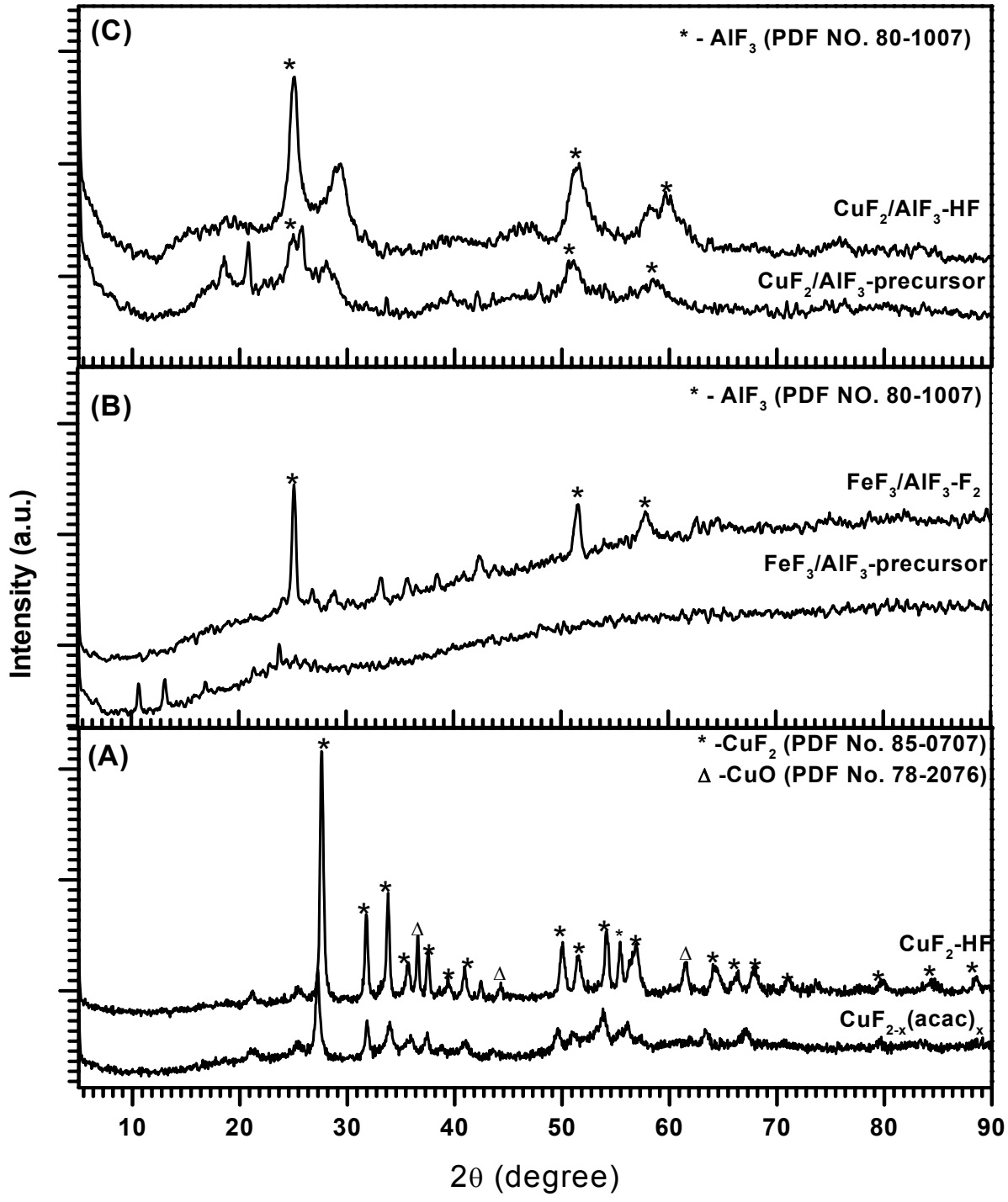


**Fig. 4.20** XRD of precursors and post-fluorinated $CuF_2$ (A), $FeF_3/AlF_3$ (B) and $CuF_2/AlF_3$ (C) samples.

### 4.3.2 $N_2$-adsorption and desorption isotherms and BJH pore size distribution

Interestingly, the $FeF_3$ samples prepared by different post-fluorination have shown different type of $N_2$ adsorption-desorption isotherms (Fig 4.21). All samples show a typical type IV adsorption isotherm, however they differ in desorption isotherm curve. The different desorption isotherms lead to the formation of hysteresis of different types indicating the presence of different shapes of pores. $FeF_3$-HF and $FeF_3$-$F_2$ have shown a H1-type of hysteresis, which is formed because of the capillary condensatation of cylindrical shape of mesopores.

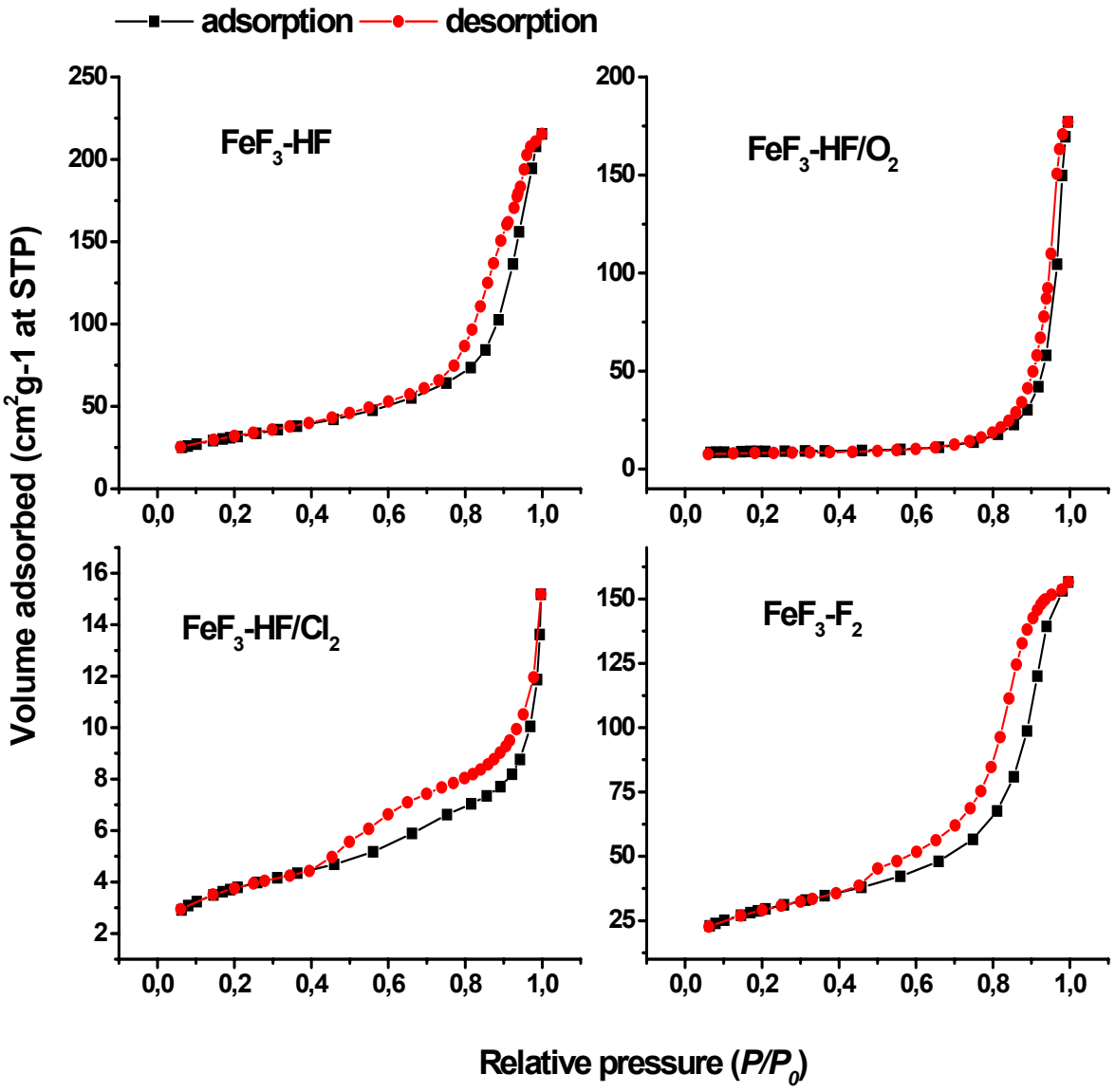


**Fig. 4.21** $N_2$-adsorption desorption isotherms of $FeF_3$ samples of different post synthesis treatments

$FeF_3$-HF/$O_2$ and $FeF_3$-HF/$Cl_2$ have shown a H3-type of hysteresis formed because of the agglomerated forming slit shaped pores (plates or edged particles like cubes). Similarly, $FeF_3$ samples obtained from different post-fluorinations have shown different pore size distributions with average pore diameter belonging to mesoporous range between 50-500 Å (Fig 4.22).

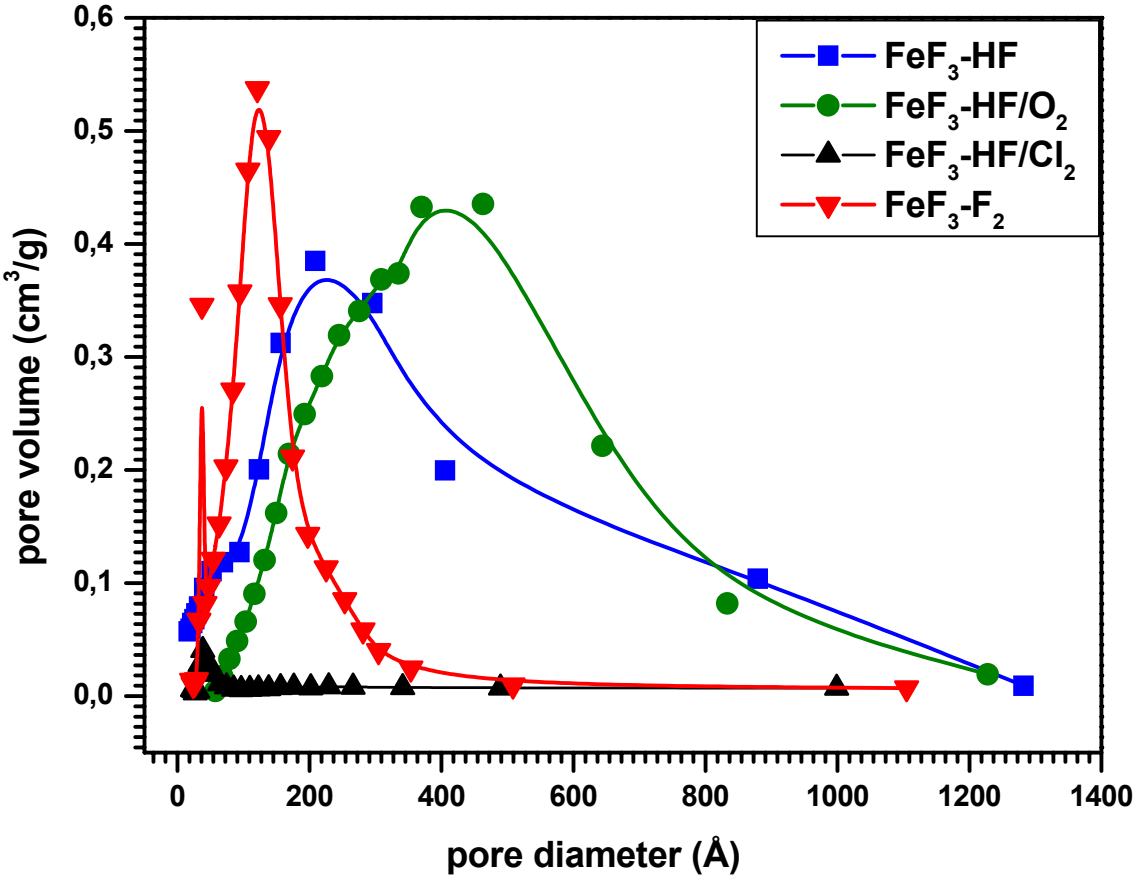


**Fig. 4.22** BJH pore size distributions of $FeF_3$ samples of different post synthesis treatments.

Among all samples $FeF_3$-HF/$Cl_2$ has shown a very small pore volume (0.02 $cm^3/g$) because of low surface area (Section 3.5). The broad pore size distribution in $FeF_3$-HF and $FeF_3$-HF/$O_2$ with respective average pore diameter has shown the presence large pores with irregular sizes. $FeF_3$-$F_2$ has shown presence of dual pore system at 37 and 91.4 Å. The most number of pores are of 91.4 Å and have shown a narrow pore size distribution indicating that all pores are of similar size.

### 4.3.3 SEM images

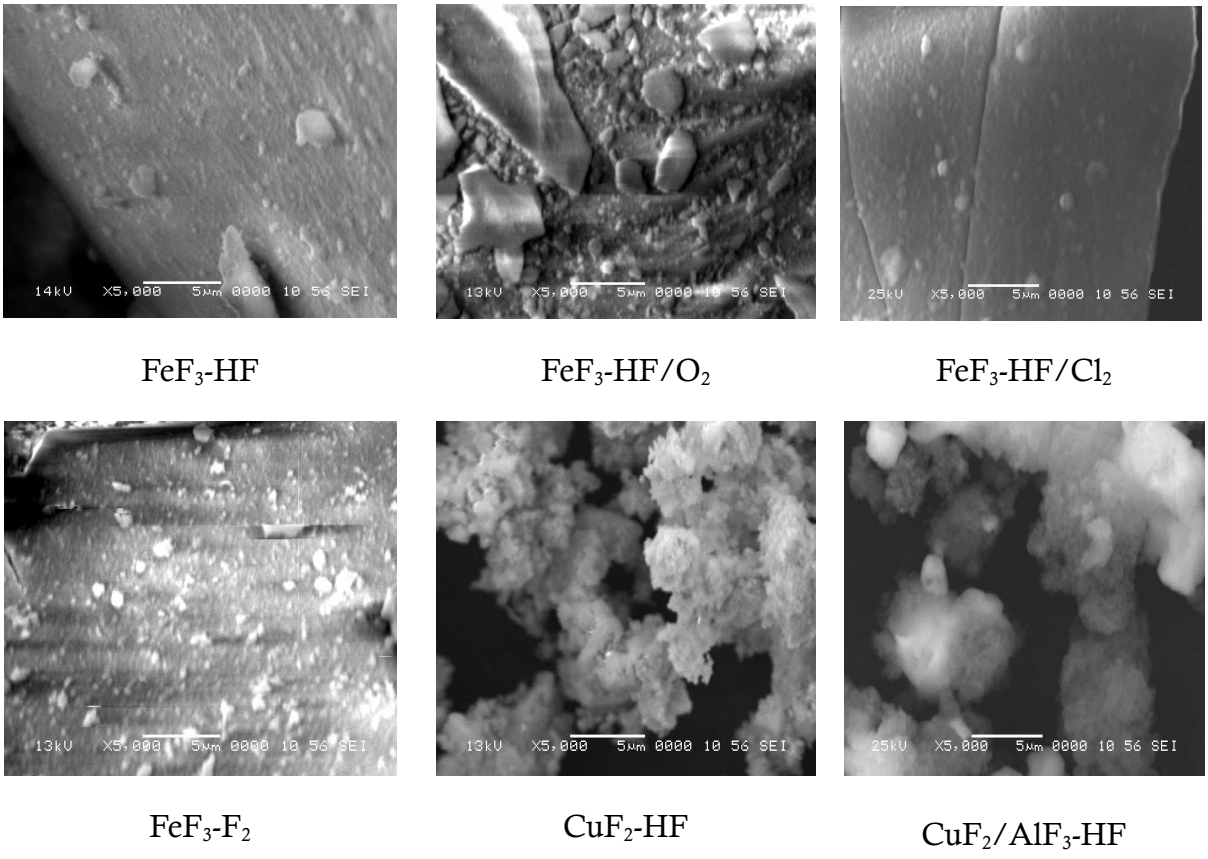


$FeF_3$-HF $FeF_3$-HF/$O_2$ $FeF_3$-HF/$Cl_2$

$FeF_3$-$F_2$ $CuF_2$-HF $CuF_2$/$AlF_3$-HF

**Fig. 4.23** SEM images of iron and copper based binary and host-guest fluorides.

Scanning electron microscopy was carried out to investigate the surface morphology and particle size distributions of these samples. SEM images have shown the formation of agglomerates with various dimensions (1-20 μm) (Fig. 4.23). The agglomerates of $FeF_3$-HF/$O_2$ are large in size compared to other $FeF_3$ samples. $CuF_2$-HF and $CuF_2$/$AlF_3$-HF have shown highly porous web like structure.

# 5 CATALYSIS

## 5.1 Dehydrofluorination of Hydrofluorocarbons

### 5.1.1 Introduction

Dehydrofluorination is a type of dehydrohalogenation reaction, in which a halohydrocarbon with α-hydrogen undergoes elimination of hydrogen halide with the formation of olefins. Fluoroolefins are widely used as monomers for the preparation of fluoropolymers. Additionally they possess the properties necessary to function as refrigerants, solvents, cleaning agents, foam blowing agents, extinguishing agents, sterilants, power cycle working fluids and thus can be used as replacements for the environmentally harmful CFCs and HCFCs. Dehydrofluorination of hydrofluorocarbons (HFCs) is always a challenging reaction since hydrofluorocarbons possess remarkable heat stability and the activation of the C-F bond is a high energy demanding phenomena. The non-catalytic dehydrofluorination of HFCs has been carried out at higher temperatures (above 500° C)[131, 149, 150], and leads to the formation of product mixtures along with the desired olefins, which are difficult to separate because of the close boiling points. At a higher temperature, fragments of lower fluorocarbons were observed because of C-C fission. An advantage of catalytic dehydrofluorination is that the reactions can be carried out at lower temperature with good olefin selectivity. Metal fluorides have been used as catalysts[151, 152] because they are known for their thermal stability and resistance against HF formed during the reaction. In the present work, performance of metal fluoride based systems prepared by the new sol-gel method for the dehydrofluorination of HFCs is demonstrated. Initially, binary fluorides with different acidities (strong to neutral) were tested. Effect of metal as well as host-guest fluorides was studied and samples prepared by non-aqueous sol-gel were compared with samples prepared by aqueous fluorination

## 5.1.2 Dehydrofluorination of 1,1,1,2-tetrafluoroethane ($CF_3CH_2F$, HFC-134a)

Dehydrofluorination of $CF_3CH_2F$ leads to the formation of trifluoroethylene ($CF_2$=CHF, HFC-1225zc) with the elimination of hydrogen fluoride (Scheme 5.1). The thermal dehydrofluorination of $CF_3CHF_2$ usually occurs at a very high temperature above 900 ºC, and above 1050 ºC formation of the $CH_2F_2$ and $C_2F_4$ was reported.[149, 150] Powell and Sharratt[131] have carried out this reaction using $AlF_3$ catalyst at 600 ºC and claimed a maximum of 37.9 % yield of $CF_2$=CHF at initial period of time (7 minutes), which was dropped to 5.7 % after 3 hours of reaction time.

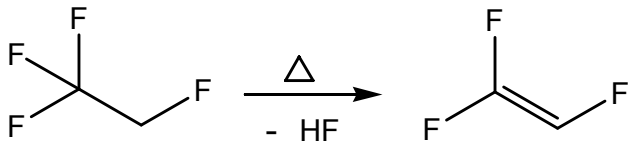


**Scheme 5.1**

The results of dehydrofluorination of 1,1,1,2-tetrafluoroethane (HFC-136a) are shown in Table 5.1.

**Table. 5.1** Catalytic activities of different metal fluorides based catalysts for gas phase hydrofluorination of 1,1,1,2-tetrafluoroethane (HFC-134a) to trifluoroethylene at various temperatures.[a]

| Sr. No. | Catalysts | C content (%)[b] | | % yield of $CF_2$=CHF at | | |
|---|---|---|---|---|---|---|
| | | BR | AR | 400 ºC | 450 ºC | 500 ºC |
| 1. | $AlF_3$ | 0.8 | 10.2 | 14.4 | 36.5 | 57.4 |
| 2. | $MgF_2$ | < d.l. | < d.l. | 0.3 | 3.1 | 7.8 |
| 3. | $CaF_2$ | < d.l. | < d.l. | 0 | 0 | 0 |
| 4. | $AlF_3$-aq | 0.7 | 7.5 | 12.9 | 25.9 | 41.1 |
| 5. | $Pd/AlF_3$ | 1.6 | 8.0 | 10.2 | 31.5 | 48.6 |
| 6. | $NbF_3/AlF_3$ | 1.2 | 8.9 | 10.5 | 24.6 | 38.1 |
| 7. | $TaF_3/AlF_3$ | 0.9 | 6.6 | 12.0 | 20.4 | 32.1 |
| 8. | $VF_3/MgF_2$ | 0.7 | 13.9 | 6.1 | 8.3 | 10.5 |

[a]-Reaction conditions: catalyst amount = ~ 200 mg, CT= 1.5 sec, GHSV = 2700 $h^{-1}$, $CF_3CH_2F$: $N_2$ ratio = 1:4, BR= before reaction, [b]-AR= after reaction, [c]-below detection limit.

At the first approximation, metal fluorides with different acidities (strongly acidic $AlF_3$, moderately acidic $MgF_2$ and neutral $CaF_2$ were tested under identical reaction conditions. Among the catalysts tested *high surface* $AlF_3$ possessing strong Lewis acidic sites has shown promising catalytic activity with 57.4 % yield for $CF_2$=CHF at 500 °C. Moderately acidic $MgF_2$ and neutral $CaF_2$ have shown very low $CF_2$=CHF yields 7.8 % and 0 % respectively, which clearly indicates that the strong Lewis acidity is responsible for dehydrofluorination. However, $AlF_3$-aq catalyst prepared by aqueous fluorination has also shown inferior activity compared to $AlF_3$ prepared by non-aqueous method. Furthermore, no beneficial influence was observed by the doping of Pd or other fluorides like $NbF_3$ or $TaF_3$ in metal fluoride in comparison to bulk $AlF_3$. Pd is probably blocking the Lewis acidic centers of $AlF_3$. $NbF_3$ and $TaF_3$ trivalent dopents have increased Brønsted acidity, which could be the possible reasons for their inferior activity. However, the yield for $CF_2$=CHF is slightly higher in $VF_3$ doped $MgF_2$ than in bulk $MgF_2$. This is probably because of higher Lewis acidity generated in $MgF_2$ because of $VF_3$ dopant, which are the active centers in dehydrofluorination. In contrast to the literature report, *high surface* $AlF_3$ has shown high selectivity for $CF_2$=CHF (100 %) and stability over for 5 h of reaction time without loss in $CH_2$=CHF yield.

### 5.1.3 Dehydrofluorination of 1,1,1,2,3,3-hexafluoropropane and 1,1,1,3,3,3-hexafluoropropane

Dehydrofluorination of $CF_3CHFCHF_2$ (mentioned as HFC-236ea hereafter) and $CF_3CH_2CF_3$ (mentioned HFC-236fa hereafter) is a subject of patent literature (Scheme 5.2 and 5.3).[151-153] 1,1,3,3,3-pentafluoropropene is a useful cure site monomer in polymerization to form fluoroelastomers.

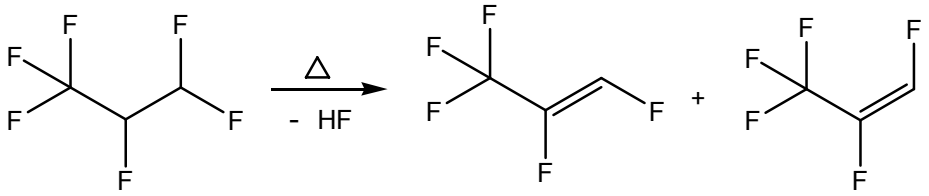


**Scheme 5.2**

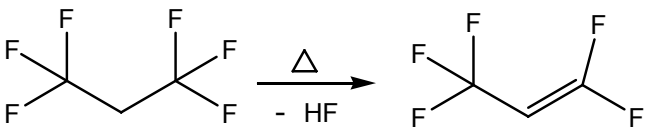


**Scheme 5.3**

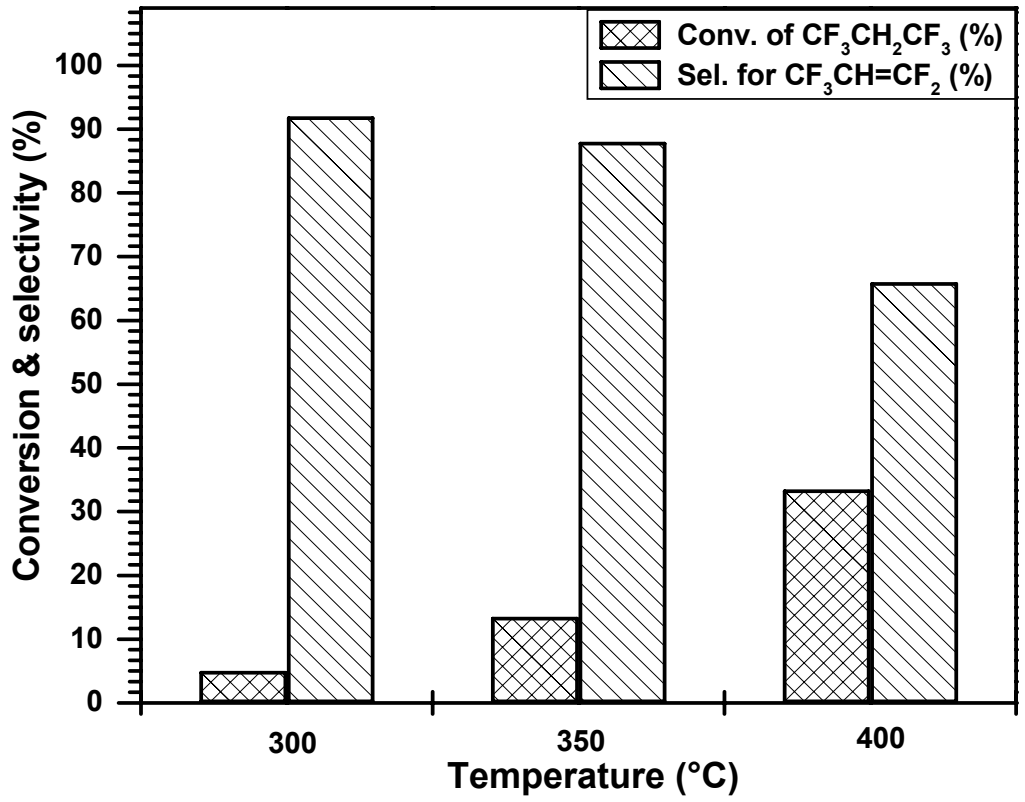


**Fig. 5.1** Dehydrofluorination of $CF_3CHFCHF_2$ over high surface $AlF_3$ at different temperatures.

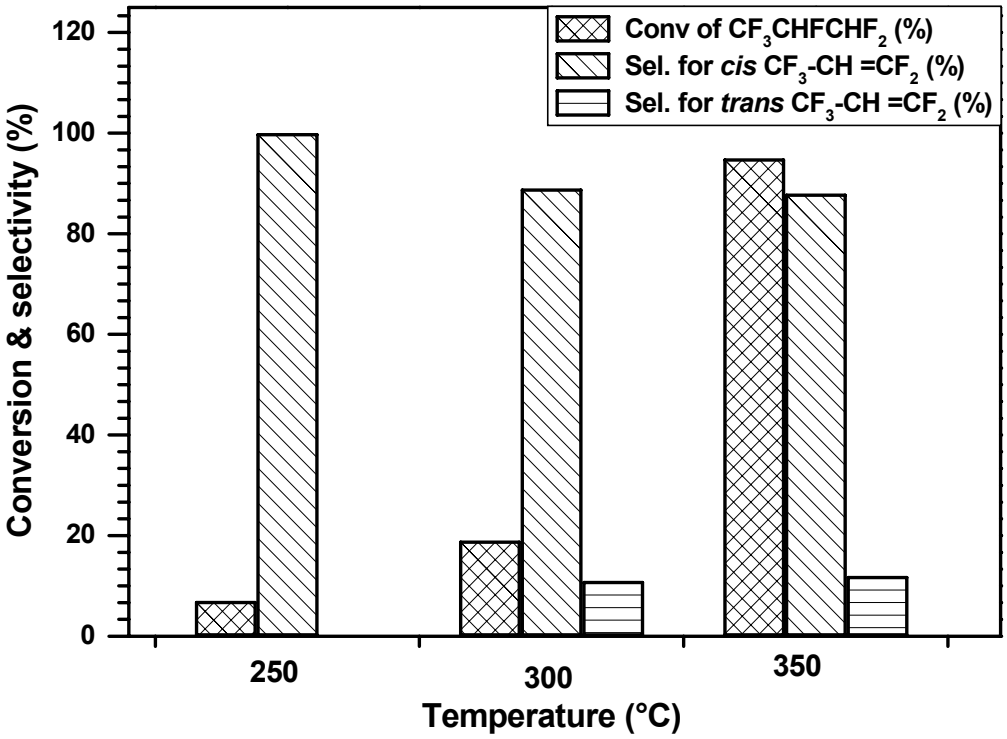


**Fig. 5.2** Dehydrofluorination of $CF_3CHFCHF_2$ over *high surface* $AlF_3$ at different temperatures.

The best $AlF_3$ catalyst was further tested for this reaction. HFC-236ea after dehydrofluorination gave cis- and trans- isomers of $CF_3CF=CHF$ (HFC-1225ye), whereas F236fa resulted in formation of $CF_3CH=CF_2$ (HFC-1225zc) as the only product. The performance of $AlF_3$ at different temperatures and selectivities for the desired products for the dehydrofluorination of HFC-236ea and HFC-236fa is presented in Fig 5.1 and Fig 5.2. Dehydrofluorination of F236ea started at a very low temperature 250 ºC with the formation of *cis*- HFC1225ye as only product. At 350 ºC, HFC-236fa conversion reached to 95 % with 100% selectivity for the fluoroolefins, 88 % for *cis*- HFC-1225ye and 12 % *trans*- HFC-1225ye. Dehydrofluorination of HFC-236fa started at a higher temperature than HFC-236ea, since it is asymmetric and more stable. At 300 ºC, conversion was only 3% with 92 % ºC HFC-1225zc selectivity. The conversion was increased to 35.5 % at 400 ºC with a decrease in HFC-1225zc selectivity (66 %), because of formation of the unidentified products.

### 5.1.4 Summary

- Among the catalysts tested for dehydrofluorination of HFC-134a, *high surface* $AlF_3$ containing strong Lewis acid sites was highly active and selective catalyst.
- Dehydrofluorination of HFC-134a was occurred out at relatively lower temperatures with high selectivity (up to 100 %) for the desired fluoroolefins with strongly acidic metal fluorides.
- $AlF_3$ catalyst was stable for 5 h or reaction time without any loss in the product yield.
- *High surface* $AlF_3$ was further very efficient for dehydrofluorination of different HFCs such as $CF_3CHFCHF_2$ and $CF_3CH_2CF_3$ giving high yield of desired fluoroolefins at low temperatures (250-500 ºC).

# 5.2 Citronellal Isomerization

## 5.2.1 Introduction

Menthol is a terpene known for its refreshing effect used as a fragrance or flavor in the production of pharmaceuticals, food products and cosmetics.[154] Therefore its synthesis is of considerable interests.[155] Since menthol has three asymmetric centers, there exist eight enantiomers forming four diastereomer pairs. Among the eight isomers of menthol only (-)-menthol possesses a characteristic odor of peppermint and produces a physiological cooling sensation on human body. Therefore selective synthesis of (-)-menthol is of immense interest to several industries and research groups. One of the major synthetic route to (-)-menthol is the Takasago process,[132] involving the acid catalyzed cyclization of (+)-citronellal to (-)-isopulegol in the presence of aqueous $ZnBr_2$, followed by Ni-catalyzed hydrogenation (Scheme 5.4).

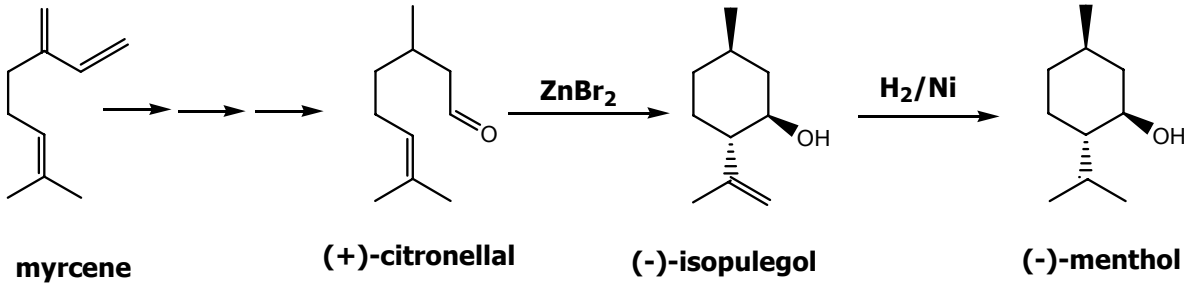


**Scheme 5.4**

The present industrial process of citronellal cyclization involves usage of large amounts of $ZnBr_2$ as homogeneous catalyst, which causes environmental problems due to the formation of large amounts of waste upon catalyst separation. The replacement of $ZnBr_2$ by a heterogeneous catalyst is one of the challenges to circumvent the problems associated with the homogeneous catalyst. Several research groups are engaged in developing a new heterogeneous bi-functional catalyst (metal/acid) for each step of menthol production and also in finding the catalyst able to carry out the synthesis of (-)-menthol in an one-pot process starting from (+)-citronellal[156-160] or from a renewable source like citral.[161,162] Thermal cyclization of (+)-citronellal leads to the formation of four isopulegol isomers with selectivities of 61 % (-)-isopulegol, 19 % (+)-neo-isopulegol, 15 % (+)-iso-isopulegol and 5 % (+)-Neo-iso-isopulegol (Scheme 5.5). Diastereoselectivity for the (-)-isopulegol is important because it is the only isomer that gets transformed to (-)-menthol after hydrogenation. For this purpose, a number of heterogeneous catalysts such as zeolite beta, MCM-41, Sn-beta, silica supported heteropoly acids have been used for cyclization of citronellal to isopulegol[163-164].

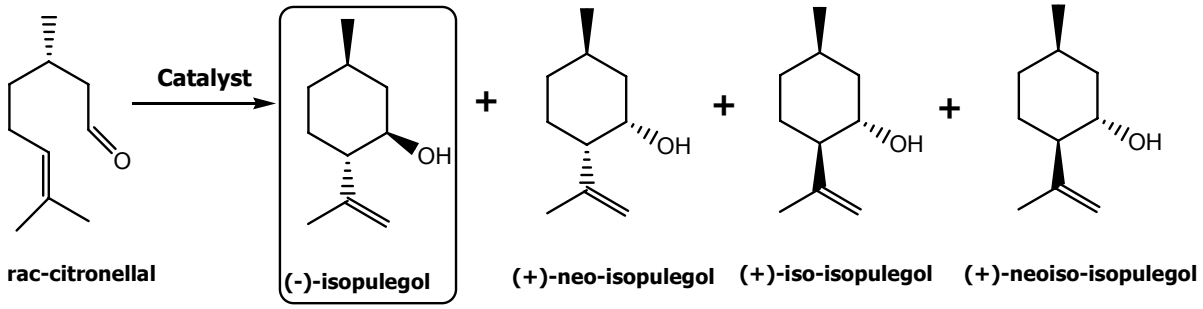


**Scheme 5.5**

Generally, these catalysts resulted in the formation of all four isopulegol isomers and the diastereoselectivity for (±)-isopulegol was in the range of 52-75 %. Very recently Yongzhong et. al. have reported a highly diastereoselective catalyst and showed that a hydroxylated surface having both Lewis and Brønsted acid sites is essential for a good activity[165]. In the present work we were interested to study the potential of metal fluoride based materials for the diastereoselective (d.s.) cyclization of citronellal to (±)-isopulegol.

## 5.2.2 Catalytic study

The catalytic activities along with their selectivities and yields for isopulegols over different metal fluoride based catalysts for the isomerization of citronellal is shown in Table 5.2.

*Catalyst screening*

**Table. 5.2** Catalytic performances of different metal fluorides for the cyclization of (±) citronellal to isopulegols.[a]

| Sr. No. | Catalyst | (%) Conv. of citronellal | (%) Sel. for isopulegol | (%) Yield for isopulegols | Distereoselectivity for(±)-isopulegol,% |
|---|---|---|---|---|---|
| 1.* | $AlF_3$ | 100 | 90.9 | 90.9 | 90 |
| 2. | $MgF_2$ | 23.8 | 85.7 | 20.4 | 89,3 |
| 3. | $CaF_2$ | 14.1 | 98.7 | 13,9 | 84.7 |
| 4. | $AlF_3$-aq | 16.4 | 100 | 16.4 | 86.4 |
| 5. | $Al(OH)_{1.5}F_{1.5}$ | 16.3 | 100 | 16.3 | 88.0 |
| 6. | $Mg(OH)_{0.4}F_{1.6}$ | 17.0 | 87.3 | 14.9 | 92.6 |

[a]-Reaction conditions: citronellal = 1 mL, catalysts amount = 50 mg, solvent = toluene (5 mL), temp = 80 °C, time = 6h, *-1h.

In this study, formation of (-)-isopulegol and (+)-neo-isopulegol as major products with traces of (+)-iso-isopulegol was observed. (+)-Neo-iso-isopulegol was not formed under

these reaction conditions. Apart from these products, there were also a few unidentified high boiling products detected. Among the catalysts tested under identical reaction conditions, *high surface* $AlF_3$ possessing strong Lewis and weak Brønsted acid sites gave a high yield for isopulegols (90%) compared to moderately acidic $MgF_2$ (23.8%) and neutral $CaF_2$ (14.1%). $AlF_3$-aq (13.9 %), $Al(OH)_{1.5}F_{1.5}$ (16.3 %) and $Mg(OH)_{0.4}F_{1.6}$ (14.9 %) have also shown low yields for isopulegols. Diastereoselectivity for (-)-isopulegol was very high only in the case of $AlF_3$ (90 %) and $Mg(OH)_{0.4}F_{1.6}$ (92.6%). Since in the presence of the $AlF_3$ sample the yield to isopulegols was the highest, this sample was further used in the reaction conditions optimization studies and in leaching and recycling tests.

***Influence of solvents***

The effect of different solvents on the catalytic activity, isopulegols yield and selectivity and diastereoselectivity to (±)-isopulegol was checked using the best $AlF_3$ catalyst under identical reaction conditions (Fig. 5.3). Among the solvents tested, non-polar toluene was found to be the best in terms of activity (100 %) as well as diastereoselectivity (90 %). In the presence of a polar solvent like isopropanol, isopulegol selectivity was very low (79 %) because of formation of unidentified by-products.

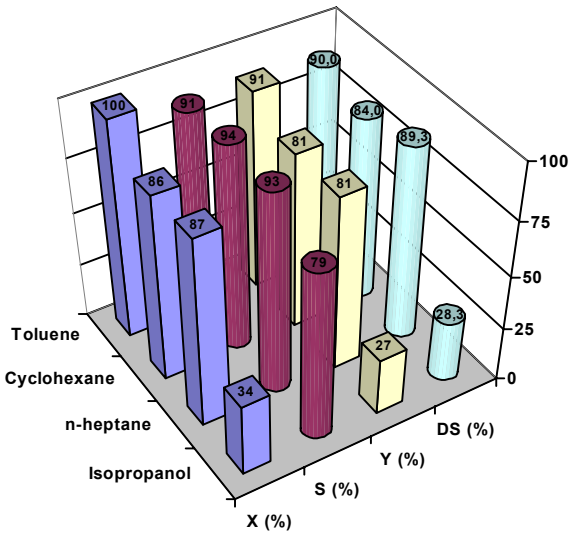


**Fig 5.3** Influence of solvents

***Influence of metal nature***

The effect of metals supported on metal fluorides was studied under identical conditions and compared with bulk $AlF_3$ (Fig. 5.4). In the presence of these catalysts the catalytic performances suffered, in some cases, only a low modification. Therefore, in the presence of $Ni/AlF_3$ the conversion decreased by 6 % and d.s. by less than 2 % while the yield to isopulegols increased by 1 %. A major modification of the catalytic performances was observed in the case of post-fluorinated samples. Therefore, the

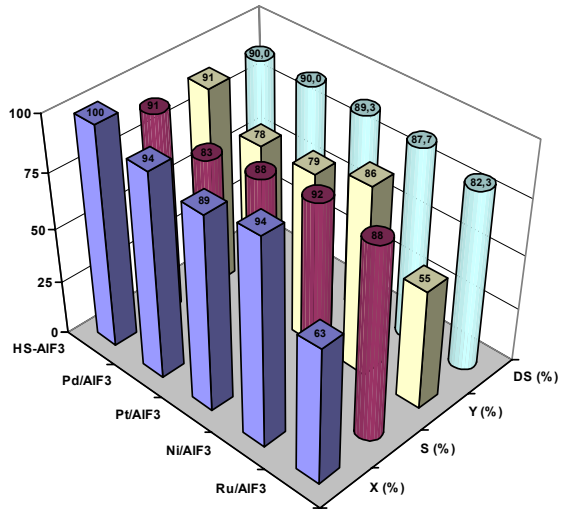


**Fig 5.4** Influence of metal supported $AlF_3$

activity decreased to ca. 58 % and d.s. to 82 %. The selectivity to isopulegols decreased by only 5 %. A possible reason for these results is the blocking of the support acidity by the metal.

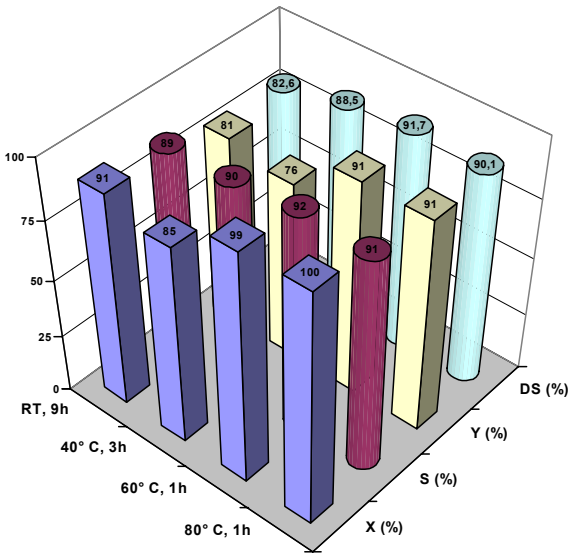


**Fig 5.5** Influence of temperature

***Influence of temperature***

The effect of temperature on the activities and selectivities was further studied at different temperatures ranging from room temperature (25 °C) to 80 °C (Fig 5.5). The catalytic activity increased proportionally to temperature. However, at 60 °C a very high diastereoselectivity of 91.7 % for (-)-isopulegol was observed.

***Influence of substrate to catalyst ratio***

To investigate whether the amount of substrate has an influence on the activities and selectivities, experiments were carried out using varying citronellal to catalyst molar ratio ($n_{ispulegol}/n_{cat}$ = 4.65, 9.3 and 13.96) keeping the amount of the $AlF_3$ catalyst constant (50 mg) under identical conditions. It was observed that $AlF_3$ could catalyze this reaction very efficiently even at higher amounts of substrate. No significant influence on isopulegol selectivity and diastereoselectivity was observed.

***Leaching and recycling study***

To analyze the stability of $AlF_3$ catalyst, leaching and recycling experiments were carried out. In the leaching test, the catalyst was separated after 15 minutes (citronellal conversion of 41.6 %) and reaction mixture was further allowed to stir for a further 3 hours. There was no increases in citronellal conversion (42 %) observed, indicating leaching of $AlF_3$ catalyst did not occur. Therefore, it can be concluded that reaction takes place in heterogeneous catalysis. In agreement to leaching test, the catalyst could be further quantitatively recovered and recycled for 3 cycles (1 fresh & 2 cycles) without any loss in activity and product selectivity indicating a good stability.

## 5.2.3 Summary

- Metal fluorides were shown to have the potential to catalyze citronellal isomerization, which is a useful step in the synthesis of menthol.

- Among the catalysts tested, $AlF_3$ was found to be excellent in terms of high catalytic activity (100 % conversion), high yield for isopulegol isomers (up to 92.5 %) and high diastereoselectivity for the desired (-) isopulegol (up to 91.7 %).
- Optimization of the reaction conditions showed that 60 °C temperature and a non-polar solvent like toluene is necessary for obtaining high diastereoselectivity for (-) isopulegol.
- $AlF_3$ supported metallic (Pd, Pt, Ni, Ru) catalysts did not show any beneficial effect for this reaction. However the lower activity was attributed to lower acidity compared to bulk $AlF_3$, which are the active sites in this reaction.
- Leaching and recycling studies have showed that the reaction was purely heterogeneous and $AlF_3$ was a stable catalyst, can be easily recovered and recycled.
- In conclusion, high surface $AlF_3$ prepared by new sol-gel method can effectively catalyze the crucial citronellal isomerization step in the industrial production of menthol by the Takasago process and can replace the homogeneous $ZnBr_2$. Additionally, $AlF_3$ supported by metal (Pd, Pt, Ni) acts as bi-functional (acid/metal) catalyst and can be used for the one-pot synthesis of (-)-menthol by hydrogenative cyclization of citral or citronellal in a cascade type of reaction.

# 5.3 Suzuki Coupling

## 5.3.1 Introduction

Due to their high surface to volume ratio, Pd nanoparticles[129-130] have extensively been investigated for C-C- cross coupling reactions.[166] Furthermore, catalysts based on Pd nanoparticles are widely used in the Suzuki coupling reaction,[133] which is at the present the standard method for synthesis of biaryls. Homogeneous as well as heterogeneous Pd catalysts have been proposed for the Suzuki coupling, the later recognized clearly as more advantageous with respect to costs, easiness in handling, reusability, selectivity and purity of obtained products.[133] Nowadays, exclusively nanostructured Pd particles on different supports are used as catalysts. The investigations of nano Pd particles deposited on oxides,[167] carbon,[168-170] zeolites,[171] hydrotalcites,[172] fluorapatite,[173] as supports have shown that the catalyst activities are strongly influenced not only by the particle size of Pd but also by the properties of the support. Besides supported catalysts, encapsulated palladium is also being used as reusable catalyst for such cross-coupling reactions. [174, 175].

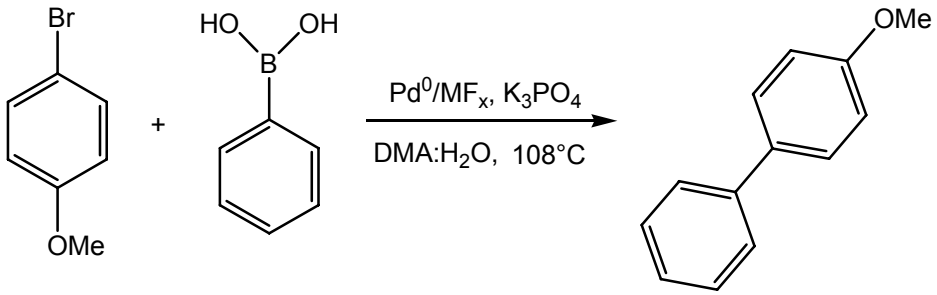


**Scheme 5.6**

In this study, the coupling of 4-bromoanisole with phenylboronic acid and $K_3PO_4$ as base was performed in order to investigate the catalytic activities of $Pd^0$/ $MF_x$-composites with different but adjusted properties in the Suzuki coupling reaction (Scheme 5.6).

## 5.3.2 Reaction study

In order to study the catalytic properties of $Pd^0/MF_x$ composites, Suzuki cross coupling of 4-bromoanisole (4-BA) and phenylboronic acid (PBA) to 4-methoxybiphenyl (4-MBP) was carried out as model heterogeneously catalyzed liquid phase reaction. Along with $Pd^0/MF_x$ catalysts, a commercially available 5 wt % Pd/C catalyst, (Aldrich, Degussa type E101 NO/W), was used as benchmark, which has been widely applied for Suzuki coupling.[168] Besides the main reaction product 4-MBP only small amounts of biphenyl (3-5 %) formed by homocoupling of PBA has been detected as byproduct in this reaction.

In Table 5.3 the yields of desired 4-MBP after 1 and 10 hr reaction times are summarized. Dramatic differences in the activities of the heterogeneous $Pd^0/MF_x$ catalysts have been observed depending on the Lewis acidic properties of $MF_x$ - support used in the non aqueous sol gel synthesis (Table 5.3, entry 1-4).

**Table. 5.3** Suzuki Coupling of 4-bromoanisole (I) with phenylboronic acid (II) and $K_3PO_4$ (III) over $Pd^0$/MFx catalysts to give 4-methoxybiphenyl (4-MBP).[a]

| Entry | Description | Reaction time (h) | 4-MBP Yield (%) |
|---|---|---|---|
| 1 | $Pd^0/AlF_3$-HF | 1 | 9 |
| 2 | $Pd^0/MgF_2$-HF | 1 | 11 |
| 3 | $Pd^0/CaF_2$-HF | 1 (10) | 88.1 (94.2) |
| 4 | $Pd^0/CaF_2$-R22 | 1 (10) | 81.9 (91.7) |
| 5 | $Pd^0/CaF_2$-Aq | 1 (10) | 48.3 (72.5) |
| 6 | $Pd^0/CaF_2$- imp | 1 (10) | 8.1 (24.4) |
| 7 | $Pd^0/Ca(OH)_{0.5}F_{1.5}$ | 1 | 30.6 |
| 8 | $Pd^0/C$ | 1 | 85.9 |

[a]- Reaction conditions: I:II: III = 1:1.5:3 (molar ratio), T = 108° C, 35 mg $Pd^0/MF_x$ catalyst, solvent 12 mL of a 5:1 mixture of DMA and $H_2O$.

Similarly, total different catalyst properties came out for the same binary catalyst system, $Pd^0/CaF_2$, depending on whether Pd nanoparticles were immobilized by impregnation of the "sol-gel $CaF_2$" support ($Pd^0/CaF_2$-imp) or "in situ"-incorporated in the course of sol-gel synthesis using anhydrous ($Pd^0/CaF_2$-HF & $Pd^0/CaF_2$-R22) or aqueous HF ($Pd^0/CaF_2$-aq). Only minor different catalytic activities were observed depending on whether the post fluorination step was carried out either with HF or with R22. The most substantial differences found in performing the coupling reactions over neutral $Pd/CaF_2$-HF (yield 88 %), or strong acidic $Pd^0/AlF_3$-HF (9 %), or moderate acidic $Pd/MgF_2$-HF (11 %) catalysts can consistently be explained on the basis that

i) the acidic centers are getting blocked by the electron donors (Lewis bases) $K_3PO_4$ and/or water used for the reaction. It seems that the hydrogen bonding network formed this way by water at the surface causes a dramatic decrease of the accessibility of the Pd nanoparticles on the surface
ii) the uniform micropores built up in case of sol gel prepared Pd nanoparticles supported on Lewis acidic $MF_x$ (Fig. 5.6) can easily be blocked by the H-network dis-

cussed above. Thus, all the Pd nanoparticles locked inside the pores are no longer available causing a remarkable decrease in reaction centers (spots) on the remaining surface of the Pd/$MF_x$-catalysts.

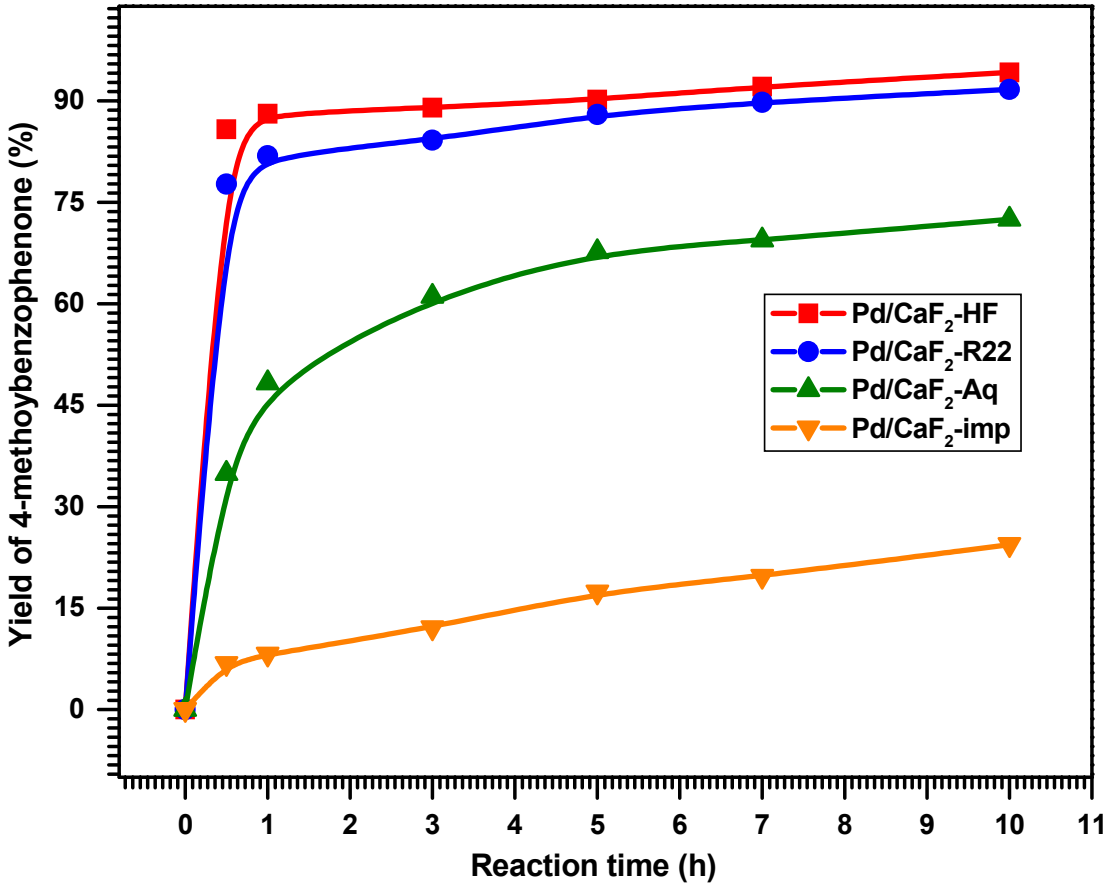


**Fig. 4.3** Catalytic activities of $Pd^0/CaF_2$ samples for Suzuki coupling of 4-bromoanisole with phenylboronic acid.

Furthermore, comparison of $Pd^0/CaF_2$ catalysts of different preparations strongly supports the advantages of non-aqueous sol-gel method (Fig. 5.6), showing that the fluorolysis of alkoxides in the synthesis of precursors becomes already influenced by the presence of small amounts of water. Obviously, OH groups, once incorporated (chemically bonded) into the $MF_x$ precursors during the sol-gel synthesis, are highly resistant against the consecutive post fluorination treatment but still accessible for interacting with bases (water) during "wetting of the catalyst" by the reaction mixture. Thus, it has apparently been demonstrated by these findings that although the latter reactions are carried out in DMA/water solutions, the history of synthesis (use of aqueous or anhydrous HF in the sol-gel process) is crucial for obtaining active catalyst phases. In attempt to clarify whether the reaction is going by homogeneous or heterogeneous pathway leaching tests were carried out. The reaction was terminated after 5 minutes - at this time conversion has already reached about 65 % and the catalyst was separated by filtration. The reaction

mixture was further stirred for 6 hours in absence of the catalyst and a marginal increase in 4-MBP yield (3-5 %) has been detected. On the other hand, with the separated catalyst nearly the same conversion (~ 55 %) as with the fresh one was observed after 5 minutes, hence, leaching can be excluded. Most probably the "reaction progress without catalyst" was due to nanoscopic $Pd^0/CaF_2$ –particles which has not been separated by a simple filtration.

### 5.3.3 Summary

Among the $Pd/MF_x$ studied, neutral $Pd^0/CaF_2$ catalysts were far more active than the catalysts supported on metal fluorides which are strongly ($Pd^0/AlF_3$) or moderately ($Pd^0/MgF_2$) Lewis acidic. High dispersion of Pd over the supports was the main feature of "sol-gel samples" as confirmed by XRD, TEM, and XPS. $Pd^0/CaF_2$ samples ($Pd^0/CaF_2$-HF & $Pd^0/CaF_2$-R22) prepared by the novel non-aqueous method were evidently much better catalysts in comparison to those prepared by using aqueous HF in the sol-gel process ($Pd^0/CaF_2$-aq) or simply by impregnation techniques ($Pd^0/CaF_2$-imp). Their high activities are due to the homogeneous distribution of Pd nanoparticles within the metal fluoride supports of very distinct morphology characterized by a suitable distribution of meso and macro pores and possessing almost none of the obvious disadvantageous micropores. However, the morphology of the metal fluoride support alone is not sufficient enough. Formation / precipitation of Pd-particles during impregnation of the sol-gel synthesized $MF_x$-support results in significantly larger and more crystalline Pd-particles, and hence, into the lower catalytic activity of $Pd^0/CaF_2$-imp. Thus, the surface morphology of these binary phases together with the homogeneous, fine dispersion of Pd nano-particles are the most important characteristics of the catalysts and both have apparently been optimal formed in case of the neutral $Pd^0/CaF_2$ composites as a direct result of the novel chemical synthesis. As confirmed by XRD and TEM measurements there are no essential agglomerations on the catalyst after its use, neither of Pd- nor of $CaF_2$- particles. Finally it can be concluded that Palladium supported on nanoscopic, high surface area metal fluorides prepared via the new sol-gel-synthesis route is catalytically at least as good as the "benchmark" Pd/C-catalyst. Moreover, the obtained $Pd^0/MF_x$ -systems for which the Lewis-acidiy of the support can be tuned over a wide range might be of great interest for reactions where beside the noble metal, active Lewis acids sited are an important requisite.

# 5.4 $CHClF_2$ Hydrodehalogenation

## 5.4.1 Introduction

Difluoromethane ($CH_2F_2$, HFC-32) is an important compound used as low boiling refrigerant, substituting environmentally harmful former chlorine containing fluorocarbons. Fluorination of $CH_2Cl_2$ by $SbF_5$[176] and/or by HF[177], as well as HF-fluorination of formaldehyde in presence of $BF_3$[178] are well established methods for its synthesis on laboratory or industrial scale. Moreover, there are many reports focusing on the selective synthesis of hydrofluorocarbons by hydrodechlorination reaction of the respective chlorofluorocarbons e.g., the formation of $CH_2F_2$ from dichlorodifluoromethane ($CCl_2F_2$, CFC-12)[33, 81-85] or from chlorodifluoromethane ($CHClF_2$, HCFC-22).[86-90] Because of the "steady state availability" of the latter compound – it is the key compound for manufacturing PTFE -, a selective and efficient synthesis method for $CH_2F_2$ based on hydrodechlorination of $CHClF_2$ as starting material is of great practical interest. Thus, attempts have already been undertaken to selectively hydrodechlorinate $CHClF_2$ but conversion into the desired $CH_2F_2$ is very low, making a technical application senseless.[86-90] Palladium supported catalysts,[124] more specifically on metal fluoride supports,[8] have generally been applied for the hydrodechlorination of chlorine containing fluorocarbons. Due to their high thermal stability and resistance against HF and/or HCl, metal fluorides have been found to be advantageous over commonly used oxidic catalysts with respect to activity, stability and desired product selectivity[35, 37, 47]. For this purpose $AlF_3$[81-83] and $MgF_2$[33-38] are the most studied compounds to be used as supports.

The hydrodechlorination of $CHClF_2$ with the aimed formation of $CH_2F_2$ was the main objective of this study. However, it turned out that this is markedly affected by competitive dismutation and dehydrochlorination reactions. Hence, these were carefully investigated, too.

## 5.4.2 Hydrodehalogenation of $CHClF_2$

Hydrodehalogenation is one of the most used methods for the selective removal of halogens from halocarbons.[125] The kinetics (conversion and selectivity) of the halogen against hydrogen exchange on saturated halocarbons strongly depends on the strength of C-X bond, the nature of catalyst, and the reaction conditions. For the reaction between $CHClF_2$ and hydrogen according to Eq. 5.1, the formation of C-C-coupling products along with the desired $CH_2F_2$ have been reported over nickel catalysts,[86] whereas over Pt supported on silica $CH_3F$ and $CH_4$ were the only products observed.[47] In our investiga-

tions, *high surface* -$AlF_3$ was first used as support though it is known as very strong solid Lewis acid.[20, 21] Hence, it was expected to activate the C-Cl bond on the Lewis acidic sites effectively, thereby enhancing the hydrodechlorination activity/selectivity.

**Table. 5.4** Hydrodehalogenation of $CHClF_2$ with hydrogen over various metal fluorides supported palladium catalysts.[a]

| Sr. No | Catalyst | Temp (°C) | $CHClF_2$ Conv. (%) | Product selectivity (%) | | | | |
|---|---|---|---|---|---|---|---|---|
| | | | | $CH_2F$ | $CH_4$ | $CHF_3$ | $CH_3F$ | Other[b] |
| 1. | $Pd^0/AlF_3$ | 260 | 85.9 | 0 | 32.1 | 31.5 | 28.2 | 8.2 |
| 2. | $Pd^0/MgF_2$ | 350 | 6.0 | 5.2 | 26.8 | 39.6 | 6.3 | 22.2 |
| 3. | $Pd^0/CaF_2$ | 350 | 2.3 | 72.7 | 27.3 | 0 | 0 | 0 |
| 4. | $Pd^0$/KMgF | 350 | 2.9 | 68.6 | 31.4 | 0 | 0 | 0 |
| 5. | $Pt^0/AlF_3$ | 290 | 95.9 | 0 | 32.9 | 44.7 | 2.2 | 20.1 |
| 6. | $Pt^0/MgF_2$ | 290 | 0.6 | 0 | 48.7 | 51.3 | 0 | 0 |
| 7. | $Pd^0/C$ | 320 | 13.6 | 4.6 | 55.5 | 33.1 | 1.8 | 5.0 |

[a-] Reaction conditions: amount of catalyst = 0.25 mL, $H_2/CHClF_2$ mole ratio = 7, GHSV = 3600 $h^{-1}$, CT=1 sec. [b-] $CH_3Cl$, $CHF_2$-$CHF_2$, $C_2H_4$, etc.

However, as a result of the reaction between $CHClF_2$ and hydrogen the following products were formed on the $Pd^0/AlF_3$ catalyst: $CHF_3$, $CH_2F_2$, $CH_3F$, and $CH_4$ (Table 5.4). The appearance of the latter three compounds might be easily explained assuming consecutive hydrodehalogenation reactions as they are displayed by Eq. 5.1. Thus, as a result of the Cl against H exchange first $CH_2F_2$ will be formed whereas the subsequent hydrodefluorination would generate $CH_3F$ and finally $CH_4$.

$$CHClF_2 \xrightarrow[-HCl]{H_2} CH_2F_2 \xrightarrow[-HF]{H_2} CH_3F \xrightarrow[-HF]{H_2} CH_4 \qquad (5.1)$$

However, the formation of $CHF_3$ as major compound contradicts this mechanistic path. The formation of $CHF_3$ can be explained via two distinctly different reaction pathways: i) fluorination of the $CHClF_2$ by HF formed in the course of the above discussed consecutive hydrodefluorination, ii) dismutation of $CHClF_2$ according Eq. 5.2a. Since $CHF_3$ appears always immediately as a major compound (cf. Fig. 5.8), it can not be formed as a consecutive product of Cl/F-exchange according to path i) as speculated above. Hence the only plausible explanation is a reaction path proceeding via consecutive dismutation reactions of $CHClF_2$ according to Eqs. 5.2 followed by hydrodechlorination.

$$2\ CHClF_2 \longrightarrow CHCl_2F + CHF_3 \qquad (5.2a)$$

$$2\ CHCl_2F \longrightarrow CHCl_3 + CHClF_2 \qquad (5.2b)$$

$$5\ CHClF_2 \longrightarrow 3\ CHF_3 + CHCl_2F + CHCl_3 \qquad (5.2)$$

Because the dismutation reactions are always dominating, the observed high degree of conversion is doubtless caused by the reactions according to Eqs. 5.2. In other words, dismutation reactions are dominant but hydrodechlorination reactions occur just with the products of dismutation. Since the reactivity of the halocarbons increases with the number of chlorine atoms in the saturated haloalkane molecule, the formation of hydrogenated compounds from chlorinated methane derivatives can easily be rationalized: $CHCl_2F \rightarrow CH_3F$; $CHCl_3 \rightarrow CH_4$. Since the starting compound, $CHClF_2$, dominantly undergoes dismutation reactions, the formation of the desired $CH_2F_2$ is suppressed. $CHF_3$ is too stable to undergo hydrodefluorination reactions under these conditions, hence, the product distribution as listed in Table 3 can be fully understood this way. Since in case of dominating dismutation reactions the ratio of the products $CHCl_3$ ($CH_4$) to $CHCl_2F$ ($CH_3F$) to $CHF_3$ must be constant irrespective of the conversion degree, even the ratio of the hydrogenated compounds should reflect this situation. The yield of these products is almost consistent with the interpretation of the reaction pathway and the conclusions drawn above. A separate hydrodechlorination using pure $CHCl_3$ under the same reaction conditions expectedly yielded almost complete conversion into methane this way confirming the high reactivity of the higher chlorinated methane homologous and supporting our conclusions drawn. Since dismutation turned out being a major competitive reaction to hydrodehalogenation, we have carried out separately dismutation reactions using bulk $MF_x$ (Fig. 5.7). For instance, the dismutation activity of *high surface* -$AlF_3$ is so extreme, that after once it has become catalytically active (between 200 to 250 °C) the temperature can be decreased to just 50 °C and it still yields 98 % conversion thus proving the excitingly high Lewis-acidity of this material. As a consequence, less Lewis acidic nano-metal fluorides with high surface areas were synthesized to be used as support for the Pd-metal in order to suppress dismutation reactions. However, even at $Pd^0/MgF_2$ catalysts dismutation reactions still occurred to be seen from the high amount of $CHF_3$ formed which clearly can be ascribed due to the Lewis acid sites at the nano-$MgF_2$ support. However, $CaF_2$ and $KMgF_3$ are neutral solids even in the form of nano-materials. In line with this, the activity of the catalysts for both, hydrodechlorination as well as dismutation, dropped down significantly. The results of the hydrodechlorination reactions using different kind of catalysts are summarized in Table. 5.4. A $Pd^0/C$ catalyst - widely used for hydrodehalogenation reactions - was employed for comparison reasons (Table 5.4). It

shows dismutation reactions at like to the Lewis acidic $Pd^0/MF_x$-catalysts resulting in unwanted hydrogenated products.

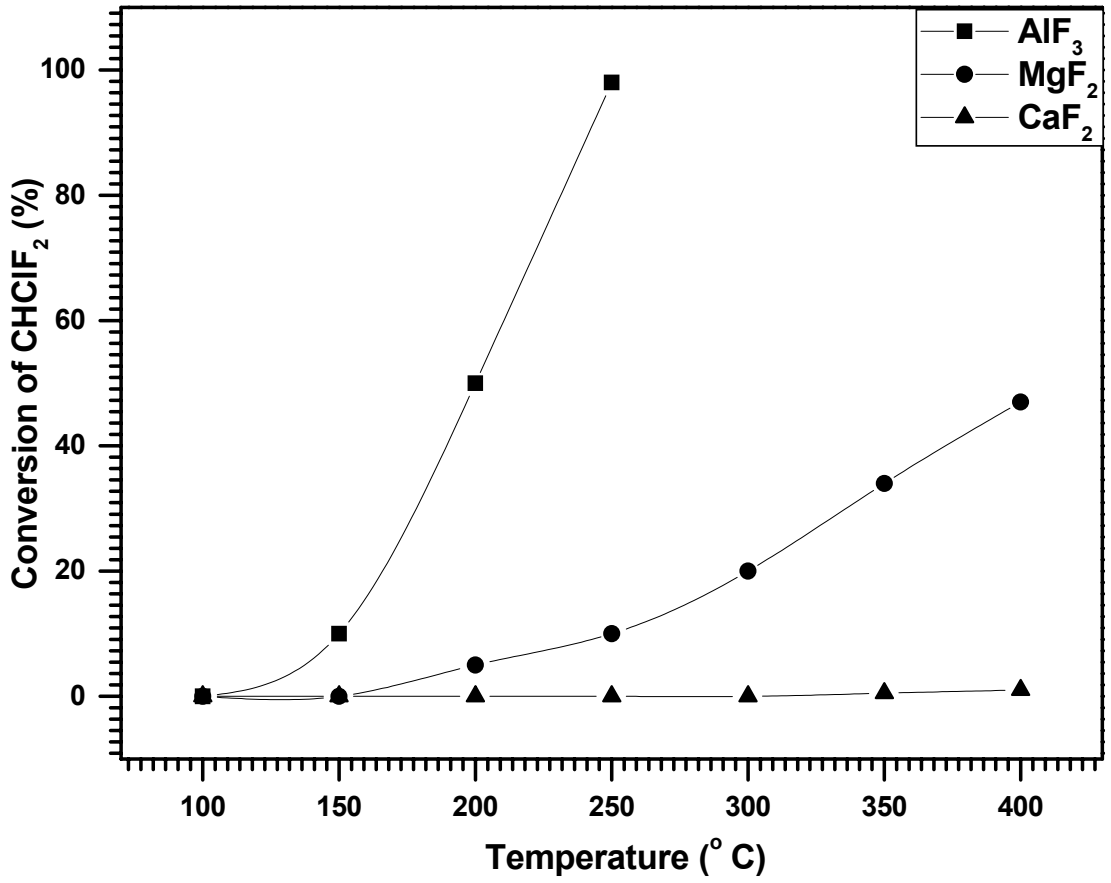


**Fig. 4.4** Conversion of $CHClF_2$ in dismutation over bulk $MF_x$. Reaction conditions: amount of catalyst = 0.4 mL, CT = 1 sec, GHSV = 3600 $h^{-1}$.

This behavior is well known since activated carbon usually contains traces of metal salts from the synthesis procedure which act as Lewis sites. Analogous Pt-based catalysts were also prepared and tested. However, their catalytic performance in both, conversion and selectivity, was significantly lower, therefore, they will not be reflected here. The significant drop in $CHClF_2$ conversion with increasing temperature over $Pd^0/AlF_3$ (Fig. 5.8) is caused by the transformation of high surface-$AlF_3$ into catalytically inactive α-AlF3, which was further confirmed by XRD of used catalyst (Fig. 5.13). Although phase transformation of high surface -$AlF_3$ into crystalline α-AlF3 does not occur at a distinct temperature but differs depending on the degree of distortion in the nano-materials[179] this phase transition temperature is un-usual low. This is unexpected behavior seems to originate from the presence of the reducing $H_2$-gas. Over $Pd^0/CaF_2$ catalysts, $CHClF_2$ conversion was low, 2.3 %, however with 78 % selectivity for $CH_2F_2$ and 22 % for methane at 320 °C without any formation of $CH_3F$ and $CHF_3$, respectively (Fig. 5.9).

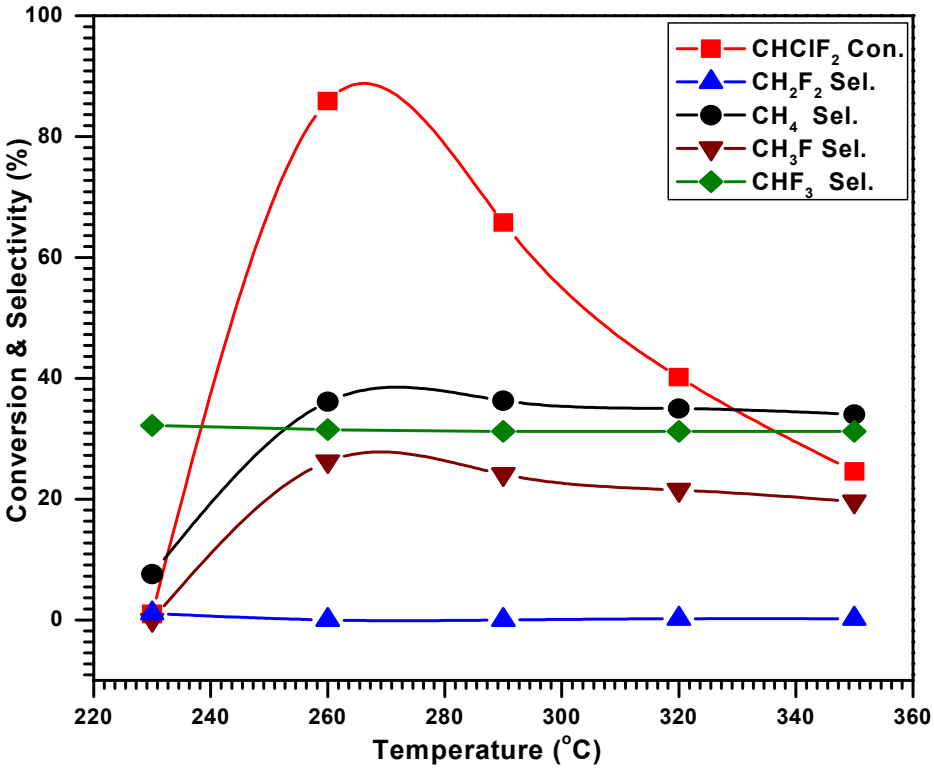


**Fig. 4.5** Hydrodehalogenation of $CHClF_2$ over $Pd^0/AlF_3$. Reaction conditions: amount of catalyst = 0.25 mL, $H_2/CHClF_2$ mole ratio =7, CT = 1 sec, GHSV = 3600 $h^{-1}$.

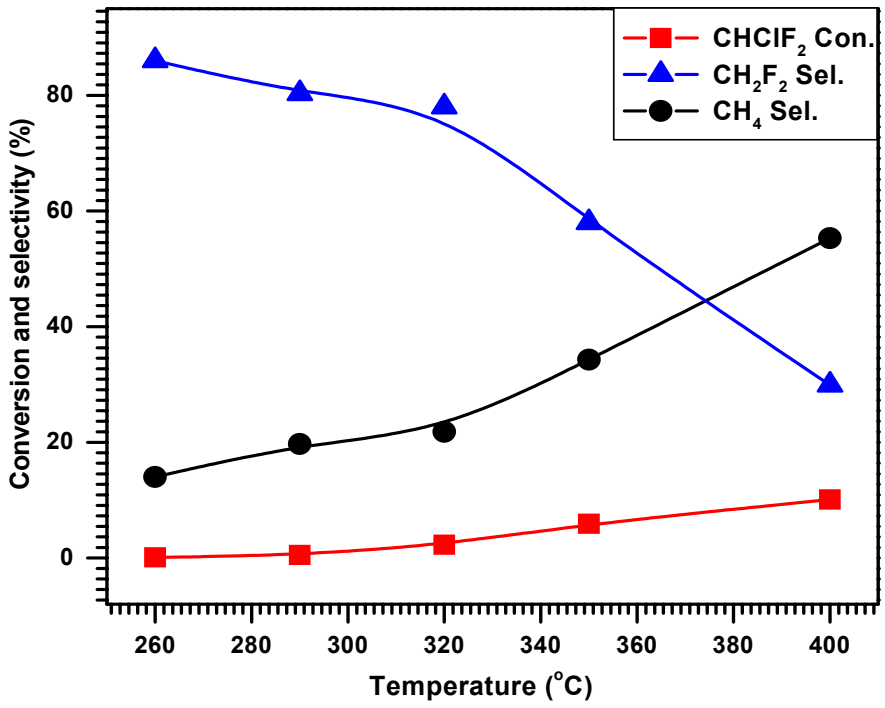


**Fig. 4.6** Hydrodehalogenation of $CHClF_2$ $Pd^0/CaF_2$. Reaction conditions: amount of catalyst = 0.25 mL, $H_2/CHClF_2$ mole ratio =7, CT = 1 sec, GHSV = 3600 $h^{-1}$.

On further temperature increase from 320 to 400 °C, the $CHClF_2$ conversion increased from 2.3 to 10 % but the selectivity for $CH_2F_2$ dropped down to 30 % whereas large amount of methane was formed (56 %). The absence of $CHF_3$ can be taken as clear evidence that dismutation –expectedly - could successfully be suppressed. The only products formed were $CH_2F_2$ and $CH_4$. The formation of these two compounds can be easily explained based on the carbene mechanism as explored for the hydrodechlorination of $CCl_2F_2$ and $CF_3$-$CCl_2F$, respectively [83, 84, 180].

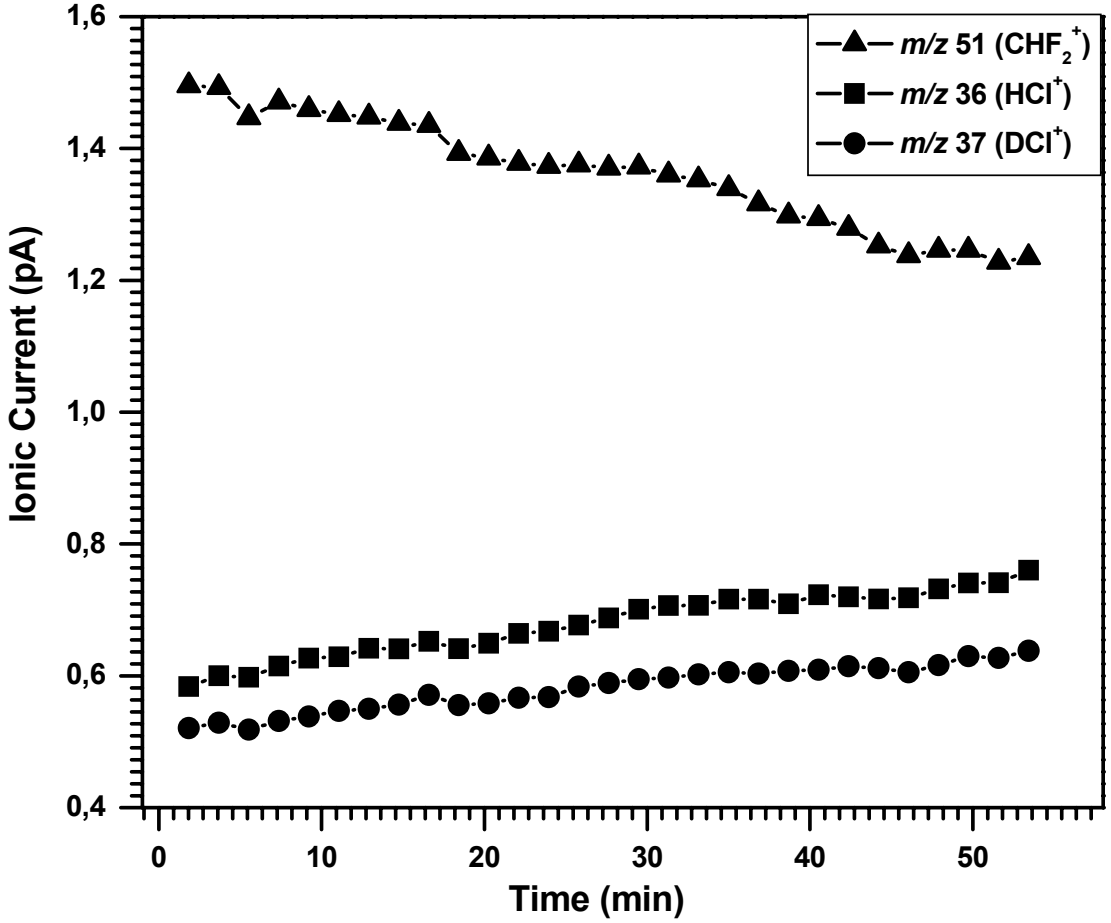


**Fig. 4.7** IC curves for *m/z* 51 ($CHF_2^+$), *m/z* 36 ($HCl^+$) and *m/z* 37 ($DCl^+$) over $Pd^0/CaF_2$ catalyst.

Our $D_2$ isotope exchange measurements with $CHClF_2$ (Fig 5.10) showed the formation of both, HCl and DCl, even in absence of $H_2$, which strongly supports the carbene mechanism. Based on the product distribution and $D_2$ isotope exchange measurement, we propose the following reaction pathway for the hydrodehalogenation of $CHClF_2$ (cf. also Scheme 5.7). In a first step, $:CF_2$ may be formed according to Eq. 5.3a becoming immediately hydrogenated by activated hydrogen at the catalysts surface.

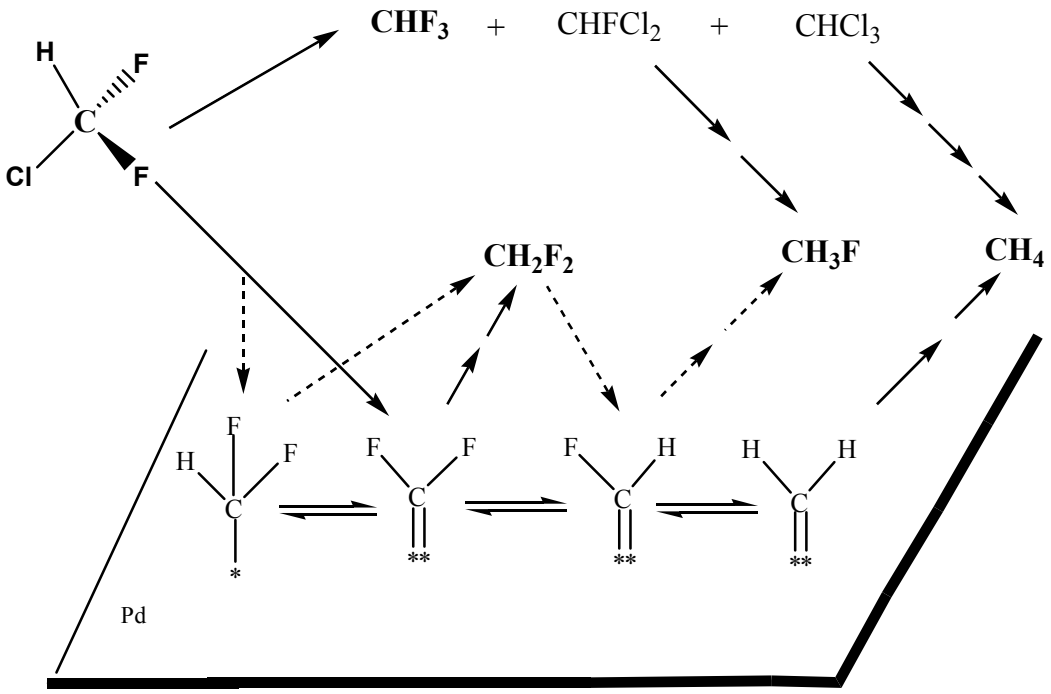


**Scheme 5.7** Proposed reaction pathway for hydrodehalogenation of $CHClF_2$.

Dismutation is the top cycle and the down cycle is hydrodechlorination

$$CHClF_2 \xrightarrow{-HCl} :CF_2 \xrightarrow{+2H} CH_2F_2 \qquad (5.3a)$$

The absence of any $CH_3F$ may be taken as a hint for the total suppression of dismutation reactions. Further on it proves that even the hydrodefluorination must occur via an intermediately formed carbene, but this time obviously a $:CH_2$ carbene will be formed according to Eq. 5.3b which further reacts with activated hydrogen forming $CH_4$.

$$CH_2F_2 \xrightarrow{-2F} :CH_2 \xrightarrow{+2H} CH_4 \qquad (5.3b)$$

The carbenes $:CF_2$ and $:CH_2$ are stable intermediates whereas a possible :CHF carbene is less probable, thus explaining the absences of $CH_3F$ because this would need the intermediate formation of a :CHF carbene. However, at high temperatures - also with pure $CaF_2$ and even without any catalyst - another reaction path becomes dominating (cf. Eq. 5.4).

### 5.4.3 Pyrolysis and co-pyrolysis

$$2CHClF_2 \xrightarrow{-2HCl} 2\,:CF_2 \longrightarrow CF_2{=}CF_2 \qquad (5.4)$$

This pyrolysis reaction (Eq. 5.4) - better it should be considered as C-C-coupling dehydrochlorination - is a well known industrial process for tetrafluoroethylene (TFE) formation which is the key intermediate for PTFE-production and was long time considered to be not influenced catalytically regarding activity and selectivity.

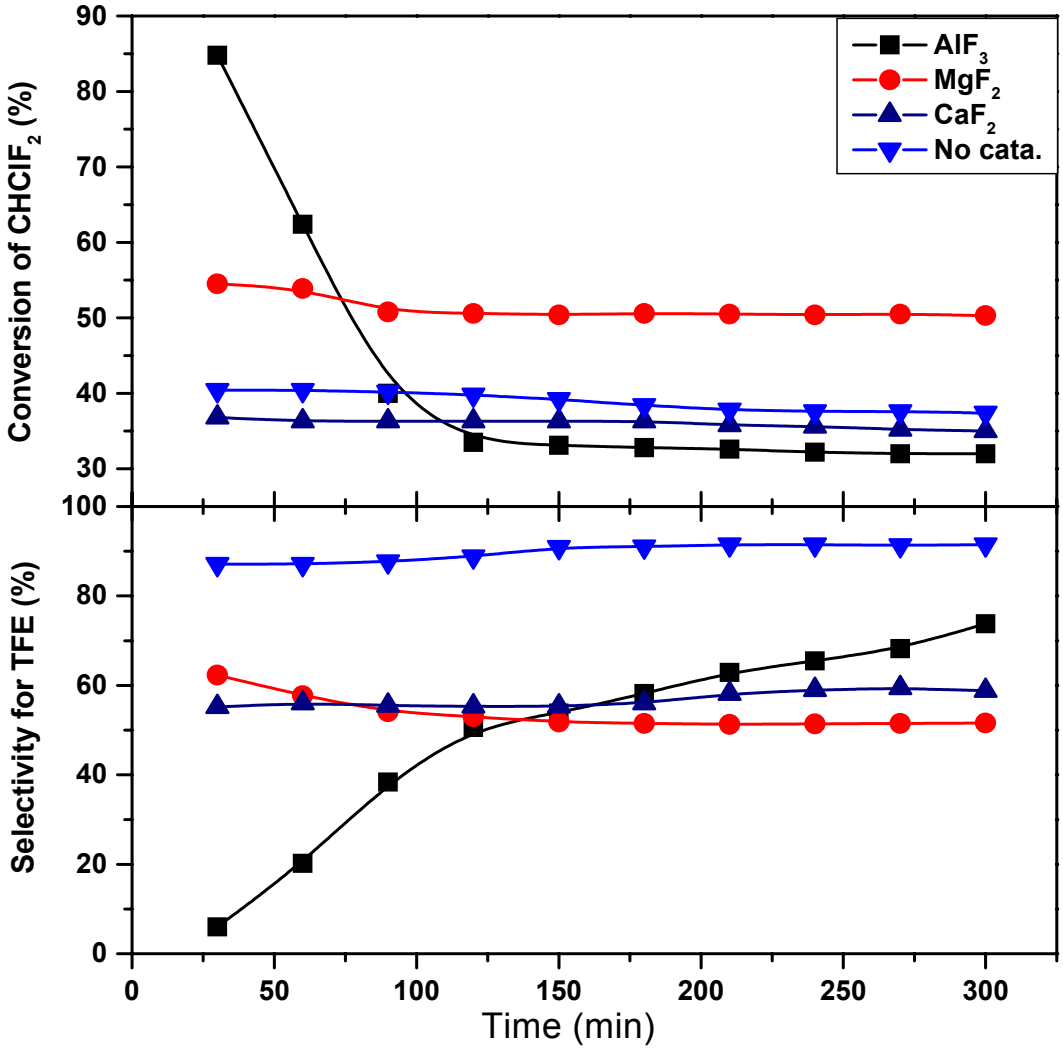


**Fig. 4.8** Pyrolysis of $CHClF_2$ at 600 °C. Reaction conditions : amount of catalyst = 0.25 mL, CT = 1 sec, GHSV = 3600 $h^{-1}$.

However, recently Sung et. al.[17] have introduced metal fluorides to increase the TFE yield, and observed a mild influence over $AlF_3$ and $CaF_2$ based bulk, mixed and Cu promoted catalysts. Hence, we have tested our sol-gel prepared *high surface* metal fluorides for $CHClF_2$ pyrolysis at 600 °C aiming enhanced TFE selectivity (Fig. 5.11). A non-catalytic run has also carried out and included for comparison. The catalytic activities we observed in our experiments follow the order $AlF_3$ > $MgF_2$ > non-catalytic > $CaF_2$ and the tetrafluoroethylene selectivity is in the order non-catalytic > $CaF_2$ > $MgF_2$ > $AlF_3$ at the initial

period (1h) of the reaction time. The $CHClF_2$ conversion decreased over $AlF_3$ with time on stream (TOS) accompanied by an increase in TFE selectivity, whereas $CHClF_2$ conversion and TFE selectivity remained stable for 300 min of TOS over $CaF_2$. Octafluorocyclobutane, hexafluoropropene, $CHF_2$-$CF_2Cl$, $CHF_2$-$CF_2$-$CF_2Cl$, $CHF_3$, and $CH_2F_2$ were the major side products.

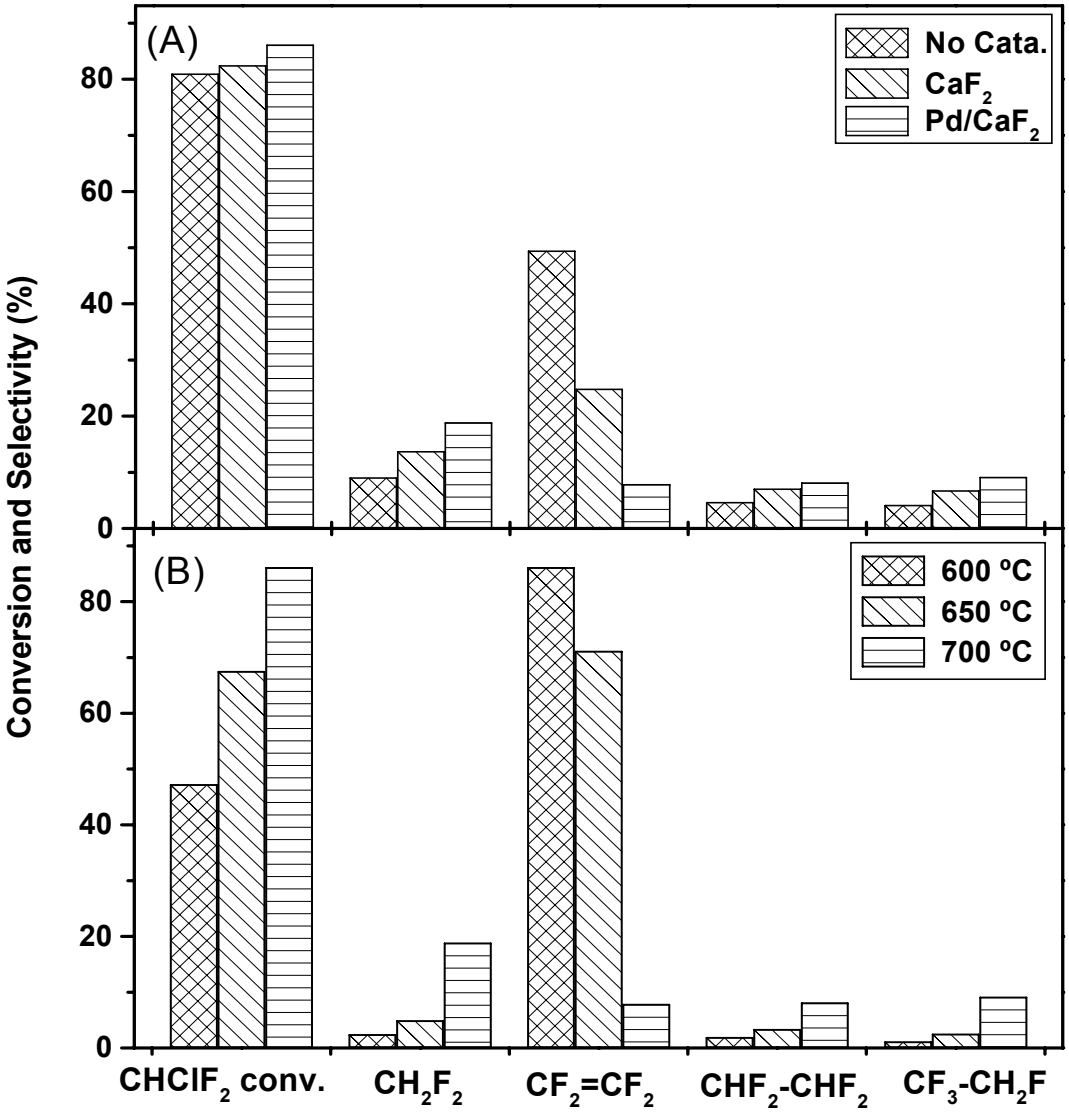


**Fig. 4.9** Co-pyrolysis of $CHClF_2$ over $CaF_2$, $Pd^0/CaF_2$ and under non-catalytic conditions at 700 °C (A). Effect of temperature (B). Reaction conditions: amount of catalyst = 0.25 mL, $H_2/CHClF_2$ mole ratio =5, temp = 700 °C, CT = 1 sec, GHSV = 3600 $h^{-1}$.

Since we were interested in $CH_2F_2$ formation, we intended to suppress the carbene dimerization according to Eq. 5.4 by adding hydrogen to the system. The dehydrochlorination of $CHClF_2$ in presence of hydrogen, co-pyrolysis, was investigated by Dolbier et al.[181] and yielded valuable compounds like $CHF_2$-$CHF_2$ and $CF_3$-$CH_2F$, along with the

formation of $CH_2F_2$ and $CF_2=CF_2$. In our experiments, expectedly higher amounts of $CH_2F_2$ were formed due to the addition of hydrogen, especially with the $Pd^0/CaF_2$ catalyst (Fig. 5.12), but still the TFE formation occurred to a noticeable degree. However, TFE is the major product in case of the non-catalytic reaction, whereas $CH_2F_2$ is the major product in case of the $Pd^0/CaF_2$ catalyzed reaction in presence of hydrogen. Interestingly enough, in all cases the formation of additional C-C-coupling products, the two isomers of $C_2H_2F_4$, in noticeable amounts were observed. Most probably, these compounds are formed by a consecutive reaction of TFE with activated hydrogen, to be seen at the significantly increased yield of the latter in presence of the $Pd^0/MF_x$ -catalysts.

**Table. 5.5** Characterization of used catalysts

| Reaction | Catalysts | Temp.[a] (° C) | Elemental Analysis (%) | | $V_{BJH\text{-}d}$[b] ($cm^3/g$) | $d_{avg}$[c] ( Å ) | $S_{BET}$[d] ($m^2/g$) |
|---|---|---|---|---|---|---|---|
| | | | C | Cl | | | |
| Hydrodehalogena- | Pd /$AlF_3$ | 350 | 2.2 | 0.4 | 0.36 | 484.9 | 30.9 |
| | Pd /$MgF_2$ | 350 | < d.l. | 0.4 | 0.14 | 150.8 | 37.6 |
| | Pd/$CaF_2$ | 400 | 0.8 | 1.1 | 0.15 | 256.5 | 24.6 |
| | Pd /$KMgF_3$ | 400 | 1.0 | 3.4 | 0.52 | 238.9 | 90.0 |
| Pyrolysis | $AlF_3$ | 600 | 19.6 | 2.3 | 0.03 | 166.6 | 9.2 |
| | $MgF_2$ | 600 | 2.2 | 0.8 | 0.03 | 362.6 | 3.8 |
| | $CaF_2$ | 600 | 20.0 | 2.4 | 0.07 | 166.6 | 18.1 |
| Co-pyrolysis | $CaF_2$ | 700 | 36.7 | 1.7 | 0.04 | 174.7 | 10.6 |
| | Pd/$CaF_2$ | 700 | 28.0 | 1.9 | 0.09 | 156.5 | 23.8 |

[a] = final reaction temperature, [b, c and d] = see footnotes table 5.4.

The used catalysts were analyzed by XRD, elemental analysis and BET surface area measurements. A significant loss in surface area (50-70 %) has been observed in case of $AlF_3$, $MgF_2$ and $CaF_2$ supported Pd catalysts used for hydrodehalogenation, but no coke formation and increase in chlorine contents (Table 5.6). In case of $Pd^0/KMgF_3$ catalyst no significant loss in surface area and no any new phases in XRD (Fig. 5.13) were observed showing its stability. On contrary, $AlF_3$ based bulk and supported Pd catalyst underwent a transformation into crystalline $\alpha$-$AlF_3$ (ASTM card no. 76-1623).

A representative bright-field TEM image of a used $Pd^0/CaF_2$ catalyst is shown in Fig. 5.14a. As can be seen, the $CaF_2$ particle size has been increased ranging now from 50 to 80 nm. Moreover, the surface of the $CaF_2$ particles seems to be flattened as a result of

the catalytic reactions which have taken place, thus being in line with the observed decrease of the BET surface area for the used catalysts (cf. Tab.5.5). Interestingly enough, the Pd-particles appear more homogeneous in the used catalysts than in the fresh ones.

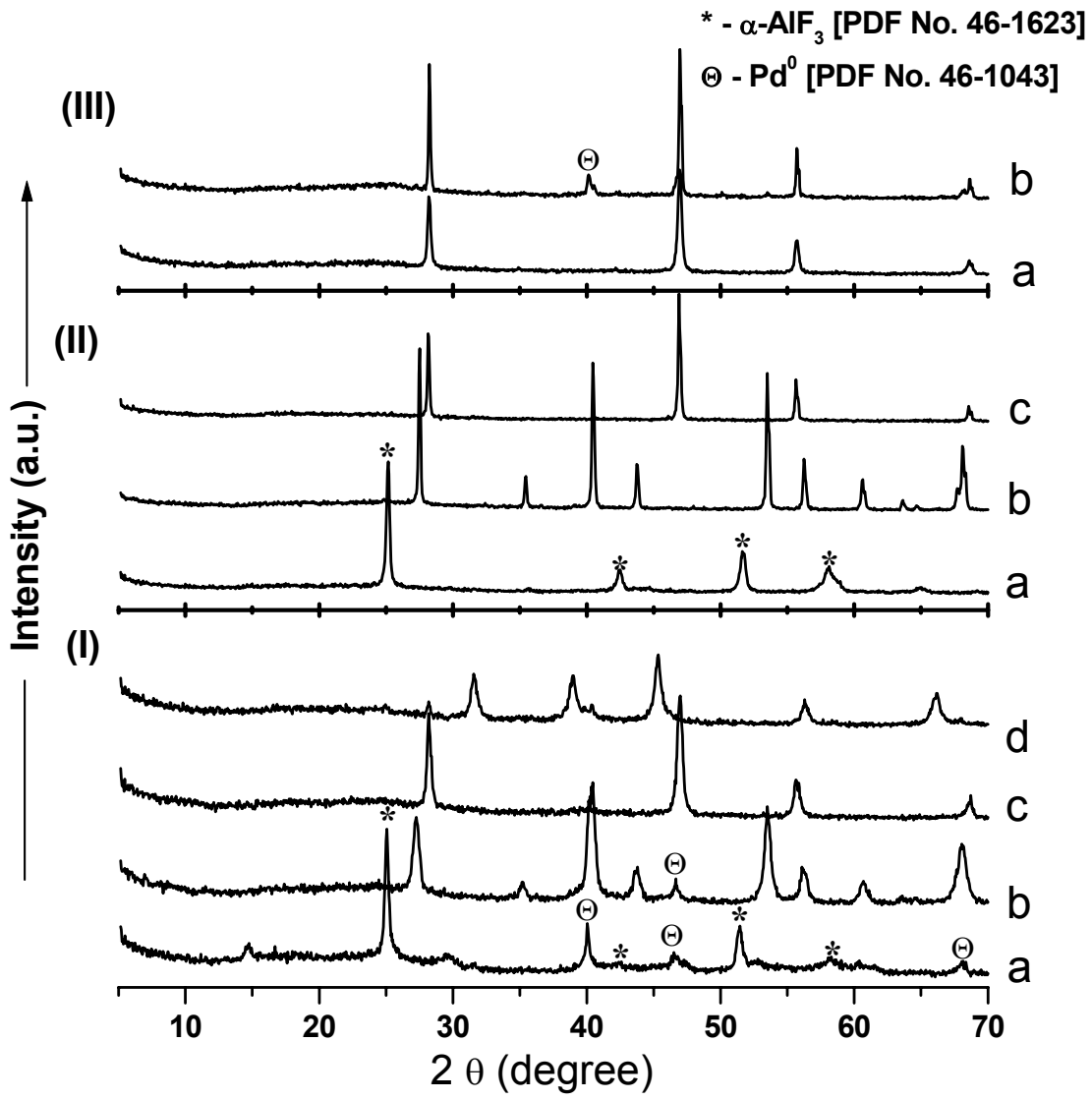


**Fig. 4.10** XRD patterns of catalysts used for (I) hydrodehalogenation (a = $Pd^0/AlF_3$, b = $Pd^0/MgF_2$, c = $Pd^0/CaF_2$ and d = $Pd^0/KMgF_3$), (II) pyrolysis (a = $AlF_3$, b = $MgF_2$ and c = $CaF_2$) and (III) co-pyrolysis (a = $CaF_2$ and c = $Pd^0/CaF_2$) of $CHClF_2$.

The majority of Pd particles are spherical with a diameter in the range of 5 to 8 nm, whereas the larger dark areas observed in the fresh sample are minor and are mainly build of agglomerates of the smaller Pd-particles. The lattice plane distance of d = 0.39(0) nm measured within the particle shown in the high-resolution TEM image of Fig. 5.14b for the used catalyst corresponds to the {100} lattice planes of Pd. However,

since $PdF_2$ and PdO also exhibit lattice constants exactly with this value the formation of $Pd^{II}$-compounds due to the intensive contact with the highly corrosive gases HCl and HF can not be excluded.

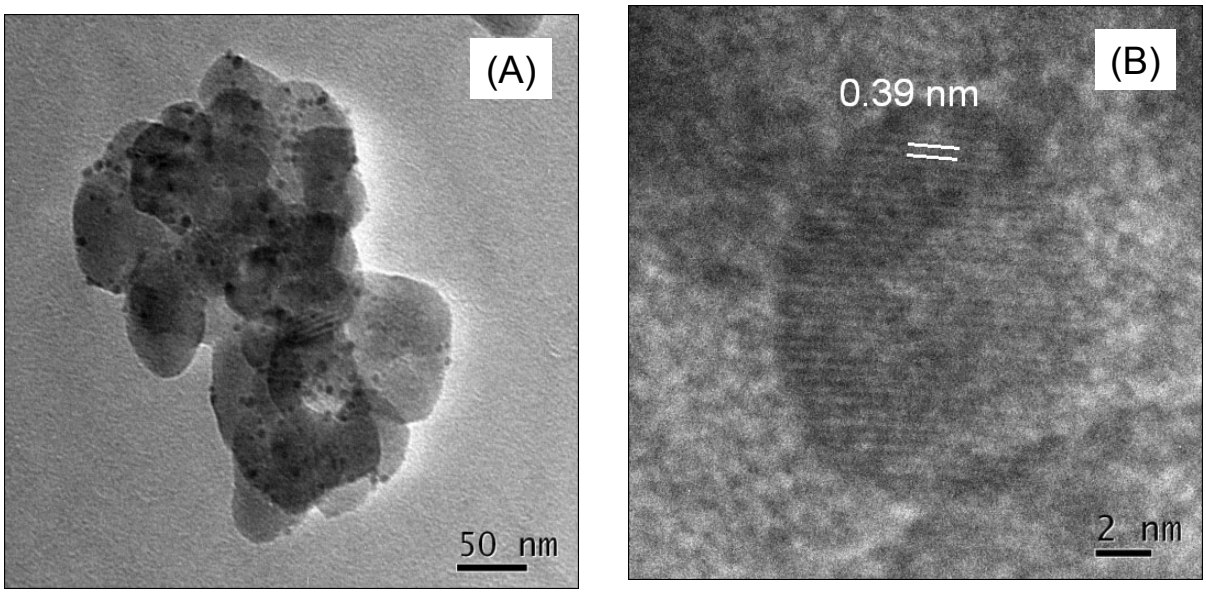


**Fig. 4.11** TEM images of $Pd^0/CaF_2$ catalysts used for hydrodehalogenation of $CHClF_2$.

### 5.4.4 Summary

Based on this study some of the important results are summarized below.

- The catalytic activity and product selectivity in hydrodehalogenation of $CHClF_2$ is strongly governed by the Lewis acidity of the $MF_x$-supports. As expected, the strong Lewis acid supports activate very efficiently the C-Cl-bond. However, it seems that also the C-F-bond becomes sufficiently enough activated to undergo halogen exchange reactions (dismutation) which is an undesired side reaction. By tuning down the Lewis acidity of the support to neutral surfaces these dismutation reactions can be totally suppressed. However, at the same time the C-Cl-bond activation goes down, too. This can be taken as a clear hint that not only the Pd-metal but to a great extend also the support has a remarkable influence on the C-X-bond activation. In order to overcome this problem, the reaction temperature has to be increased, this way opening the "window" to another unwanted side reaction – the C-C-coupling dehydrochlorination. Hence, at least three different reactions compete to each other, dismutation, hydrodechlorination and dehydrochlorination. Unfortunately, dismutation dominates in presence of Lewis acidic catalysts whereas neutral catalysts demand

higher reaction temperatures at which dehydrochlorination reactions dominate. This way, there is no "reaction window" at which hydrodechlorination of $CHClF_2$ can be performed with high conversion degrees and high selectivities at the same time. However, for fluorine free chlorocarbons, the highly Lewis acidic nano-metal fluoride supported Pd catalysts seem to be superior because competitive dismutation can not take place.

- Based of the catalytic results and H/D isotope exchange experiments a carbene mechanism involving dismutation coupled with consecutive hydrogenation reactions is proposed for hydrodehalogenation of $CHClF_2$ over metal fluorides supported Pd catalysts.
- As expected the catalysts used here are chemically robust even at elevated temperature (gas phase products are HCl and HF), however the surface area declines significantly which is not only due to the high temperature but especially due to the presence of hydrogen and/or HX in the gas phase.

# 5.5 Oxidative fluorination of benzene

## 5.5.1 Introduction

Fluorinated aromatics are widely used as intermediates for the synthesis of pharmaceuticals and agrochemicals[182] with its production exceeding 4000 metric tons per year. In particular, fluorobenzene is extensively used as a starting material for the industrial-scale manufacture of many fungicides and drugs. There are several methods for the synthesis of fluorinated compounds but the classical method for the synthesis of fluorobenzene is the Balz-Schieman reaction,[183] involving diazotization of an aromatic amine in the presence of tetrafluoroboric acid (Scheme 5.8). However, this method produces large quantities of unwanted waste such as $NaBF_4$ and NaCl and suffers from a poor atom economy associated with fine chemical manufacturing.

Cl/F-exchange has also been widely used for the synthesis of aliphatic and aromatic fluorocarbons. This method involves first step chlorination of hydrocarbon followed by catalytic Cl/F exchange with HF, yielding 2 moles of HCl for every C-F bond produced.[80] There is strong demand for an economical and environmentally benign method for conversion of hydrocarbons to fluorocarbons, selectively, without generating large quantities of waste.

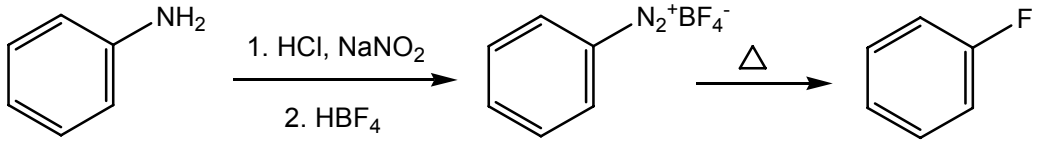


**Scheme 5.8**

The direct synthesis of C-F bonds by fluorination of C-H bonds with HF is thermodynamically unfavorable. Several fluorinating reagents, such as $XeF_2$, $CF_3OF$, $CH_3CO_2F$, $CsSO_4F$, and elemental $F_2$ have been documented in literature for oxidative or electrophilic fluorination of benzene. However synthesis of these compounds involves $F_2$, they are relatively expensive, highly toxic, and often dangerous to use, hence not used for the commercial manufacture of fluoroaromatics. Alternatively, transition metal fluorides like $CoF_3$, $KCoF_4$, $AgF_2$, $CeF_3$, and $MnF_3$ have been examined as fluorinating reagents. However, these reagents resulted into polyfluoro- or perfluoro- compounds when used for fluorination of benzene or other aromatics. Therefore, a development of metal fluorides for selective monofluorination is of great demand. Subramanian and Manzer have first disclosed $CuF_2$ based first fluorides ($E^0$ = 0.36 V) for the selective fluorination of ben-

zene[134, 185] and proposed a general principle that the reactivity, regenerability and selectivity is depend on the redox potentials [$E^0$] of the metal fluorides [Table 5.6].

**Table 5.6** Oxidation-reduction potential for metals in various oxidation states.

| $E^0 > 1$ | $1 > E^0 > 0$ | $E^0 < 0$ |
|---|---|---|
| $Co^{3+} + e^- \longleftrightarrow Co^{2+}$ | $Cu^{2+} + 2e^- \longleftrightarrow Cu^0$ | $Al^{3+} + 3e^- \longleftrightarrow Al^0$ |
| $Ag^{2+} + e^- \longleftrightarrow Ag^{1+}$ | $Fe^{3+} + e^- \longleftrightarrow Fe^{2+}$ | $Mg^{2+} + 2e^- \longleftrightarrow Mg^0$ |
| $Ce^{3+} + e^- \longleftrightarrow Ce^{2+}$ | $Ag^{1+} + e^- \longleftrightarrow Ag^0$ | $Zn^{2+} + 2e^- \longleftrightarrow Zn^0$ |
| $Pb^{4+} + 2e^- \longleftrightarrow Pb^{2+}$ | $Hg^{2+} + 2e^- \longleftrightarrow Cu^0$ | $Co^{2+} + 2e^- \longleftrightarrow Co^0$ |

For example, use of metal fluorides with $E^0 > 1$ which are strong oxidizing agent's, result in exhaustive fluorination and can only be regenerated with elemental fluorine. Those fluorides with $E^0 < 0$ are easy to prepare from HF and $O_2$ but are not strong enough to oxidize C-H bond. The most attractive fluorides are the ones with redox potential in the range $1 > E^0 > 0$. Dolbier has further studied the $CuF_2$ for oxidative fluorination of benzene[185-187] and found improvement in fluorobenzene yield with $CuF_2$:$AlF_3$ (1:2) mixed fluoride based materials.[185]

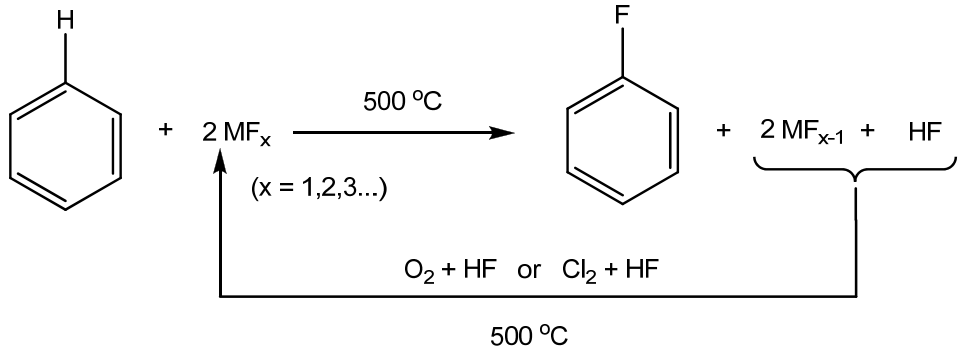


**Scheme 5.9**

In this study, the main objective was to investigate the potential of $FeF_3$ for oxidative fluorination of benzene, since it possesses a redox potential in the same range that of copper (0.77 V) and it is cheaper than copper. Second objective was to carry out catalytic fluorination in a continuous process.

## 5.5.2 Activities of $FeF_3$ and $CuF_2$ based fluorides

The results of oxidative fluorination of benzene over the different $FeF_3$ based reagents are shown in Table 5.7. The activity of $FeF_3$ samples was compared with$CuF_2$ and

$CuF_2/AlF_3$. Fluorobenzene was the only main and desired product. Difluorobenzenes (*o-* , *m-* & *p-*) were also observed in very little amount (< 0.2 %) in few cases. Iron fluorides fluorinated with the strong fluorinating agent $F_2$, were active for fluorination with fluorobenzene with yields of 1.8 % and 4 % over $FeF_3$-$F_2$ & $FeF_3/AlF_3$-$F_2$ respectively. Traces of fluorobenzene formation was observed over $FeF_3$-HF and $FeF_3$-OF, whereas chlorobenzene formed in small amount (2 %) was the only product over $FeF_3$-CF.

**Table 5.7** Oxidative fluorination of benzene with $CuF_2$ and $FeF_3$ based fluorides

| Sr. No. | Reagent | Amount of reagent used (g) | Amount of benzene used (□ L) | Yield of fluorobenzene (%) |
|---|---|---|---|---|
| 1. | $FeF_3$-HF | 1 | 394 | traces |
| 2. | $FeF_3$-HF/$O_2$ | 1 | 394 | traces |
| 3. | $FeF_3$-HF/$Cl_2$ | 1 | 394 | 0* |
| 4. | $FeF_3$-$F_2$ | 1 | 394 | 1.8 |
| 5. | $FeF_3/AlF_3$-$F_2$ | 1.6 | 250 | 4.0 |
| 6. | $CuF_2$-HF | 1 | 875 | 3.0 |
| 7. | $CuF_2/AlF_3$-HF | 1.2 | 393 | 7.5 |

**Reaction conditions**: temperature = 500 °C, flow of argon= 15 mL/min,

*- 2% chlorobenzene formation was observed.

The chlorobenzene formation suggests the presence of an intermediate chloride based phase like "ironchlrofluoride" in this material and acting as chlorinating agent. The yield of fluorobenzene was 3 % over $CuF_2$ and 7.5 % in case of $CuF_2/AlF_3$. The higher yield in cases of $AlF_3$ doped systems can be attributed to high surface area of $AlF_3$, which offers a homogeneous dispersion of active $FeF_3$ and $CuF_2$ and preventing their sintering. Additionally, the strong Lewis acidity might also be enhancing the fluorination activity. The used reagent were further successfully regenerated with $O_2$/HF or $Cl_2$/HF or $F_2$ and re-used for the next cycle.

### 5.5.3 Catalytic oxidative fluorination in presence of $Cl_2$ as oxidant

Metal fluorides prepared by sol-gel method have shown the potential to fluorinate aromatic ring and the final reduced material can be regenerated to original fluoride state via oxidative fluorination. This promoted us to examine a catalytic fluorination of benzene in a continuous process by passing benzene along with HF and oxidant. For this purpose, $Cl_2$ was used as oxidant since $O_2$ and $F_2$ are too strong and can oxidize benzene. Few ex-

periments were carried out using $FeF_3$ at different temperatures (200, 350 and 500 °C). Chlorobenzene and polychlorobenzenes were the only formed products without any traces of fluorobenzene. $Cl_2$ used for oxidation purpose is acting as chlorinating agent in presence of acidic $FeF_3$.

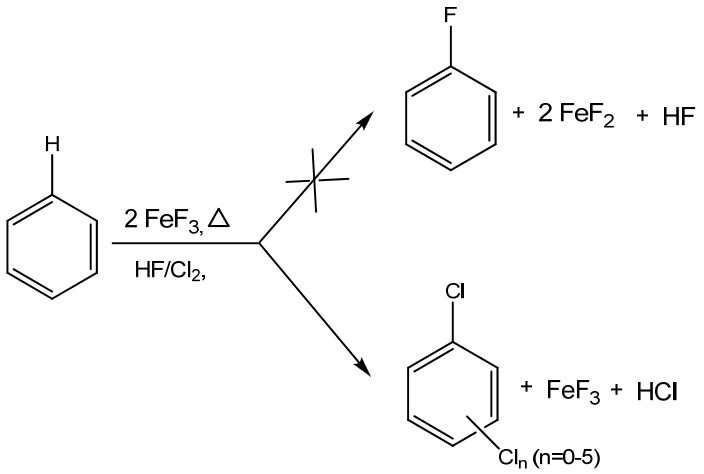


**Scheme 5.10**

## 5.5.4 Mechanistic aspects

The proposed mechanism for oxidative fluorination of benzene using $FeF_3$ is shown in scheme 5.11

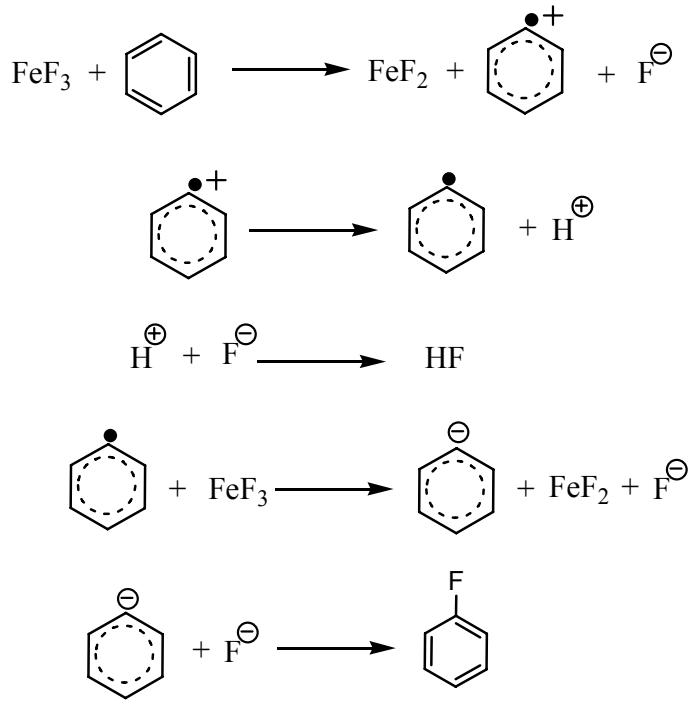


**Scheme 5.11**

### 5.5.5 Summary

- Iron(III) fluoride prepared by new sol-gel synthesis has a potential for selective monofluorination of benzene. The activity as well as the product selectivity was influenced by the structural properties of $FeF_3$ obtained by different post-fluorinations.
- $FeF_3$-$F_2$ sample obtained via sol-gel synthesis and post-fluorination by fluorine was the only better active and selective.
- Preliminary efforts have been made to carry out catalytic fluorination in continuous process by in-situ oxidizing the used low valent $FeF_2$ to $FeF_3$ but unfortunately chlorination of benzene is the dominating reaction to oxidative fluorination leading to polychlorinated benzenes as product.

# 6 SUMMARY

Using non-aqueous sol-gel fluorination of defined metal organic compounds a wide variety of nanoscopic metal fluoride based catalysts have been prepared. Bulk and surface properties of these new catalytic materials were extensively characterized as well as their efficiencies evaluated in selected reactions of academic and industrial importance.

## Synthesis

- The newly developed synthesis of nanoscopic metal fluorides involves two main steps: i) Fluorolysis of metal alkoxide solutions leading initially to a stable sol-state and after the removal of solvent to a gel precursor (reversible sol-gel process, controlled by colloid chemistry) and ii) Post-treatment of the latter via a solid-gas fluorination process to transfer the dry gel into catalytically active nanoscopic metal fluorides. The synthesis of a wide variety of metal fluorides with the expected characteristic properties has clearly shown that the fluorolysis of metal alkoxide solutions is a general sol-gel process leading to non crystalline solids containing high surface areas. As a final product of sol-gel process we obtained in all case highly but not completely fluorinated material (dry gel) containing some residual alkoxide groups and strongly bounded solvent molecules in their structures. They are catalytically inactive. By applying a mild post-fluorination step the precursors can be converted into pure metal fluorides of nanoscopic dimensions with high catalytic activity. The sol-gel synthesis step (fluorolysis) can not only be performed with metal alkoxides but in some cases also with acetylacetonates. Starting with $Fe(acac)_3$ or $Cu(acac)_2$ we successfully prepared nanoscopic iron and copper fluorides, respectively. In the case of the synthesis of "palladium-doped" metal fluorides, the two step process was extended by an additional reduction step with hydrogen to obtain highly dispersed metallic palladium in and/or on the metal fluorides. It was shown that the reduction step

can be performed at a low temperature and that does not have a significant influence on the final metal fluoride properties.

- The properties of the nanostructured metal fluorides depend on the conditions of fluorolysis (metal cation, alkoxide rest and solvents) as well as on the post-fluorination processes (fluorinating gas, time and temperature).

- The optimal conditions for the synthesis of distinctly different metal fluoride based catalysts have been worked out and a wide variety of nano-solids were prepared this way: Binary fluorides ($MgF_2$, $CaF_2$, $FeF_3$, $CuF_2$), hydroxy fluorides [$AlF_{3-x}(OH)_x$, $MgF_{2-x}(OH)_x$], complex fluorides ($KMgF_3$ and $K_3AlF_6$), metal fluoride supported Pd nanoparticles ($Pd^0/AlF_3$, $Pd^0/MgF_2$, $Pd^0/CaF_2$), host-guest fluorides ($FeF_3/AlF_3$, $CuF_2/AlF_3$). As a direct result of the new synthetic route the obtained solid catalysts possess nearly the exact properties as predicted from the $MF_x$ molecular structures, a fact which does not hold for crystalline metal fluorides. Thus, very strong ($AlF_3$) or moderate ($MgF_2$) solid Lewis acids, bi-acidic [$AlF_{3-x}(OH)_x$, $MgF_{2-x}(OH)_x$] or neutral ($CaF_2$, $KMgF_3$) compounds as well as materials with redox ($FeF_3$, $CuF_2$) or bi-functional ($Pd^0/AlF_3$, $Pd^0/MgF_2$) properties have been prepared.

# Characterization

The bulk and surface characterizations of newly prepared metal fluoride based catalysts were carried out by the following methods:

- Powder *XRD measurements* have shown that $AlF_3$ and $Pd^0/AlF_3$ samples are amorphous, but broad XRD reflections have been observed for $MgF_2$, $CaF_2$ and $KMgF_3$ based bulk as well as supported Pd samples, which are in accordance with highly distorted solid structures. The lowest intensity of Pd reflection (appearing at $2\theta = 40.1°$) in XRD of $Pd^0/CaF_2$ samples prepared by our method reveals the presence of uniform nano- sized crystalline Pd particles as well as their significantly higher dispersion in comparison to samples prepared by aqueous fluorination ($Pd^0/CaF_2$-aq) or simple impregnation ($Pd^0/CaF_2$-imp) methods.

- The *$N_2$-adsorption / desorption isotherms* obtained from BET surface area measurements have mostly shown an adsorption with characteristic H1 type hysteresis, suggesting well ordered and uniform mesoporous solid structures. The average pore diameter (40-400 Å) for all investigated samples attests the general formation of mesoporous morphology for the products of the new developed synthetic route. However, $CaF_2$

based sol-gel samples were the only exception with broad and bimodal pore size distribution.

- Multinuclear *MAS NMR spectroscopy* provided resonance signals corresponding to pure metal fluorides, but from the very large half widths of the observed signals (FWHM of kilohertz range), the high distortions in their structures were evident.

- The acidities (Lewis and/or Brønsted) of the samples were determined by *$NH_3$-TPD* and *FTIR-PAS*. $NH_3$-TPD results demonstrated that $AlF_3$ and $Pd^0/AlF_3$ samples are strong and $MgF_2$ and $Pd^0/MgF_2$ moderate Lewis acids while $CaF_2$ or $KMgF_3$ as well as their supported Pd samples are completely neutral solids. The absorption frequencies in FTIR-PAS corresponding to characteristic vibrations for chemically adsorbed pyridine on Lewis acidic (1454 $cm^{-1}$) and on Brønsted acidic (1545 $cm^{-1}$) sites were always observed with the strongest solid Lewis acid $AlF_3$, showing that despite post-fluorination and $H_2$-reduction steps, some acidic protons are still present on the solid surfaces ($AlF_3$, $Pd^0/AlF_3$). The extraordinary acidity of solid $AlF_3$ was further confirmed by dismutation reactions, which have only been performed with the two strongest Lewis acids as catalysts (solid ACF and liquid $SbF_5$).

- *XPS* of $Pd^0/MF_x$ - precursors have shown the presence of $Pd^{2+}$-ions and also some partial reduction occurring already during the post-fluorination and before the actually reduction step. The finally reduced samples contain only pure metallic Pd. Characteristic values of Pd binding energies (BE) have been determined within the $Pd^0/MF_x$ samples prepared by different synthetic routes, e.g. $Pd^0/CaF_2$ from the sol-gel synthesis has shown the lowest BE values (0.8 eV lower than the samples prepared by aqueous fluorination or impregnation methods). This fact was attributed to particle size effects and is in agreement with the formation of uniform nano sized particles during the sol-gel synthesis step. Furthermore, it was found that acidity strengths of the supports also have strong influences on Pd ($3d_{5/2}$) - BE., e. g. the measured value of 337.0 eV for $Pd^0/AlF_3$ is higher by 1.5 eV than that of $Pd^0/CaF_2$, revealing an active interaction between metal and support.

- *Microscopic studies (SEM, TEM & AFM)* were performed with the aim to determine surface morphologies and particle size distributions. Highly porous "landscapes" with homogenously distributed crystallites were observed in SEM images of $MF_x$ - samples prepared by our new sol-gel synthesis. Homogeneously dispersed Pd particles between 2 and 5 nm on the *high surface area* metal fluorides ($MF_x$ particle size distribution from 10 to 50 nm) was the main characteristic feature of these samples. In contrast, agglomerates of significantly larger Pd particles of about 100 nm were observed

within the samples prepared by either aqueous ($Pd^0/CaF_2$-aq) or impregnation ($Pd^0/CaF_2$-imp) methods, respectively. Although these samples also contain nano-sized Pd particles, they possess very low catalytic activities.

# Catalysis

The novel metal fluoride based catalysts with relevant properties were tested in various reactions of industrial and academic importance and their efficiencies were compared with those of the standard catalysts. The synthesis of fluorinated olefins (by dehydrofluorination of hydrofluorocarbons) and the reactions compelling the citronellal isomerization are two examples of catalytic reactions that are only enabled with the assistance of acids of defined functionalities and strengths. For these reactions binary metal fluorides ($MF_x$) as well as hydroxy [$AlF_{3-x}(OH)_x$, $MgF_{2-x}(OH)_x$] and host-guest fluorides were "tailored" as catalysts with adjusted Lewis and Brønsted acid strengths. As for the Suzuki cross coupling and hydrodehalogenation of $CHClF_2$, these occur exclusively on metallic surfaces. $Pd^0/MF_x$ catalysts prepared by different methods were investigated and compared. Finally, because of their promising redox properties for a possible selective synthesis of $C_6H_5F$ from $C_6H_6$, the $FeF_3$ and $CuF_2$ based catalysts were tested in the oxidative fluorination of benzene.

- *Dehydrofluorination of hydrofluorocarbons:* Due to its strong Lewis acidity, $AlF_3$ was found to be a very efficient catalyst for the activation of the C-F bond in the dehydrofluorination reactions of hydrofluorocarbons. Thus $CF_3CH_2F$, $CF_3CHFCHF_2$ and $CF_3CH_2CF_3$ were converted with high yield over *high surface* $AlF_3$ into $CF_2CHF$, $CF_3CFCHF$ and $CF_3CHCF_2$ respectively. The selective elimination of HF proceeded with a high efficiency already at quite low temperatures and the catalyst was stable for a very long period of time without any losses of activity.

- *Citronellal isomerization:* Metal fluorides were found to catalyze very efficiently the isomerization of citronellal, a reaction which represents the crucial step of the Takasago process for the industrial production of menthol. Among the catalysts tested, $AlF_3$ showed the best yield (92.5 %) in performing the cyclization of citronellal to isopulegol and the highest diastereoselectivity for the (-) isomer (91.7 %). No leaching of the catalyst in the solution was observed and the solid catalyst can be used repeatedly without significant losses in activity and selectivity.

- *Suzuki coupling* was used as a probe reaction for the $Pd^0/MF_x$ catalyst samples. The highest activity was reached with Pd nanoparticles deposited on the neutral surface of $CaF_2$. It was found that the catalytic activity of Pd for the Suzuki coupling reaction

depends on the acidity of the supports: the higher the acidity of $MF_x$, the less active are the Pd nanoparticles. $Pd^0/CaF_2$ from the sol-gel synthesis was not only a much better catalyst in comparison to the corresponding samples prepared by aqueous HF fluorination ($Pd^0/CaF_2$-aq) or impregnation ($Pd^0/CaF_2$-imp), but also slightly better as the "benchmark" Pd/C.

- *$CHClF_2$ hydrodehalogenation* was carried out in the presence of hydrogen aiming at selective formation of $CH_2F_2$ with the removal of HCl (hydrodechlorination). Unfortunately, the catalytic activity is strongly governed by the Lewis acidity of $MF_x$-supports. Lewis acidic supports activate very efficiently the C-Cl-bond, but at the same time also the C-F-bond, leading to undesired side reactions. Hence, it was found that at least three different reactions compete with each other (dismutation, hydrodechlorination, dehydrochlorination), and no "selective reaction window" leading to $CH_2F_2$ was found.

- *Oxidative fluorination of benzene*: Sol-gel prepared $FeF_3$ and $CuF_2$ were investigated as to potentials for the selective monofluorination of benzene as well as for their "regeneration abilities" ($FeF_2$ to $FeF_3$ / Cu to $CuF_2$) by $HF/O_2$ or $HF/Cl_2$. The obtained results excluded the possibility of performing fluorination in a continuous catalytic process. Although the selective fluorination of benzene was possible as a batch process, it was shown that the efficiency of the process is negatively influenced by the regeneration step. Thus, the regenerated high valent metal fluorides have shown marginal decreases in their fluorination activities.

# 7 EXPERIMENTAL

## 7.1 Catalysts Synthesis

### 7.1.1 Sol-gel synthesis of binary fluorides

The binary fluorides were prepared either directly from the corresponding alkoxides dissolved into a dry solvent (mostly alcohol) or starting with the metals, which were converted into the alkoxides just before the fluorolysis step was performed. Adding stepwise anhydrous alcoholic HF to the 0.4 - 0.5 M alkoxide solutions, until a slight stoichiomeric excess of fluorine with respect to $MF_x$ was reached, led to the formation of colloidal solutions (sols), which were stirred for about 5h and allowed to age overnight (12-15h). There after the sol went into the wet gel which was dried under vacuum at ca. 65 °C. The obtained highly but not completely fluorinated $MF_{x-y}(OR)_y$-xerogels, the so called "precursors", were post-fluorinated by applying a general time / temperature - regime with gaseous $CHClF_2$ or HF to obtain the completely fluorinated active catalysts $MF_x$. The general two step procedure is described subsequently for the synthesis of $AlF_3$ and $MgF_2$. For comparison purpose, $AlF_3$ samples were prepared also by using aqueous HF (instead of alcoholic HF) for the "sol-gel" fluorination step.

*Synthesis of high surface aluminium fluoride ($AlF_3$)*

i) Synthesis of $AlF_{3-x}(O^iPr)_x$ precursor: In a PTFE reactor (250 ml capacity), 12.161 g (59.54 mmol) of $Al(O^iPr)_3$ was placed along with 150 mL of dry isopropanol under argon atmosphere and stirred at room temperature until a clear solution was formed (~ 1h). To this 21.7 mL (8.5 M) HF/$^i$PrOH (HF/Al = 3.1) solution was added drop wise using a plastic pipette under inert atmosphere and employing ice cold water to control exothermic reaction. This led to the formation of a sol, which was stirred for 5h and allowed to age overnight (12-15h). The sol was then transformed into a thick gel which was dried

under vacuum at 65 °C with a gentle stirring. The obtained highly but not completely fluorinated $AlF_{3-x}(O^iPr)_x$-xerogel so called "precursor" was post-fluorinated to obtain a completely fluorinated $AlF_3$ [CAUTION : HF is a highly toxic and irritant compound causing severe burns if it comes in contact with skin. Appropriate safety precautions must be used]

ii) Post-fluorination of $AlF_{3-x}(OiPr)_x$ precursor: The obtained $AlF_{3-x}(OiPr)_x$ precursors was post-fluorinated with $CHClF_2$ in gas phase. 1.5 g was placed in the center of the reactor (l = 45 cm, i.d. = 6 mm) on a silver wool plug. $CHClF_2$ (flow rate 5 ml/min) and $N_2$ (20 ml/min) have been passed through, controlled by a digital mass flow meter (MKS instruments). The reactor temperature was controlled by a temperature regulator (HORST GmbH) and raised from 100 to 300 °C for 8-10 h. The white colored precursor was transformed into brownish after post-fluorination. The post-fluorinated samples were collected under inert atmosphere and stored in glove box to avoid any contact with moisture.

*Synthesis of magnesium fluoride ($MgF_2$)*

$Mg(OMe)_2$ was first prepared by reaction of Mg turnings (1.56 g, 64.2 mmol) with excess of dry methanol (100 mL) of under stirring and inert atmosphere at room temperature. A gentle heating was applied for complete and faster reaction. The formation of milky $Mg(OMe)_2$ takes lace with the evolution of $H_2$-gas. This obtained Mg(OMe) was transferred to the PTFE reactor and 15 mL (8.5 M) HF/MeOH (HF/Mg = 2.1) was added drop wise with a plastic pipette. This led to the formation of a sol, which was stirred for 5h and allowed to age overnight (12-15h). The sol was then transformed into a thick gel which was dried under vacuum at 50 °C with a gentle stirring. The obtained $MgF_{2-x}(OMe)_x$-precursor was post-fluorination with $CHClF_2$ similarly as described for $AlF_3$

*Synthesis of aluminium fluoride by aqueous HF-fluorination ($AlF_3$-aq)*

5.77 g (28.28 mmol) of $Al(O^iPr)_3$ was dissolved in 100 ml of isopropanol and 3.85 ml (22.8 M) $HF/H_2O$ was added. The obtained gel was dried and post-fluorinated with $CHClF_2$ similar to high surface $AlF_3$ prepared by non-aqueous method. The sample obtained this way was denominated as $AlF_3$-aq.

## 7.1.2 Sol-gel synthesis of hydroxyfluorides [$MF_{x-y}(OH)_y$]

*Synthesis of $AlF_{1.5}(OH)_{1.5}$*

Similar to the synthesis of high surface $AlF_3$, $AlF_{3-x}(OiPr)_x$ precursor was prepared by fluorination of $Al(O^iPr)_3$ (12 g, 56.87 mmol) with stoichiometric amount (HF/Al=1.5) of HF/ $^i$PrOH (10.37 mL, 8.5 M). The formed sol was transformed into a gel which was

dried under vacuum at 65 °C with a gentle stirring. The obtained precursor was calcined in a temperature programmed furnace at 350 °C in flowing air (75ml/min) for 5 h.

*Synthesis of $MgF_{1.4}(OH)_{0.6}$*

1.56 g (64.2 mmol) of Mg metal was allowed to dissolve in appropriate amount of dry methanol in a schlenk flask attached to reflux condenser. The reaction commences with the evolution of hydrogen gas to give a whitish colored magnesium methoxide solution which was used for the fluorination. Magnesium methoxide was fluorinated using 7.55 mL (8.5 M) anhydrous HF/MeOH (HF/Mg = 1) resulted in the formation of viscous gel, which was dried under vacuum at 50 °C with a gentle stirring to obtain $Mg(OH)_xF_{2-x}$-precursor. The obtained precursor was calcined in a temperature programmed furnace at 350 °C in flowing air (75ml/min) for 5 h.

### 7.1.3 Sol-gel synthesis of complex fluorides ($M^1M^2F_x$)

*Synthesis of $KMgF_3$*

In a PTFE reactor $Mg(OMe)_2$ prepared from Mg (0.807 g, 33.22 mmol) and excess of methanol was places along with 4.27 g (38.08 mmol) $KO^tBu$ under inert atmosphere. The mixture was stirred at room temperature to get a clear solution. Fluorination was carried out by drop wise addition of 11.7 mL (8.5 M) HF/MeOH anhydrous solution. This led to the formation of a sol, which was stirred for 5h and allowed to age overnight (12-15h). The sol was then transformed into a gel which was dried under vacuum at 50 °C with a gentle stirring. The obtained material was post-fluorination in gas phase by $CHClF_2$. $K_3AlF_6$ was prepared similarly using $KO^tBu$ and $Al(O^iPr)_3$ as starting materials.

### 7.1.4 Synthesis of metal fluorides supported Pd catalysts ($Pd^0/MF_x$)

*Sol-gel synthesis of $Pd^0/MF_x$ (M = Al, Mg, Ca)*

A typical sol-gel method used for synthesis of $Pd^0/MF_x$ involves the three major steps: i) fluorolysis of metal alkoxides in an alcoholic solvent and in presence of $Pd(acac)_2$ by anhydrous HF ii) gas phase post-fluorination of "$Pd/MF_{x-y}(OR)_y$-precursors" by HF or $CHClF_2$ followed by iii) $H_2$-treatment for the complete reduction of Pd-species.

i) Synthesis of $Pd^{II}/MF_{x-y}(OR)_y$ catalyst precursors: for the synthesis of $Pd^{II}/AlF_3$, 11.55 g (56.55 mmol) of aluminium isopropylate was dissolved in a PTFE reactor in 100 mL $^i$PrOH. 715 mg (6.72 mmol) of $Pd(acac)_2$ dissolved in 2-3 mL chloroform was added to the vigorously stirred clear solution. Liquid phase fluorination was carried out by drop wise addition of HF/$^i$PrOH (HF/Al = 3.1) lead to the formation of yellowish colored

sol, which was further stirred vigorously for 5h and aged for 12-15h. After drying at 65 °C under vacuum (4-5h) the $Pd^{II}/MF_{x-y}(OR)_y$ precursor was obtained.

ii) Post fluorination of $Pd^{II}/MF_x(OR)_y$: All catalyst precursors were fluorinated either with $CHClF_2$ or with HF gas phase. A sample of about 1.5 g was placed in the center of the reactor. $CHClF_2$ (flow rate 5 ml/min) and $N_2$ (20 ml/min) have been passed through, controlled by a digital mass flow meter (MKS instruments). The reactor temperature was controlled by a temperature regulator (HORST GmbH) and raised from 100 to 300 ºC for 5-8 h. The samples post-fluorinated with $CHClF_2$ are denoted as $Pd/MF_x$-R22. For HF-post-fluorination, the $Pd^{II}/MF_x(OR)_y$-precursor was treated with HF (HF flow = 4mL/min and argon flow = 20 mL/min) at 120 °C for 4h. The samples post-fluorinated with HF are denoted as $Pd/MF_x$-HF.

iii) Reduction of $Pd^{II}/MF_x$ post-fluorinated samples: The $Pd^{II}/MF_x$ samples, post-fluorinated with $CHClF_2$, were reduced at 200 ºC for 5 h by a mixture of hydrogen and argon (1:4; 75 mL/min) using a temperature programmed furnace and increasing the oven temperature by 3 ºC /min. $Pd^0/CaF_2$ used for $D_2$ isotope exchange experiments was reduced by using $D_2$ instead of $H_2$.

By following this general procedure and strategy used for binary fluorides $Pd^0/AlF_3$, $Pd^0/MgF_2$ and $Pd^0/CaF_2$, $Pt/AlF_3$ and $Ni/AlF_3$ were prepared.

*Synthesis of $Pd^0/CaF_2$ by aqueous HF-fluorination ($Pd^0/CaF_2$-aq)*

$Pd/CaF_2$-aq was prepared following same procedure used for non-aqueous sol-gel synthesis only instead of dry HF/MeOH aqueous HF (40 %) was used for fluorination followed by usual steps of post-fluorination with $CHClF_2$ and reduction described above.

*Synthesis of $Pd^0/CaF_2$ by impregnation ($Pd^0/CaF_2$-imp)*

$Pd/CaF_2$-imp was prepared by impregnation of 1.9 g of $CaF_2$ obtained by sol-gel method (procedure described in section 7.2.2) with 286 mg of $Pd(acac)_2$ dissolved in 10 mL of $CHCl_3$. The mixture was stirred for 2h and dried under vacuum. The obtained material was reduced directly at 200 ºC for 5 h without any further post-fluorination.

*Sol-gel Synthesis of $Pd^0/CaF_{1.5}(OH)_{0.5}$*

$Pd^0/CaF_{1.5}(OH)_{0.5}$ was prepared by fluorination of a methanolic solution of $Ca(OCH_3)_2$ and $Pd(acac)_2$ with 1.5 equivalents of aHF, thus leading to a nominal composition [$Pd/CaF_{1.5}(OH)_{0.5}$]. After removal of the solvent the sample was calcined at 350 ºC in air atmosphere and additionally reduced at 200 °C by $H_2$ gas. The Pd content was adjusted in all catalysts to 5 wt %.

## 7.1.5 Synthesis of copper and iron fluorides

*Synthesis of $FeF_3$*

6.2 g $Fe(acac)_3$ (17.55 mmol) was dissolved in dry methanol ( 100 mL) in a PTFE-reactor under inert atmosphere and fluorination was carried out using 6.46 mL (8.5 M) HF/MeOH anhydrous solution and at room temperature. There was no sol formation observed, but a gel like product was obtained. The product was dried under vacuum at 45 ºC with a gentle stirring. Following four different post-fluorination conditions were used for the obtained $FeF_3$-x$(acac)_x$-precursor and the samples are denoted according to the reagents used for post-fluorination.

i) $FeF_3$-HF: The $FeF_3$-x$(acac)_x$-precursor was post-fluorinated with HF (HF flow = 4mL/min and argon flow = 20 mL/min) at 400 °C for 4h.

ii) $FeF_3$-HF/$O_2$: The $FeF_3$-x$(acac)_x$-precursor was post-fluorinated using the mixture of HF and oxygen (HF flow = 4mL/min, $O_2$ = 2mL/min and argon flow = 20 mL/min) at 400 °C for 4h.

iii) $FeF_3$-HF/$Cl_2$: The $FeF_3$-x$(acac)_x$-precursor was post-fluorinated using the mixture of HF and chlorine (HF flow = 4mL/min, $Cl_2$ = 2mL/min and argon flow = 20 mL/min) at 400 °C for 4h.

iv) $FeF_3$-$F_2$: The $FeF_3$-x$(acac)_x$-precursor was first heated in argon at 200 °C to remove organics then post-fluorinated by $F_2$ ($F_2$ flow = ~ 5 mL/min, argon flow = 20 mL/min) at 200 °C for 2h.

*Synthesis of $CuF_2$*

9.13 g $Cu(acac)_2$ (50.26 mmol) was dissolved in dry methanol (150 mL) in a PTFE-reactor under inert atmosphere and fluorination was carried out using 12.4 mL (8.5 M) HF/MeOH anhydrous solution and at room temperature. This led to the formation of a sol, which was stirred for 5h and allowed to age overnight (12-15h). The sol was then transformed into a gel which was dried under vacuum at 50 ºC with a gentle stirring. The obtained precursor was post-fluorinated with HF (HF flow = 4mL/min and argon flow = 20 mL/min) at 400 °C for 4h.

## 7.1.6 Synthesis of host-guest fluorides

*Synthesis of $FeF_3/AlF_3$ (1:2)*

12.79 g (36.21 mmol) of $Fe(acac)_3$ and 5.98 g of $Al(O^iPr)_3$ (29.28 mmol) were dissolved separately using isopropanol (~ 150 mL) under inert atmosphere and mixed together.

This mixture was fluorinated using 38.95 mL (8.5M) dry HF/ $^{i}$PrOH solution. This led to the formation of a sol, which was stirred for 5h and allowed to age overnight (12-15h). The sol was then transformed into a gel which was dried under vacuum at 50 ºC with a gentle stirring. The obtained precursor was first heated in argon at 200 °C to remove organics then post-fluorinated by $F_2$ ($F_2$ flow = ~ 5 mL/min, argon flow = 20 mL/min) at 200 °C for 2h. The sample is denoted as $FeF_3/AlF_3$-$F_2$

*Synthesis of $CuF_2/AlF_3$ (1:2)*

4.04 g (22.25mmol) of $Cu(acac)_2$ and 9.09 g (44.53 mmol) of $Al(O^{i}Pr)_3$ were dissolved separately using isopropanol (~150 mL) under inert atmosphere and mixed together. This mixture was fluorinated using 21.7 mL (8.5M) dry HF/ $^{i}$PrOH solution. This led to the formation of a sol, which was stirred for 5h and allowed to age overnight (12-15h). The sol was then transformed into a gel which was dried under vacuum at 50 ºC with a gentle stirring. The obtained precursor was post-fluorinated with HF (HF flow = 4mL/min and argon flow = 20 mL/min) at 400 °C for 4h. The sample is denoted as $CuF_2/AlF_3$-HF

Similarly $VF_3/MgF_2$ (10 mol % of $VF_3$), $TaF_3/AlF_3$ (10 mol % of $TaF_3$), $NbF_3/AlF_3$ (10 mol % of $NbF_3$) were also prepared using respective metal precursors.

# 7.2 Catalyst Characterization

## 7.2.1 Elemental analysis

C, H, N -analysis was performed using Leco CHNS-932 analyzer with extension of VTF 900. Wherever necessary, analysis of chloride was carried out by mercurimetric titration after burning the substance in oxygen by the Schoeniger flask technique[188]. For the determination of fluoride, about 0.2-0.5 g of the sample was dissolved by melting in a mixture of 0.5 g of $K_2CO_3$ and 0.5 g of $Na_2CO_3$ in a platinum crucible for 30 min. After cooling down, the obtained mixture was dissolved in water. The fluoride content in the aqueous solution was determined with an $F^-$ sensitive electrode (FSE).

## 7.2.2 X-ray diffraction (XRD)

The phase composition and crystallinity of the samples were analyzed by X-ray powder diffraction which was carried out with XRD 7, Rich. Seiffert & Co., Freiberg using Cu Kα (Cu $K\alpha_{1,2}$, λ = 1.5418 A) radiation. The spectra were recorded at room temperature.

### 7.2.3 Solid state MAS NMR spectroscopy ($^{19}F$ and $^{27}Al$)

All MAS NMR spectra were measured on a Bruker AVANCE 400 spectrometer.

$^{19}F$ MAS NMR spectra were recorded at [$\upsilon_L$ ($^{19}F$) = 376.5 MHz] and excitation pulses length of a 2 μs using a 2.5 mm probe. The samples were characterized at room temperature at a spinning speed from 25 to 30 kHz to reduce most of the $^{19}F$ dipolar interactions and to obtain high-resolution spectra. Chemical shifts of fluorine resonance were recorded relative to $C_6F_6$ as a secondary standard ($\delta_{iso}$ = -166.61 ppm against $CFCl_3$).

$^{27}Al$ MAS NMR spectra were recorded [$\nu_L$ ($^{27}Al$) = 104.2 MHz] using an excitation pulse lengths of about 1 μs. All $^{27}Al$ spectra were collected using 2.5 mm rotors at a spinning rate of 25 kHz. 1 M aqueous solution of $AlCl_3$ was used as reference for the chemical shift of $^{27}Al$. The recycle delay was chosen as 1 s and the accumulation number was 16384, necessary for the highly disordered samples.

### 7.2.4 Thermal analysis (TA-MS)

The thermal behaviour was studied by TA-MS measurements. A NETZSCH thermoanalyzer STA 409 C *Skimmer®* system, equipped with a BALZERS QMG 421, was used to record the thermoanalytical curves (TG, DTA).[189] A DTA-TG sample carrier system with platinum crucibles (baker, 0.8 ml) and Pt/PtRh10 thermocouples was used. A sample of 44-62 mg was measured versus empty reference crucible. Constant purge gas flow of 70 ml/min $N_2$ / 10 % $H_2$ and heating rate of 10 K/min were applied. The determination of the initial ($T_i$), extrapolated onset ($T_{on}^{ex}$) and peak ($T_P$) temperatures was performed following international recommendations.[190]

### 7.2.5 $N_2$ adsorption-desorption isotherm

Nitrogen adsorption measurements were carried out at -196°C using Micromeritics ASAP 2020. The BET surface area, $S_{BET}$, was obtained by applying the BET equation.[191] The total pore volume was evaluated from the amount of nitrogen adsorbed at the highest relative pressure of 0.99. The pore-size distribution was estimated by applying the BJH method to the desorption isotherm.[192] Before each measurement, the samples were degassed at 4 $\times 10^{-3}$ mbar at 200 °C for 10-12h.

### 7.2.6 FTIR photoacoustic spectroscopy (FTIR-PAS)

The Lewis acid sites (LPy) and Brønsted acid sites (BPy) were measured with FTIR photoacoustic spectroscopy after pyridine adsorption (FTIR-PAS). Pyridine was loaded

at 150 °C, and the FTIR spectra of pyridine adsorbed samples were recorded with MTEC 200 photoacoustic cell (FTIR system 2000) Perkin-Elmer instrument at RT between 4000 and 400 $cm^{-1}$. The intensities of bands at 1445 $cm^{-1}$ (LPy), 1490 $cm^{-1}$ (LPy + BPy) and 1540 $cm^{-1}$ (BPy) were used for the evaluation of LPy and BPy.[146]

### 7.2.7 Temperature programmed desorption of ammonia ($NH_3$- TPD)

The strength of acidic sites was measured quantitatively by $NH_3$-TPD. Samples of about 200 mg were heated at 350 °C for 1h under Ar, and thereafter ammonia was loaded at 120 °C. Then, the sample was purged in a nitrogen flow until no ammonia could be detected in the gas phase. After cooling down this sample to 80 °C, desorption of $NH_3$ during heating (10 °C per minute) was monitored between 80 to 500 °C by FTIR (Perkin-Elmer System 2000). The total amount of $NH_3$ desorbed was determined by absorption in excessive sulfuric acid and back titration with NaOH.

### 7.2.8 X-ray photoelctron spectroscopy (XPS)

XP spectra were recorded on VG ESCALAB 220 iXL with AlKα radiation (1486.6 eV). The binding energy was referenced to the C1s peak at 284.8 eV.

### 7.2.9 Transmission electron microscopy (TEM)

Samples for TEM measurements were prepared by a two-step procedure. First the $Pd/MF_x$ powder was dispersed in methanol applying ultrasonic bath. Second a single droplet of the methanol- $Pd/MF_x$ dispersion was transferred to a TEM grid covered by a continuous carbon film. After complete evaporation of methanol the samples were studied in a TEM HITACHI H8110 operated at an acceleration voltage of 200 kV.

### 7.2.10 Scanning electron microscopy

SEM images were recorded using scanning electron microscope JSM-60460 (Jeol Ltd., Tokyo, Japan) combined with a Röntec (Berlin, Germany) energy dispersive X-ray (EDX) machine.

### 7.2.11 Atomic force microscopy

Samples for AFM measurements were prepared by dip coating technique using clean silicon substrates (15 × 15 mm). The film of dip coated $Pd/MF_x$-gel was prepared, dried in oven at 110 °C for 1 h and reduced at 200 °C in mixture of $H_2$ and argon for 2 h. All

AFM measurements were performed at room temperature in air using AFM instrument made up of commercial microscope head (Topometrix TMX 2000 Explorer, Santa Clara, CA), a piezoelectric scanning table (P-517.2 CL) and a Z piezo (P-753.11 C) for XY and Z positioning respectively (both from Physik instrument GmbH & Co., Waldbronn, Germany and equipped with integrated capacitive displacement sensors). Measurements were carried out by static plowing and employing contact mode. The details of the instrumental setup and measurements are given elsewhere [193]

### 7.2.12 $D_2$ isotope exchange measurements

The D/H-isotope exchange experiments were carried out in a quartz reactor with on-line coupled mass spectrometer. Initially $Pd^0/CaF_2$ (200 mg) was heated under vacuum at 350 °C for 2 h, and thereafter 5 mbar of a gas mixture from $CHClF_2$ and $D_2$ (1:7) was loaded thereafter. The changes of the gas phase composition during the reaction were analyzed by MS technique using a quadrapole mass spectrometer QMG4211 (Pfeiffer Vacuum GmbH). The detailed instrumental setup is described elsewhere.[39]

## 7.3 Catalytic Reactions

### 7.3.1 Dehydrofluorination of hydrofluorocarbons

Dehydrofluorination experiments were carried out as like to the hydrodechlorination. Ina typical experiment about 200 mg of the catalysts was loaded in quartz reactor and activated at 400 °C for 2 h. $CF_3$-$CH_2F$ (134a) was passed over catalyst by using $N_2$ as diluent ($N_2$/134a = 4). The HF formed during the reaction was neutralized using dilute alkali (1M NaOH) solution. The reaction products were analyzed by offline gas chromatograph (GC, HP-5890) on PoraPLOT Q capillary column (30m × 0.32mm i.d.). The products were further confirmed by $^1$H NMR spectroscopy.

### 7.3.2 Citronellal isomerization

Liquid phase citronellal isomerization reactions were carried out in closed sample vials. 1 ml of citronellal was along with 5 mL toluene was placed in reaction vial and a 50 mg catalyst was added in to vial. The reaction mixture was stirred at 80 °C. Reaction samples were collected after certain intervals and analyzed offline by gas chromatography Shimadzu 2010 instrument fitted with capillary column (DB-5, *l* = 30 m, i.d. = 0.25 mm, f.t. = 0.25μm ). Distereoselectivity for isopulegol formation was measured by using $^1$H NMR.

### 7.3.3 Hydrodehalogenation of $CHClF_2$

The reactions under investigation were carried out in a fixed bed microflow reactor. Appropriate amounts of catalysts were placed at the center of a quartz reactor (*l* = 45 cm, i.d. = 4 mm) and flow rates of the gases were controlled by mass flow controllers. In a typical run of hydrodehalogenation, 0.25 mL volume of catalyst (~ 180-280 mg $Pd^0/MF_x$) was used. Contact time (CT) was 1 sec and the gas hourly space velocity (GHSV) 3600 $h^{-1}$, a $H_2/CHClF_2$ molar ratio of 7 was maintained by adjusting the flow rates: $CHClF_2$ (1.5ml/min), $H_2$ (10.5 ml/min) and $N_2$ (3 ml/min). The reaction products were passed through 1M NaOH and analyzed by offline gas chromatograph (GC, HP-5890) on PoraPLOT Q capillary column (30m × 0.32mm i.d.). No efforts were made to quantify HCl and/or HF amounts in course of the reactions since it has been proven under analogous conditions in our lab[104] that the carbon mass balance was almost complete (100%) within the GC-detection limits. Hence, the amount of hydrogenated C1-compounds corresponds to the HX amount formed. To keep the analysis reasonably easy to handle, the amount of HX was, therefore, not followed. The identity of all products was additionally confirmed by $^{19}F$ and $^{1}H$ NMR. Dismutation, pyrolysis, co-pyrolysis of $CHClF_2$ and hydrodechlorination of $CHCl_3$ was carried out similarly. The used reaction conditions are described below tables and/ figures.

### 7.3.4 Suzuki Coupling

In a 50 mL two-necked round bottomed flask equipped with a condenser and magnetic stirrer 1 mmol 4-BA (187.4 mg), 1.5 mmol PBA (181.7 mg), 3 mmol $K_3PO_4$ ( 636.5 mg), and 35 mg catalyst were mixed in 12 mL of a 5:1 mixture of DMA (N, N-dimethyl acetamide) and water as solvent and heated at 108 ºC under stirring. The reaction progress was monitored by gas chromatography using Shimadzu 2010 instrument fitted with capillary column (Inowax) and flame ionization detector. About 0.5 mL of reaction sample was collected with a plastic syringe, dried over $MgSO_4$ and analyzed offline after centrifugation. Products were identified by GC-MS (Shimadzu-17A, MS-QP-5000) and quantified by GC using authentic samples for calibration.

### 7.3.5 Oxidative fluorination of Benzene

For the oxidative fluorination of benzene 0.5-1 g of fluoride based fluorinating reagent was loaded in a stainless steel reactor (*l* = 50 cm, i.d. = 6 mm). Vapors of Benzene in stoichiometric amount with fluoride required for selective monofluorination (e.g. 875 µL of benzene for 1 gm $CuF_2$ or 394 µL of benzene for 1 gm of $FeF_3$) were passed using $N_2$ as carrier gas (flow rate 15 mL/min) at 500 °C C. The products were condensed using

ice-cold water and then analyzed by gas chromatography using Shimadzu 2010 instrument fitted with capillary column (Inowax) and flame ionization detector and confirmed by $^{19}F$, $^{1}H$ & $^{13}C$-NMR spectroscopy.

# 7.4 Chemicals, suppliers and purities

## Solids

| | |
|---|---|
| Aluminium *iso*-propylate, $Al(O^iPr)_3$ | Aldrich, 98+ % |
| Calcium, turnings, Ca | Aldrich, 99 % |
| Copper(II) acetylacetonate | Strem Chemicals, 98+% |
| Iorn(III) acetylacetonate | Aldrich, 98% |
| Magnesium, turnings, Mg | Aldrich, 99.98 % |
| Nickel(II) acetylacetonate | Strem Chemicals, 95% |
| Phenylboronic acid, $C_6H_5B(OH)_2$ | Aldrich, 97 % |
| Palladium(II) acetylacetonate | Fluka, 34 % Pd |
| Platinum(II) acetylacetonate | Aldrich, 97 % |
| Potassium *tert*-butoxide | (Aldrich, 95 %) |
| Tripotassium phosphate, $K_3PO_4$ | Alfa Aesar, 97% |

## Liquids

| | |
|---|---|
| Benzene, $C_6H_6$ | Fluka, 99.5 % |
| 4-bromoanisole | Acros organics, 98% |
| Citronellal | Across, 93 % |
| Chloroform, $CHCl_3$ | Across, 99+ % |
| Chloroform-d, $CDCl_3$ | Chemotrade, 99.8 % |
| Hydrofluoric acid | Fluka, 40% in $H_2O$ |
| Isopropanol, | Across, 99.5 % |
| Methanol, $CH_3OH$ | Across, 99+ % |
| N,N-dimethyl acetamide | Fluka, 99.5 % |
| Toluene, $C_6H_5$-$CH_3$ | Across, 99.5 % |

## Gases

| | |
|---|---|
| Argon, Ar | Air Liquid, 4.8 |

| | |
|---|---|
| Chlorine, $Cl_2$ | Air Liquid, 2.8 |
| Chlorodifluoromethane, $CHClF_2$ | Solvay Fluor GmbH, 99 % |
| Deuterium, $D_2$ | Messer Griesheim, 99.7 % |
| Fluorine, $F_2$ | Air Liquid, 99 % |
| 1,1,1,3,3,3-hexafluoropropane, $C_3H_2F_6$ | ABCR GmbH Co.KG, 97 % |
| 1,1,2,3,3,3-hexafluoropropane, $C_3H_2F_6$ | ABCR GmbH Co.KG, 98 % |
| Hydrogen fluoride, HF | Solvay Fluor GmbH, |
| Nitrogen, $N_2$ | Air Liquid, 5.0 |
| Oxygen, $O_2$ | Air Liquid, 5.0 |
| 1,1,1,2-tetrafluoroethane, $C_2H_2F_4$ | Solvay Fluor GmbH, 99 % |

# References


[1] R. A. Sheldon, I. Arends, U. Hanefeld, *Green Chemistry and Catalysis*, Wiley-VCH Verlag GmbH & Co. KGaA, Weinheim, 2007.

[2] E. Kemnitz, D.H. Menz, *Prog. Solid State. Chem.*, 26 (1998) 97-153.

[3] E. Kemnitz, J. M. Winfield *Advanced Inorganic Fluorides: Synthesis, Characterization and Applications,* Elsevier Amsterdam, 2000, 367-401.

[4] S. Rüdiger, U. Groß, E. Kemnitz, *J. Fluorine Chem.*, 128 (2007) 353-368.

[5] S. Rudiger, E. Kemnitz, *Dalton Trans.*, (2008) 1117-1127.

[6] T. Krahl, E. Kemnitz *J. Fluorine Chem.,* 127 (2006) 663-678.

[7] M. Wojciechowska, M. Zielinski, M. Pietrowski, *J. Fluorine Chem.,* 120 (2003) 1-11.

[8] B. Coq, F. Medina, D. Tichit, A. Morato, *Catal.Today*, 88 (2004)127-137.

[9] N. Herron, W. Farneth, *Adv. Mater.,* 8 (1996) 959-968.

[10] S. V. Kuznetsov, V. V. Osiko, E. A. Tkatchenko, P. P. Fedorov, *Russ. Chem. Rev.*, 75 (2006) 1065-1082.

[11] J. Lucas, F. Smektala, J. I. Adam, *J. Fluorine Chem.,* 114 (2002) 113-118.

[12] M. Ahrens, G. Scholz, S. Redmer, E. Kemnitz, *Solid State Sci.*, 9 (2007)833-837.

[13] H. Krüger, E. Kemnitz, A. Hertwig, U. Beck, *Thin Solid Films,* 516 (2008) 4175-4177.

[14] S. Fujihara, M. Tada, T. Kimura, *Thin Solid Films*, 304 (1997) 252-255.

[15] P. A. Sermon, R. Badheka, *J. Sol-Gel Sci. Technol.*, 32 (2004) 149-153.

[16] G. G. Amatucci, N. Pereira *J. Fluorine Chem*., 128 (2007) 243-462.

[17] D. J. Sung, D. J. Moon, S. Moon, J. Kim, S.-I Hong, *Appl. Catal. A,* 292 (2005) 130-137.

[18] C. J. Brinker, G. W. Scherer, *Sol Gel Science: The Physics and Chemistry of the Sol Gel Processing*, Academic Press, San Diego, 1990.

[19] R. Tleimat-Manzalji, T. Manzalji, G. M. Panjonk, *J. Non-Cryst. Solids,* 147 (1992) 744-747.

[20] E. Kemnitz, U. Groß, S. Rüdiger, C. S. Shekar, *Angew. Chem. Int. Ed.,* 42 (2003) 4251-4254.

[21] S. K. Rüdiger, U. Groß, M. Feist, H. A. Prescott, S. C. Shekar, S. I. Troyanov, E. Kemnitz, *J. Mater. Chem.,* 15 (2005) 588-597.

[22] A. Wander, C. L. Bailey, S. Mukhopadhyay, B. G. Searle, N. M. Harrison, *J. Mater. Chem.*, 16 (2006) 1906-1910.

[23] A. Wander, C. L. Bailey, B. G. Searle, N. M. Harrison, *J. Phys. Chem. B,* 109 (2005) 22935-22938.

[24] K. O. Christe, D. A. Dixon, D. McLemore, W. W. Wilson, J. A. Sheehy, J. A. Boatz, *J. Fluorine Chem.,* 101 (2000) 151-153.

[25] J. Krishna Murthy, U. Gross, S. Rüdiger, V. V. Rao, V. V. Kumar, A. Wander, C. L. Baily, N. M. Harrison, E. Kemnitz, *J. Phys. Chem., B*, 111 (2006) 8314-8319.

[26] M. Wojciechowska, K. Nowinska, W. Kania, A. Nowacka, *React. Kinet. Catal. Lett.,* 2 (1975) 229-236.

[27] J. Haber, M. Wojciechowska, *J. Catal.,* 110 (1988) 23-36.

[28] J. Haber, M. Wojciechowska, *Catal. Lett*., 10 (1991) 271-278.

[29] M. Wojciechowska, S. Lomnicki, J. Bartoszwicz, J. Glosar, *J. Chem. Soc. Faraday Trans.,* 91 (1995) 2207-2211.

[30] M. Wojciechowska, J. Haber, S. Lomnicki, *J. Mol. Catal*., 141 (1999) 155-170.

[31] M. Wojciechowska, M. Pietrowski, S. Lomnicki, B. Czajka, *Catal Lett*., 46 (1997) 63-69.

[32] M. Wojciechowska, M. Pietrowski, S. Lomnicki, *J. Chem. Soc. Chem. Commun*., (1999) 463-464.

[33] A. Maliowski, W. Juszczyk, J. Pielaszek, M. Bonarowska, M. Wojciechowska, Z. Karpinski, *J. Chem. Soc. Chem. Commun*., (1999) 685-686.

[34] V. Narayana Kalevaru, B. David Raju, V. Venkat Rao, A. Martin, *Catal. Commun*., 9 (2008) 715-720.

[35] V. Narayana Kalevaru, B. David Raju, S. Khaja Masthan, V. Venkat Rao, P. Kanta Rao. *Catal. Lett*., 84 (2002) 27-30.

[36] J. Krishna Murthy, U. Groß, S. Rüdiger, E. Kemnitz, *Appl. Catal.*, A 278 (2004) 133-138.

[37] J. Krishna Murthy, U. Groß, S. Rüdiger, E. Ünveren, W. Unger, E. Kemnitz, *Appl. Catal.*, A 282 (2005) 85-91.

[38] H. Berndt, H. B. Zahed, E. Kemnitz, M. Nickkho-Armiy, M. Pohl, J. M. Winfield, *J. Mater. Chem*., 12 (2002) 3499-3507.

[39] I. K Murwani, E. Kemnitz, T. Skapin, M. Nickkho-Amiry, J. M. Winfield, *Catal. Today*, 88 (2004) 153-168.

[40] M. Wojciechowska, R. Fiedorow, *J. Fluorine Chem.*, 15 (1980) 443-452.

[41] J. Krishna Murthy, U. Gross, S. Rüdiger, E. Kemnitz, J. M. Winfield, *J. Solid State Chem.*, 179 (2006) 743-750.

[42] G. Scholz, I. Dörfel, D. Heidemann, M. Fiest, R. Stösser, *J. Solid. State. Chem.*, 179 (2006) 1119-1128.

[43] P. T. Patil, A. Dimitrov, H. Kirmse, W. Neumann, E. Kemnitz, *Appl. Cata. B,* 78 (2008) 80-91.

[44] P. T. Patil, A. Dimitrov, J. Radnik, E. Kemnitz, *J. Mater. Chem.,* 18 (2008) 1632-1635.

[45] K. Tanabe, *Bull. Chem. Soc. Japan,* 47 (1974) 1064.

[46] E. Kemnitz, Y. Zhu, B. Adamczyk, *J. Fluorine Chem.* 114 (2002) 163-170.

[47] R. H. Hina, R. Kh. Al-Fayyoumi, *J. Mol. Catal. A.*, 207 (2004) 27-33.

[48] N. Herron, D. L. Thorn, R. L. Harlow, F. Davidson, *J. Am. Chem. Soc.*, 115 (1993) 3028-3029.

[49] W. Kleist, C. Haeßner, O. Storcheva, K. Köhler, *Inorg. Chim. Acta*, 359 (2006) 4851-4854.

[50] A. K. Ghosh, R. A. Kydd, *Catal. Rev.-Sci. Eng.*, 27 (1985) 539-589.

[51] V. R. Choudhary, *Ind. Eng. Chem., Prod. Res. Dev.*, 16 (1977) 12-22.

[52] T. Skapin, E. Kemnitz, *Catal. Lett.,* 40 (1996) 241-247.

[53] L. M. Rodiguez, J. Alcaraz, M. Hernandez, M. Dufaux, Y. Ben Taarit, M. Vinat, *Appl. Catal A,* 189 (1999) 53-61.

[54] R. I. Hegde, M. A. Barteau, *J. Catal.,* 120 (1989) 387-400.

[55] L. E. Manzer, *Science*, 249 (1990) 31-35.

[56] K. Early, V. I. Kovalchuk, F. Lonyi, S. Deshmukh, J. L. d'Itri, *J. Catal.* 182 (1999) 129-127.

[57] O. Boese, W. E. S. Unger, E. Kemnitz, S. L. M. Schoeder, *Phys. Chem. Chem. Phys.*, 4 (2002) 2824-2832.

[58] T. Skapin, E. Kemnitz, *J. Non-Crys. Solids*, 225 (1998) 163-167.

[59] H. Bozorgzadeh, E. Kemnitz, M. Nickkho-Amiry, T. Skapin, J. M. Winfield, *J. Fluorine Chem.,* 107 (2001) 45-52.

[60] H. Bozorgzadeh, E. Kemnitz, M. Nickkho-Amiry, T. Skapin, J. M. Winfield, *J. Fluorine Chem.,* 110 (2001) 181-189.

[61] J. L. Delattre, P. J. Chupas, C. P. Grey, A. M. Stacy, *J. Am. Chem. Soc.* 123 (2001) 5364-5365.

[62] E. K. L. Y. Hajime, J. L. Delattre, A. M. Stacy, *Chem. Mater.,* 19 (2007) 894-902.

[63] Fujihara, in *Handbook of Sol-Gel science and Technology*, ed. S. Sakka, Kulwer, Boston, 2005, vol. 1, pp. 203-224.

[64] C. Zhao, S. Feng, Z. Chao, C. Shi, R. Xu, J. Ni, *Chem. Commun*., (1996) 1641-1642.

[65] D. Dambournet, A. Demourgues, C. Martineau, S. Pechev, J. Lhoste, J. Majimel, A. Vimont, J.-C. Lavalley, C. Legein, J.-Y. Buzare, F. Fayon, A. Tressaud, *Chem. Mater.,* 20 (2008) 1459-1469.

[66] M. Pitrowski and M. Wojciechowska, *J. Fluorine Chem.,* 128 (2007) 219-223.

[67] A. M. Mailhot, A. Elyamani, R. E. Riman, *J. Mater. Res.*, 7 (1992) 1534-1540.

[68] H. -X. Mai, Y. -W. Zhang, R. Si, Z.-G. Yan, L. Sun, L. P. You, C. -H. Yan, *J. Am. Chem. Soc.,* 128 (2006) 6426-6436.

[69] J.Labeguerie, P. Gredin, J. Marot, A. De Kazak, *J. Solid State Chem.*, 178 (2005) 3197-3205.

[70] S. Fijihara, T. Kato, T. Kimura, *J. Sol-Gel Sci. Technol.,* 26 (2003) 953-956.

[71] S. Fujihara, *Recent Res. Dev. Mater. Sci.*, 3 (2002) 619-631.

[72] A. C. Pierre, G. M. Pajonk, *Chem. Rev.,* 102 (2002) 4243-4265.

[73] A. P. Wight, M. E. Davis, *Chem. Rev.,* 102 (2002) 3589-3614.

[74] Z.-L. Lu, E. Lindner, H. A. Mayer, *Chem. Rev.,* 102 (2002) 3543-3578.

[75] J. A. Schwarz, C. Contescu, A. Contescu, *Chem. Rev.,* 95 (1995) 477-510.

[76] L. L. Hench, J. K. West, *Chem. Rev.,* 90 (1990) 33-72.

[77] T. Krahl, R. Stösser, E. Kemnitz, G. Scholz, M. Feist, G. Silly, J.- Y. Buzare, *Inorg. Chem.* 42 (2003) 6474-6483.

[78] L. Kolditz, V. Nitzsche, G. Heller, R. Stoesser, *Z. Anorg. Allg. Chem.*, 476 (1981) 23-32.

[79] E. Kemnitz, A. Hess, *J. Prakt. Chem.,* 334 (1992) 591-595.

[80] L. E. Manzer, V. N. M. Rao, *Adv. Catal.*, 39 (1993) 329.

[81] B. Coq, J. M. Cognion, F. Figueras, D. Tournigant, *J. Catal.*, 141 (1993) 21-33.

[82] B. Coq, F. Figueras, S. Hub, D. Tournigant, *J. Phys. Chem.*, 99 (1995) 11159-11166.

[83] S. Deshmukh, J. L. d'Itri, *Catal. Today*, 40 (1998) 377-385.

[84] E. J.A.X. van de Sant, A. Wiersma, M. Makkee, H. van Bekkum, J. A. Moulijn, *Recl. Trav. Chim. Pays-Bas.*, 115 (1996) 505-510.

[85] P. K. Ramarao, K. S. Ramarao, A. H. Padmasri, *CATTECH* , 7 (2003) 218-225.

[86] A. Morato, F. Medina, J. E. Sueiras, Y. Cesteros, P. Salagre, L. C. De Menorval, D. Tichit, B. Coq, *Appl. Catal. B,* 42 (2003) 251-264.

[87] A. Morato, C. Alonso, F. Medina, Y. Cesteros, P. Salagre, J. E. Sueiras, D. Tichit, B. Coq, *Appl. Catal. B*, 32 (2001) 167-179.

[88] A. Morato, C. Alonso, F. Medina, J. L. Garreta, J. E. Sueiras, Y. Cesteros, P. Salagre, D. Tichit, B. Coq, *Catal. Lett.*, 77 (2001) 141-146.

[89] A. Morato, C. Alonso, F. Medina, P. Salagre, J. E. Sueiras, R. Terrado, A. Giralt, *Appl. Catal. B*, 23 (1999) 175-185.

[90] H. Yu, E. M. Kennedy, A. D. Azar, Y. Sakata, B. Z. Dlugogorski, *Ind. Eng. Chem. Res.*, 44 (2005) 3442-3452.

[91] S. C. Kellner, V. N. M. Rao, US 4872381, (1989) to Du Pont.

[92] S. C. Kellner, F. N. Tebbe, US 5243108, (1993).

[93] H. P. Aytam, V. Akula, K. Janamanchi, S. R. R. Kamaraju, K. R. Panja *J. Phys. Chem.*, B 106 (2002) 1024-.

[94] J. Estelle, J. Ruz, Y. Cesteros, R. Fernandez, P. Salagre, F. Medina, J. E. Sueiras, *J. Chem. Soc. Farady Trans.*, 92 (1996) 2811-2816.

[95] A. Hess, E. Kemnitz, A. Lippitz, W. E. S. Unger, D. -H. Menz *J. Catal.*, 148 (1994) 270-280.

[96] E. Kemnitz, A. Hess, G. Rother, S. Troyanov, *J. Catal.*, 159 (1996) 332-339.

[97] J. Krishna Murthy, U. Groß, S. Rüdiger, E. Ünveren, E. Kemnitz, *J. Fluorine Chem.,* 125 (2004) 937-949

[98] S. Rüdiger, G. Eltnany, U. Groß, E. Kemnitz, *J. Sol-Gel Sci. Technol.,* 41 (2007) 209-311.

[99] G. Eltnany, S. Rüdiger, E. Kemnitz, *J. Mater. Chem.,* 18 (2008) 2268-2275.

[100] G. Eltnany, Ph. D. Thesis, Humboldt University of Berlin, 2007.

[101] B. Adamczyk, Ph. D. Thesis, Humboldt University of Berlin, 2000.

[102] E. Ünveren, Ph. D. Thesis, Humboldt University of Berlin, 2004.

[103] G. Scholz, R. König, J. Petersen, B. Angelow, *Chem. Mater.,* 20 (2008) 5406-5413.

[104] A. Hess, E. Kemnitz, *Appl. Catal. A,* 82 (1992) 247-257.

[105] K.-U. Niedersen, K. Fiedler, E. Kemnitz, *J. Fluorine Chem.*, 126 (2005) 1017-1027.

[106] E. Kemnitz, K.-U. Niedersen, *J. Catal.,* 155 (1995) 283-289.

[107] K.-U. Niedersen, E. Schreier, E. Kemnitz, *J. Catal.,* 167 (1997) 210-214.

[108] O. Bose, B. Adamczyk, K. Fiedler, E. Kemnitz, *Catal. Lett.,* 54 (1998) 211-216.

[109] B. Adamczyk, A. Hess, E. Kemnitz, *J. Mater. Chem.*, 6 (1996) 1731-1735.

[110] H. Yang, H. Quan, M. Tamura, A. Sekiya, *J. Mol. Catal. A: Chem.,* 233 (2003) 99-104.

[111] H. Lee, H. S. Kim , H. Kim, W. S. Jeong, I. Seo, *J. Mol. Catal. A: Chem.,* 136 (1998) 85-89.

[112] Y. Zhu, K. Fiedler, St. Rüdiger, E. Kemnitz, *J. Catal.,* 219 (2003) 8-16.

[113] I. K. Murwani, K. Scheurell, E. Kemnitz, *Catal. Commun.*, (2008) DOI: 10.1016/j.catcom.2008.08.025.

[114] K. Scheurell, G. Scholz, A. Pawlik, E. Kemnitz, *Solid State Sci.,* 10 (2008) 873-883.

[115] K. Scheurell, E. Kemnitz, *J. Mater. Chem.,* 15 (2005) 4845-.4853.

[116] H. A. Prescott, Z-J. Li, E. Kemnitz, J. Deutsch, H. Lieske, *J. Mater. Chem.*, 15 (2005) 4616-4628.

[117] S. S. Pröckl, W. Kleist, K. Köhler, *Tetrahedron*, 61 (2005) 9855-9859.

[118] S. M. Coman, S. Wuttke, A. Vimont, M. Daturi, E. Kemnitz, *Adv. Synth. Catal.*, (2008) communicated.

[119] S. Wuttke, S. M. Coman, G. Scholz, H. Kirmse, A. Vimont, M. Daturi, S. L. M. Schroeder, E. Kemnitz, *Chem Eur. J.*, (2008) communicated.

[120] A. Mantilla-Ramirez, G. Ferrat-Torres, J.M. Dominguez, C.Aldana-Rivera, M. Bernal, *Appl. Catal. A* 143 (1996) 203-214.

[121] L. M. Rodriguez, J. Alcaraz, M. Hernandez, M. Dufaux, Y. Ben. Taarit, *Appl. Catal. A*, 189 (1999) 53-61

[122] M. Moreno, A. Rosas, J. Alcaraz, M. Hernandez, S. Toppi, P. Da Costa, *Appl. Catal. A*, 251 (2003) 369-383.

[123] S. M. Coman, P. T. Patil, S. Wuttke, E. Kemnitz, (unpublished results)

[124] F. J. Urbano, J. M. Marinas, *J. Mol. Catal.*, 173 (2001) 329-345.

[125] F. Alonso, I. P. Beletskaya, M. Yus, *Chem. Rev.*, 102 (2002) 4009-4091.

[126] J. Tsuji, *Palladium Reagents and Catalysts,* John Wiley & Sons Chichester, UK, 2004.

[127] R. B. Bedford, C. S. J. Cazin, D. Holder, *Coord. Chem. Rev.*, 248 (2004) 2283-2321.

[128] H.-U. Blaser, A. Indolese, A. Schnyder, H. Steiner, M. Studer, *J. Mol. Catal. A: Chem.,* 173 (2001) 3-18.

[129] C. Yang, C. Wan and C. Lee, in *Encyclopedia of Nanoscience and Nanotechnology*, ed. H. L. Nalwa, ASP, Valencia, CA, USA, 2004, vol. 8, pp. 397–413.

[130] D. Astruc, *Inorg. Chem.,* 46 (2007)1884-1894.

[131] R. L. Powell, A. P. Sharratt, WO 9605157 (1996) to ICI.

[132] S. Otsuka, K. Tani, T. yamagata, S. Akutagawa, H. Kumobayashi, M. Yagi, EP 68506, 1972 (to Takasago).

[133] N. Miyaura, A. Suzuki, *Chem. Rev.*, 95 (1995) 2457-2483.

[134] M. A. Subramanian, L. E. Manzer, *Science*, 297 (2002) 1665.

[135] M. L. Toebes, J. A. van Dillen, K. P. de Jong *J. Mol. Catal.,* 173 (2001) 75-98.

[136] S. Rüdiger, U. Gross, S. Chandra Shekhar, V. Venkat Rao, M. Sateesh, E. Kemnitz, *Green Chem.,* 4 (2002) 541-545.

[137] M. Ahrens, Ph. D. Thesis, Humboldt University of Berlin, 2008.

[138] M. Ahrens, G. Scholz, M. Feist, E. Kemnitz, *Solid State Sci.,* 8 (2006) 798-806.

[139] C. Stosiek, G. Scholz, G. Eltnany, Rainer Bertram, E. Kemnitz, *Chem. Mater.*, 20 (2008) 5687-5697.

[140] S. Wuttke, G. scholz, S. Rüdiger, E. Kemnitz, *J. Mater. Chem.,* 17 (2007) 4980-4988.

[141] P. J. Chupas, M. F. Ciraolo, J. C. Hanson. C. P. Grey, *J. Am. Chem. Soc.*, 123 (2001) 1694-1702.

[142] R. König, G. Scholz, E. Kemnitz, *Solid State Nucl. Magn. Reson.*, 32 (2007) 78-88.

[143] R. König, G. Scholz, T. H. Thong, E. Kemnitz, *Chem. Mater.,* 19 (2007) 2229-2237.

[144] R. König, G. Scholz, R. Bertram, E. Kemnitz, *J. Fluorine Chem.,* 129 (2008) 598-606.

[145] R. K. Harris, P. Jackson, *Chem. Rev.,* 91(1991) 1427-1440.

[146] A. Hess, E. Kemnitz, *J. Catal.*, 149 (1994) 449-457.

[147] G. Leofanti, M. Padovan, G. Tozzola, *Catal. Today*, 41 (1998) 207-219.

[148] B. Schleich, D. Schmeisser, W. Gopel, *Surf. Sci.,* 191 (1987) 367-384.

[149] G. E. Millward, R. Hartig, E. Tchuikow-Roux *J. Phys. Chem.,* 75 (1971) 3195-3201.

[150] G. E. Millward, E. Tchuikow-Roux, *J. Phys. Chem.,* 76 (1972) 292-298.

[151] V. N. M. Rao, M. A. Subramanian, US 6031141 (2000) to DuPont.

[152] V. N. M. Rao, S. A. C. Sievert, R. N. Miller, WO 2006/050215, (2006), to Du-Pont.

[153] R. N. Miller, M. J. Nappa, V. N. M. Rao, A. C. Sievert, US 2006/0106263, (2006) to DuPont.

[154] J. O. Bledsoe, Jr., in *Encyclopedia of Chemical Technology (Kirk-Othmer), 4th Ed.,* Wiley-Interscience, New York, 1998, vol. 23, p. 858.

[155] Y. Nakatani, K. Kawashima, *synthesis*, (1978) 147-148.

[156] A. Corma, M. Renz, *Chem. Commun.*, (2004) 550-551.

[157] F. Iosif, S. Koman, V. Parvulescu, P. Grange, S. Delsarte, D. De Vos, P. Jacobs, *Chem. Commun.,* (2004) 1292-1293.

[158] P. Martens, F. Verpoort, A.-N. Parvulescu, D. De Vos, *J. Catal.,* 243 (2006) 7-13.

[159] Y. Nie, W. Niah, S. Jaenicke, G.-K. Chuah, *J. Catal.*, 248 (2007) 1-10.

[160] K. A. De Silva Rocha, P. A. Robles-Dutenhefner, E. M. B. Sousa, E. F. Kozhevnikova, I. V. Kozhevnikov, E. V. Gusevskaya, *Appl. Catal. A*, 317 (2007) 171-174.

[161] A. F. Trasarti, A. J. Marchi, C. R. Apesteguia, *J. Catal.,* 247 (2007) 155-165.

[162] P. Mäki-Arvela, N. Kumar, D. Kubicka, A. Nasir, T. Heikkilia, V.-P. Lehto, R. Sjöholm, T. Salmi, D. Y. Murzin, *J. Mol. Cata*. A: *Chem,* 240 (2005) 72-81.

[163] S. Imachi, K. Owada, M. Onaka, *J. Mol. Catal.* A: *Chem*, 272 (2007) 174-181.

[164] K. A. De Silva, P. A. Robles-Dutenhefner, E. M. B. Sousa, E. F. Kozhevnikova, I. V. Kozhevnikov, E. V. Gusevskaya, *Catal. Commun.*, 5 (2004) 425-429.

[165] Z. Yongzhong, N. Yuntong, S. Jaenicke, G.-K. Chuah, *J. Catal.*, 229 (2007) 404-413.

[166] N. T. S. Phan, M. Van Der Sluys, C. W. Jones, *Adv. Synth. Catal.*, 234 (2006) 609-679.

[167] D. D. Das, A. Sayari, *J. Catal.,* 246 (2007) 60-65.

[168] F.-Xavier Felpin, T. Ayad, S. Mitra *Eur. J. Org. Chem.*, (2006) 2679-2690.

[169] R. Narayanan, M. A. El-Sayed, *J. Catal.,* 234 (2005) 348-355.

[170] R. G. Heidenreich, K. Khöler, J. G. Krauter and J. Pietsch, *Synlett,* 7 (2002) 1118-1122.

[171] K. Shimizu, R. Maruyama, S. Komai, T. Komama, Y. Kitayama, *J. Catal.*, 227 (2007) 2002-209.

[172] B. M. Choudhary, S. Madhi, N. C. Chowdari, M. L. Kantam, B. Sreedhar, *J. Am. Chem. Soc.,* 124 (2002) 14127-14136.

[173] M. L. Kantam, K. B. Shiva Kumar, P. Srinivas, B. Sreedhar, *Adv. Synth. Catal.,* 349 (2007) 1141-1149.

[174] S. V. Ley, C. Ramarao, R. S. Gordon, A. B. Homes, A. J. Morrison, I. F. McConvey, I. M. Shirley, S. C. Smith, M. D. Smith, *Chem. Commun.*, 10 (2002) 1134-1135.

[175] C. K. Y. Lee, A. B. Holmes, S. V. Ley, I. F. McConvey, B. Al-Duri, G. A. Leeke, R. C. D. Santos, J. P. K. Seville, *Chem. Commun.*, 16 (2005) 2175-2177.

[176] A. L. Henne, *J. Am. Chem. Soc.*, 59 (1937) 1400-1401.

[177] P. B. Logsdon, WO 24696 A1, (2000) to AlliedSignal Inc.

[178] J. L. Butcher, P. D. Bujac, WO 9506625 A1, (1995) to ICI.

[179] U. Gross, S. Rüdiger, E. Kemnitz, K.-W. Brzezinka, S. Mukhopadhyay, C. Bailey, A. Wander, N. Harrison, *J. Phys. Chem.,* A 111 (2007) 5813-5819.

[180] V. Y. Borovkov, F. Lonyi, V. I. Kovalchuk, J. L. d'Itri, *J. Phys. Chem. B*, 104 (2000) 5603-5609.

[181] R. Romelar, V. Kruger, J. Marshall, W. R. Dolbier Jr., *J. Am. Chem. Soc.* 123 (2001) 6767-6772.

[182] C. D. Hewitt, M. J. Silvester, *Aldrichimica Acta*, 21 (1988) 3-10.

[183] G. Balz, G. Schiemann, *Chem. Ber.,* 60 (1927) 1186.

[184] M. A. Subramanian, US 006166273 A, (2000) to DuPont.

[185] K. M. Janmanchi, W. R. Dolbier, Jr., *Org. Process Res. Dev.*, 12 (2008) 349-354.

[186] W. R. Dolbier, Jr., G. Buvaneswari, US 007012165 B2 (2006) to university of Fluorida.

[187] W. R. Dolbier, Jr., G. Buvaneswari, US 2005009689 A1 (2005) to university of Fluorida.

[188] Schöniger, *Mikrochim. Acta*, (1956) 869.

[189] E. Kaisersberger, E. Post, *Thermochim. Acta,* 295 (1997) 73-93.

[190] J. O. Hill (Ed.), For Better Thermal Analysis III, Special Edn. of the Intern. Confederation for Thermal Analysis (ICTA), 1991.

[191] S. Brunauer, P. H. Emmett, E. J. Teller, *J. Am. Chem. Soc.*, 60 (1938) 309-319.

[192] E.P. Barret, L.G. Joyner, P.P. Halenda, *J. Am. Chem. Soc.,* 73 (1953) 373-380.

[193] M. Heyde, K. Rademann, B. Capella, M. Geuss, H. Sturm, T. Spangenberg, H. Niehus, *Rev. Sci. Instrum,* 72 (2001) 136-141.

# List of Abbreviations, Acronyms, and Symbols

| | |
|---|---|
| Å | Angstrom, 10 pm, $10^{-10}$ m |
| $acac_2$ | acetylacetonate |
| ACF | aluminium chlorofluoride |
| AFM | atomic force microscopy |
| Ar | argon |
| a.u. | arbitrary units |
| aq | aqueous |
| BE | binding energy |
| BET | Brunauer-Emmett-Teller and their adsorption model |
| BJH | Barret-Joyner-Halenda and their adsorption model |
| BPy | Pyridine coordinated to Brønsted acid sites |
| °C | degree Celsius |
| Cat | catalyst |
| CFC's | chlorofluorocarbons |
| CT | contact time |
| DMA | N,N-dimethyl acetamide |
| DTA | differential thermal analysis |
| DTG | differential thermogravimetry |
| $E^0$ | oxidation reduction potential |
| eV | electron volt |
| FC | fluorocarbon |
| FID | flame ionization detector |
| FTIR | Fourier transform infrared spectroscopy |
| FWHM | full width at half maximum |
| GC | gas chromatography |
| GHSV | gas hourly space velocity |
| h | hour |
| HFCs | hydrofluorocarbons |
| HCFCs | hydrochlorofluorocarbons |
| *HS*- | high surface area |
| Hz | hertz |
| IC | ionic current |
| imp | impregnation |
| $^{i}Pr$ | isopropyl |
| LPy | pyridine coordinated to Lewis acid sites |
| $N_2$ | nitrogen |

| | |
|---|---|
| NMR | nuclear magnetic resonance |
| M | molar |
| mmol | millimole |
| MAS | magic angle spinning |
| -Me | methyl |
| $MF_x$ | metal fluorides |
| MS | mass spectroscopy |
| *m/z* | mass fragment |
| μL | microliter |
| nm | nanometer |
| -OR | alkoxide |
| PAS | photoacoustic spectroscopy |
| PDF No. | powder diffraction file number |
| $P/P_0$ | relative pressure |
| ppm | parts per million |
| -pre | precursor |
| -post | post-fluorinated sample |
| R-12 | dichlorodifluoromethane |
| R-22 | chlorodifluoromethane |
| RT | room temperature |
| S | selectivity for the defined product |
| $S_{BET}$ | specific surface area calculated by BET method |
| SEM | scanning electron microscopy |
| STP | standard temperature pressure |
| T | temperature |
| TEM | transmission electron microscopy |
| TG | thermo gravimetric analysis |
| TPD | temperature programmed desorption of ammonia |
| X | conversion of defined reactant |
| XRD | X-ray diffraction |
| XPS | X-ray photoelectron spectroscopy |
| Y | yield of the defined product |
| QCC | quadrupole coupling constants |
| FSE | fluoride sensitive electrode |
| d.s. | diastereoselectivity |
| δ | chemical shift |
| Δ | Heat |

# List of Publications

## Articles in Scientific Journals

1. **P. T. Patil**, A. Dimitrov, J. Radnik, E. Kemnitz. Sol-gel synthesis of metal fluoride supported Pd catalysts for Suzuki coupling *J. Mater. Chem.* 18 (2008) 1632.
2. **P. T. Patil**, A. Dimitrov, H. Kirmse, W. Neumann, E. Kemnitz. Non-aqueous sol-gel synthesis, characterization and catalytic properties of metal fluorides supported palladium nanoparticles. *Appl. Catal. B* : 78 (2008) 80.
3. S. M. Coman, **P. T. Patil**, S. Wuttke, E. Kemnitz. Cyclization of citronellal over heterogeneous inorganic fluorides-highly chemo- and diastereoselective catalysts to (±)-isopulegol. *Chem. Commun.* (2009) 460.
4. **P. T. Patil**, A. Dimitrov, E. Kemnitz. Low temperature selective dehydrofluorination of hydrofluorocarbons over high surface metal fluorides. (manuscript in preparation).
5. **P. T. Patil**, A. Dimitrov, E. Kemnitz. Iron (III) fluoride: Synthesis, characterization and potential for oxidative fluorination of benzene. (manuscript in preparation).
6. **P. T. Patil**, K. M. Malshe, P. Kumar, M. K. Dongare, E. Kemnitz. Benzoylation of anisole over borate zirconia solid acid catalyst. *Catal. Commun.* 3 (2002) 411.
7. **P. T. Patil**, K. M. Malshe, S. P. Dagade, and M. K. Dongare. Regioselective nitration of o-Xylene to 4-nitro o-xylene over solid acid catalysts. *Catal. Commun.* 4 (2003) 429.
8. S. K. Maurya, **P. T. Patil**, S. B. Umbarkar, M. K. Gurjar, M. K. Dongare, S. Rüdiger and E. Kemnitz. Vapour phase oxidation of 4-fluorotoluene over Vanadia-Titania catalyst. *J. Mol. Catal*. 234 (2005) 51.
9. S. K. Maurya, M. K. Gurjar, K. M. Malshe**, P. T. Patil**, M. K. Dongare and E. Kemnitz. Nitration of Fluorotoluenes by using Nitric acid over Solid Acid Catalysts. *Green chem.* 5 (2003) 720.
10. K. M. Malshe, **P. T. Patil**, S. B. Umbarkar and M. K. Dongare. Selective C- methylation of phenol with methanol over borate zirconia solid catalyst. *J. Mol. Catal*. 212 (2004) 337.
11. S. B. Umbarker, A. V. Biradar, S. M. Mathew, S. B. Shelke, K. M. Malshe, **P. T. Patil**, S. P. Dagade, S. P. Niphadker and M. K. Dongare. Vapor phase nitration of benzene using mesoporous $MoO_3/SiO_2$ solid acid catalyst. *Green Chem.* 8 (2006) 488.
12. B. R. Madaje, **P. T. Patil,** S. S. Shindalkar, S. B. Benjamin, M. S. Shingare, M. K. Dongare. Facile transesterification of ketoesters with alcohols using borate zirconia solid acid catalyst. *Catal. Commun.* 5 (2004) 411.
13. S. S. Shindalkar, B. R. Madaje, R. V. Hangarge, **P. T. Patil,** M. K. Dongare and M. S. Shingare Borate zirconia mediated Knoevenagel Condensation reaction in water. *J. Korean Chem. Soc.* 49 (2005) 377.

# Patents

1. M. K. Dongare, **P. T. Patil**, K. M. Malshe. Vapor phase nitration of benzene using nitric acid over molybdenum silica catalyst. *US 20040024267* A1 (EP 1386907 A2).
2. M. K. Dongare, **P. T. Patil,** K. M. Malshe. An improved process for the preparation for the preparation of 4-nitro o-Xylene. *US 2004192977* A1 (IN 2003DE00262)
3. M. K. Dongare, **P. T. Patil**, K. M. Malshe. Improved process for the preparation of microporous crystalline titanium silicates. Mohan K. Dongare. *EP 1386885* A1.
4. M. K. Dongare, **P. T. Patil**, K. M. Malshe. Catalytic alkylation process for the preparation of a mixture of alkyl phenols. IN 2003DE00302 (IN 2003DE00309).

# Presentations

## Oral Presentations

1. **P. T. Patil**, A. Dimitrov, E. Kemnitz. Catalytic applications of sol-gel derived nanoscopic metal fluorides. Oral presentation, *41 Jarestreffen Deutscher Katalytiker* 2008, Weimar, Germany.
2. **P. T. Patil**, A. Dimitrov, U. Groß, S. Rüdiger, E. Kemnitz. Metal fluorides supported platinum and palladium: novel heterogeneous catalysts. Oral presentation, *1st international IUPAC conference on green-sustainable chemistry* (IUPAC ICGC 1) 2006, Dresden, Germany.

## Poster Presentations

3. **P. T. Patil**, A. Dimitrov, E. Kemnitz. Metal fluorides supported palladium based novel heterogeneous catalysts. Poster presentation, *40 Jarestreffen Deutscher Katalytiker* 2007, Weimar, Germany.
4. **P. T. Patil**, K. M. Malshe, and M. K. Dongare. Regioselective nitration of o-Xylene to 4-nitro o-Xylene over solid acid catalysts. Poster presentation, *5th National Symposium in Chemistry* (NSC-5) 2003, CLRI Chennai, India.
5. **P. T. Patil**, Kusum M. Malshe, Pradeep Kumar, Mohan K. Dongare. Benzoylation of Anisole Over Borate Zirconia Solid Acid Catalyst. Poster presentation, *4th National Symposium in Chemistry* (NSC-4) 2002, NCL Pune (India).
6. **P**. **T. Patil**, Kusum M. Malshe, and Mohan K. Dongare. Synthesis of substituted coumarins by Pechmann condensation using borate zirconia solid acid catalyst. Poster presentation, *16th National Symposium and 1st Indo-German Conference on catalysis* 2003, IICT Hyderabad, India.
7. K. M. Malshe, **P. T. Patil**, S. B. Umbarkar and M. K. Dongare. Selective C- methylation of phenol with methanol over borate zirconia solid catalyst. Poster presentation, *National Workshop on catalysis* 2004, CLRI Chennai, India.
8. S. B. Umbarkar, K. M. Malshe, **P. T. Patil,** M. K. Dongare. Vanadia-titania thin films for catalysis. Poster presentation, *Symposium on modern trends in inorganic chemistry* (MTIC-X), 2003, IIT Bombay, India.

# Acknowledgements

*I take this opportunity to express my deepest sense of gratitude and reverence to my research supervisor,* ***Prof Dr. Erhard Kemnitz*** *for giving me an opportunity to do Ph. D. in his group and also for giving an interesting topic for study. His constant inspiration, invaluable guidance and constructive criticism helped me a lot to do this work. This thesis would not have taken present shape without his guidance and care. My everlasting gratitude goes to him.*

*Secondly, I woe my words of gratitude to my intermediate supervisor Dr. A. Dimitrov for his advice, valuable discussions throughout this work which helped me to solve many problems.*

*My sincere thank to Dr. U. Groß, Dr. S. Rüdiger, and Dr. G. Scholz, for their valuable guidance, fruitful discussions and making corrections in my publications as well as thesis work.*

*I am grateful to Dr. M. Feist for thermal analysis, Dr. S. Rüdiger for SEM measurements, Dr. G. Scholz for MAS-NMR measurements, Dr. K. Scheurell for H/D exchange measurements, Frau Bräßer for TPD and FTIR-PAS measurement, Mr. H. Krüger for AFM measurements, Dr J. Radnik (LIKAT) for XPS measurements, Dr. H. Kirmse (Institute für Physik, HUB) and Dr. M. Pohl (LIKAT) for TEM measurements, Frau Kätel and Dr. A. zehl for elemental analysis.*

*It gives me great pleasure to thank my former and present colleagues Dr. J. Krishnamurthy, Dr. S. Coman, Dr T. Karl, Dr. M. Ahrens, Dr. Prescott, Dr. I. Murwani, Dr. G. Eltanany, Dr. Z. Li, Mr. S. Wuttke, Mr. R. König, Mr. C. Stosiek, Mr. I. Buchem and all other members of Prof. Kemnitz' group including secretary frau I. Rauch for their help, valuable guidance and keeping friendly atmosphere. My special thanks to Frau Hartwich for drying solvents and improving my German language (Danke!). I also thank to my practical students Mr. G. Breadt and Ms. M. Russew for performing some of the experiments.*

*I wish to thank Dr. A. Martin for giving access to characterization methods at LIKAT and also to his group members, especially of Dr. V. Narayana Kalewaru, for their cooperation.*

*My special thank to Dr. M. K. Dongare and Dr. S. G. Hegde NCL pune (India) for giving me essential training to do research in heterogeneous catalysis, their support during my struggling days and always promoting me to do meaningful work. I am also grateful to Dr. R. A. Mane, Prof. M. S. Shingare (BAMU) and many of my teachers, lecturers and professors, who always promoted me to get the higher education.*

*I would like to thank my friends Sudhir, Raj, Dilip, Atul, Amit, Tushar, Bapu, Bondgesir, Ankush, Manoj, Vivek, Satish, Anil, Chandan, Ananya, Kusum, and several others in germany or in India, for their inspiration, encouragement and help. I also thank to my M. Sc. mates Santosh Khyade, Abhijeet Deshpande, Jairaj Thete, Dhanaji Thorat and Ganesh Ghate for their friendship over years and for their encouragement to do the best.*

*I thank to staff members of administration, NMR, glassblowing section, workshop and chemical store at institute of Chemistry (HUB) for all kind of help they have done for me during my research stay at this institute.*

*A big thank to my all family members: Parents: Sou. Bhartidevi Patil & Shri Tukaram Patil, Sisters: Sou. Anuja karbhari and Sou. Shailaja Salunke, Brother Ravi & sister in law sau. Sarita, Brother in laws: Shri Deelip Karbhari and Ranjeet Salunke, dear Nephews: Rupesh & Ajay, and nieces: Rajani & Guddi for their everlasting love, tremendous support, and encouragement through out my education.*

*Finally, I wish to acknowledge, the financial support from the EC and CSIR-DLR (Indo-German) Projects. I also acknowledge Nachwunschsförderungsgesezt (NaFöG) for financial assistance for last one year of this thesis.*

***Pratap T. Patil***

# Selbständigkeitserklärung

Hiermit erkläre ich, die vorliegende Dissertation selbständig und nur unter Verwendung der angegebenen Hilfsmittel und Quellen angefertigt zu haben.